NASA CONTRACTOR REPORT

NASA CR-595

TROPOSPHERIC WATER VAPOR CONTENT AND SURFACE TEMPERATURES FROM TIROS IV RADIATION DATA

by Ehrhard Raschke

Prepared by
UNIVERSITY OF MUNICH
Munich, Germany
for Goddard Space Flight Center

NATIONAL AERONAUTICS AND SPACE ADMINISTRATION • WASHINGTON, D. C. • SEPTEMBER 1966

NASA CR-595

TROPOSPHERIC WATER VAPOR CONTENT AND SURFACE TEMPERATURES FROM TIROS IV RADIATION DATA

By Ehrhard Raschke

Prepared under Grant No. NsG-305 by
UNIVERSITY OF MUNICH
Munich, Germany

for Goddard Space Flight Center

NATIONAL AERONAUTICS AND SPACE ADMINISTRATION

For sale by the Clearinghouse for Federal Scientific and Technical Information
Springfield, Virginia 22151 – Price $3.00

ABSTRACT:

Radiometric measurements within the 6.3 micron band of water vapor and the 8-12 micron atmospheric window were made over a five month period from February to June 1962 from the TIROS IV meteorological satellite. Simultaneous measurements in these two spectral intervals have been analyzed to infer the spatial and temporal variations on a quasi-global scale of the following three quantities: (1) the mean temperature of the cloud top, land, or ocean surfaces, (2) the mean relative humidity of the upper troposphere, and (3) in conjunction with radiosonde temperature data, the water vapor mass above the 500 mb level.

The results show three major regions of high moisture content over South America, Africa and the Western Equatorial Pacific with several other lesser regions near the Intertropical Convergence Zone. The subtropical highs of both hemispheres are regions of low moisture content, as it might be expected from the general atmospheric circulation pattern. A minimum average zonal moisture occurs in the months of February and March in the Northern Hemisphere near 20° latitude. In the months of May and June it occurs in the Southern Hemisphere near the same latitude.

At equatorial latitudes the average surface temperatures indicate a persistent minimum along a narrow band identified with the Intertropical Convergence Zone. Elsewhere the magnitudes and patterns of the mean surface temperatures are associated with semi-permanent weather regions, as well as synoptic scale weather features occuring along storm tracks in middle latitudes, especially in the winter season in each hemisphere.

CONTENTS

LIST OF FIGURES

LIST OF TABLES

1. INTRODUCTION:

Water vapor in the earth's atmosphere is of great importance in all processes which are connected with the planetary circulation, with the planetary heat balance, with the hydrologic cycle, and also with the life on earth. The knowledge of its vertical and horizontal distribution, and of the seasonal changes should give more insight into these processes.

In the past years only a little number of authors determined the global distribution of the total water vapor mass (STARR et al., 1958; BANNON and STEELE, 196o), of the relative humidity (SZAVA-KOVATS, 1938; TELEGADAS and LONDON, 1954) and of the precipitation (e.g. MÖLLER, 195o). These analyses have been based largely on radiosonde measurements. However, because of the extremely limited number of stations over most parts of the earth's surface and because of sizeable errors of measurements the validity of these water vapor analyses still have been open to question.

Global measurements of the thermal radiation of the atmospheric water vapor within several ranges of the electromagnetic spectrum from satellites should promise to yield better determinations, once methods are developed to extract from them informations about the vertical water vapor profile or the total water vapor content. Up to now, such measurements have been made only from the meteorological satellites TIROS II, TIROS III and TIROS IV in only one narrow spectral interval (5.8 - 6.8 microns) centered within the 6.3 micron band of water vapor. MÖLLER (1961) has shown that the upward going infrared radiation in this spectral range is a measure for the mean relative humidity of the troposphere if the temperature

profile is known. Later MÖLLER (1962) and RASCHKE (1965) developed an evaluation method in which they included simultaneously measured radiation in the atmospheric water vapor window between 8 and 12 microns to account for the temperature of high cloud surfaces. This method has been used in this period of the Grant NsG-3o5 to evaluate the TIROS IV radiation data. Since this method has been reported on formerly (MÖLLER and RASCHKE, 1964; RASCHKE and TANNHÄUSER, 1965; RASCHKE, 1965), it shall be discussed here only briefly.

TIROS IV measured the infrared radiation from the earth into space over about a five month period (February 8 to June 3o, 1962). During this period an optical degradation of the sensors (G.S.F.C., 1963) occured which necessitated a correction of all measured data.

The results, (1) the mean relative humidity of the upper troposphere, (2) the effective surface temperature, and in conjunction with climatological data on the temperature (3) the water vapor mass above 5oo mb, are presented here in quasiglobal distribution maps of monthly and of ten-day averages (appendices A 1 and A 2) between 55°N and 55°S.

2.o PRINCIPLE OF EVALUATIONS:

2.1 Equation for transfer of upward going infrared radiation.

A radiometer on a platform outside the earth's atmosphere measures within a sufficient small aperture angle $\Delta\omega$ the intensity $\bar{I}(\Theta)$ of upward going infrared radiation. This can also be calculated from the vertical distribution of temperature and of an absorbing gas using the following well known equation:

$$I(\theta)=\Delta w \int_{o}^{\infty} \phi_\nu B_\nu[T(\log p_o)]\tau_\nu[\theta,w(\log p_o)]d\nu \qquad (1)$$

$$+ \quad \Delta w \int_{o}^{\infty} d\nu \int_{\log p_s}^{\log p_o} \phi_\nu B_\nu[T(\log p)]\frac{d\tau_\nu[\theta,w(\log p)]}{d \log p} d \log p$$

where ν is the wave number, B_ν the Planck function, T the ambient temperature, p the ambient pressure, θ the zenith angle of the radiation, τ_ν the spectral transmittance of the atmosphere between a level at ambient pressure and the satellite, and w the mass of absorbing gas in the vertical between the two levels. The subscript "o" refers to the lower boundary, which has been assumed to be a blackbody, although cloud sufaces and the ground have not the emissivity 1.o (e.g. BUETTNER, 1965). The subscript "s" refers to the satellite. The function ϕ_ν describes the spectral filter function of the instrument.

Equation 1 is valid only in that region of the atmosphere where the local thermodynamic equilibrium exists (up to about 4o km). Further it can be assumed that the scattering of infrared radiation by air molecules is negligible except if ice particles and water droplets are present (DEIRMENDIJAN, 1959; ZDUNKOWSKI et al., 1965). Absorption and emission by aerosols have been proved (KONDRATIEV, 1961; ROBINSON, 1962; LEUPOLT, 1965), but it is very difficult to include them quantitatively into calculations of radiation fluxes.

Equation (1) shows that the total value of $I(\theta)$ consists of contributions of radiation emitted from the lower boundary (first term) and from a gas within

the atmosphere above that boundary (second term). In spectral intervals of high absorptivity of that gas (in band centers or in line centers) only radiation emitted in the upper layers can penetrate the atmosphere to space, while in spectral intervals of less absorptivity radiation from lower layers can penetrate to space.

According to the second term in Equation (1) the intensities are determined by the vertical distribution of the temperature and of the concentration of the absorbing gas in those layers. KING (1958) demonstrated the validity of this fact for determinations of the vertical distributions of the temperature and of absorbing gases from satellite measurements. KAPLAN (1959) later showed that from simultaneous measurements in different spectral ranges of the 15 micron CO_2-band with different absorptivities in principle the vertical temperature profile can be determined because of the constant mixing ratio of carbondioxide in the atmosphere up to about 40 km. The curves in Fig.2.1 show that depending on the absorptivity of CO_2 in each particular interval the center of gravity of emission (second term of equation 1) is located in particular layers.

Mathematical difficulties occuring in evaluations of those measurements have been discussed by several authors (KING, 1963; 1964; McCLATCHEY, 1965; TWOMEY, 1965; RODGERS, 1965; WARK and FLEMING, 1966). Also several techniques for measurements have been developed in the past years (DREYFUS and HILLEARY, 1962; HANEL and CHARNEY, 1965; HOUGHTON, 1961; SMITH and PIDGEON, 1964). Up to now only HILLEARY, WARK and JAMES (1965) obtained satisfactory results from balloon borne measurements.

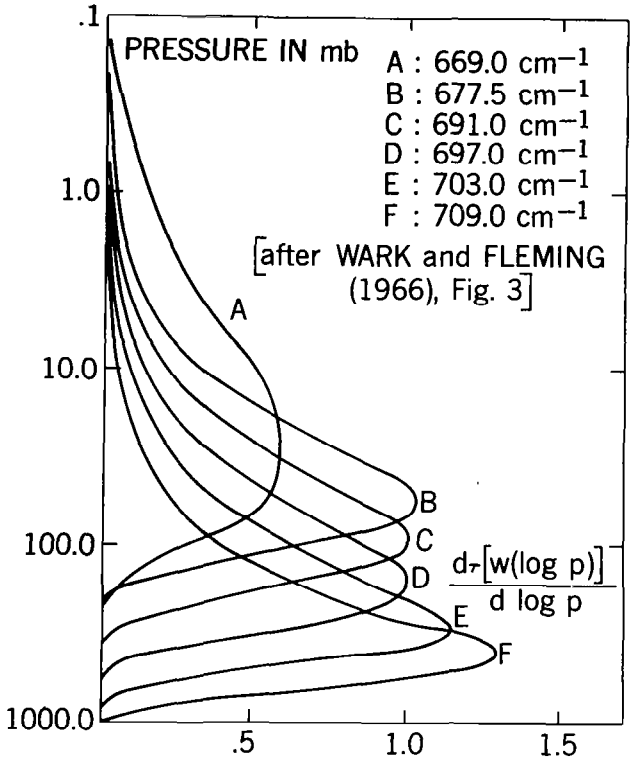

Fig.2.1: Weighting functions $\frac{d\tau_\nu[w(\log p)]}{d \log p}$ of the upward outgoing radiation within several narrow spectral intervals of the 15-micron-band of carbon dioxide

If the temperature profile is known, then in principle also the vertical distribution of an absorbing gas can be obtained from a similar set of measurements in one of its absorption bands. Inasmuch as remote soundings are made only in the infrared the the results will be disturbed by the presence of clouds dust and haze layers because ice crystals and water droplets in those layers have other optical properties than the gases.

In spectral ranges of centimeter waves and microwaves, where the scattering by larger particles is small, the temperature profile can be obtained by measurements in the region of strong O_2 lines near λ = 5 mm (SMITH, 1961; MEEKS and LILLEY, 1962; FOW, 1964). The vertical distribution of water vapor or the total water vapor mass can be derived from measurements in H_2O lines near 1.35 cm, 1.63 mm or at wavelengths shorter than 1 mm (see also KATZ, 1963). Here, however, the absorptivity of water droptlets must taken into account. Further the emissivity of the ground in that spectral range departs widely from that in the infrared region depending on the ground cover.

Determinations of the vertical structure of the lower atmosphere, in particular of the troposphere from satellite measurements of the emitted electromagnetic radiation are therefore of a sophisticated nature. They will not replace completely convential methods of meteorological observations.

2.2 Evaluation method

Up to now one of the inversion methods mentioned above could not be applied on satellite measurements,

because former meteorological satellites (TIROS II, TIROS III and TIROS IV) carried radiometers with only three channels for measurements of infrared radiation (Table 2.1).

	spectr.interv.	
channel 1	5.8-6.8 μ	center of 6.3 μ-band of water-vapor
channel 2	8 μ - 13 μ	atmospheric window
channel 4*	7 μ - 3o μ	total infrared radiation
* not aboard of TIROS IV		

Table 2.1: Spectral ranges of infrared sensor of TIROS II, TIROS III, and TIROS IV

FROM TIROS VII only radiation between 8 and 13 μ and additionally within the 15 μ -band of carbon dioxide (stratospheric temperatures) has been measured.

Within the region of sensitivity of channel 4 about 8o % of the total emerging infrared radiation of the earth and its atmosphere will be measured. As the absorption by water vapor in the rotation spectrum from 17 to about 5o microns is less than the absorption in the 6.3 micron band it was proposed by MÖLLER and RASCHKE (1963) and by YAMAMOTO (1965) to derive from channel 4 measurements the mean relative humidity of the lower troposphere or the total water mass. Since channel 4, however, measures radiation emitted from the ground (or from clouds), from H_2O and additionally from CO_2 and O_3 such determinations are of a complex nature. A quantitative analysis of these

measurements in that sense requires an accuracy of measurements which is much higher than the actual accuracy.

Therefore, only from the measurements of the remaining two channels parameters of the atmospheric structure could be derived. (Fig.2.2)

Channel 1 measures radiation emitted from atmospheric water vapor in the center of its 6.3 micron band. The absorptivity here is high enough that in a cloudless atmosphere only radiation emitted from layers above 600 mb can penetrate to space (Fig.2.3). The center of gravity of emitted radiation is located between 200 and 600 mb depending on the water vapor concentration in these layers. The contribution from layers below and above these boundaries is comparatively small because of the high absorptivity of H_2O in this spectral range and of the low concentration of H_2O in the stratosphere respectively.

If no high clouds are present the measured values of channel 1 primarily depend on the vertical temperature distribution and on the water vapor concentration between 600 mb and 200 mb (second term of Equ.1). MÖLLER (1961) could show, that they are a measure of the mean relative humidity within these layers, if only the tempeture lapse rate is known even without exact knowledge of the temperatures themselves. The lapse rates, however, do not show much of variability.

These humidity values obtained from channel 1 data are weighted means. Since the level of the center of gravity of emission changes its height with the water vapor concentration, the humidity values are not representative for a fixed level.

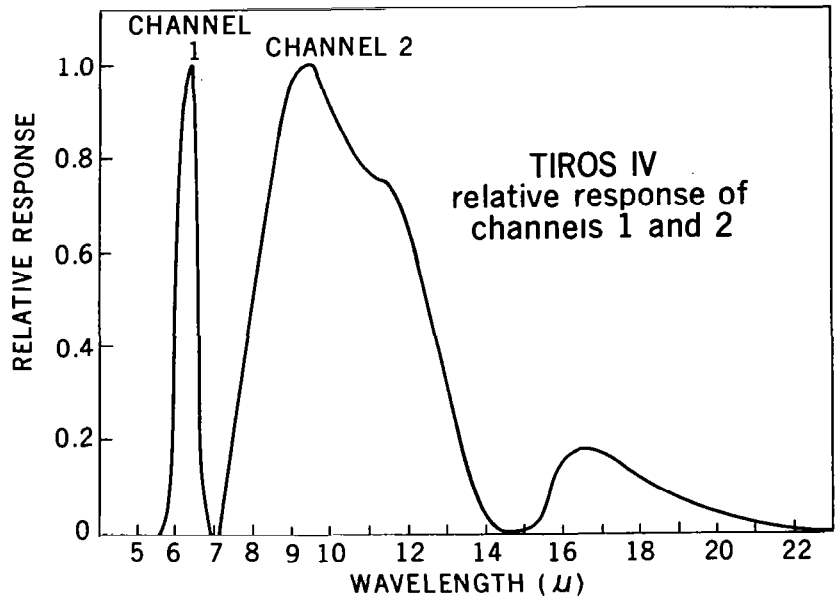

Fig.2.2: Filter functions ϕ_ν of the channels 1 and 2. (ν = 1/wavelength)

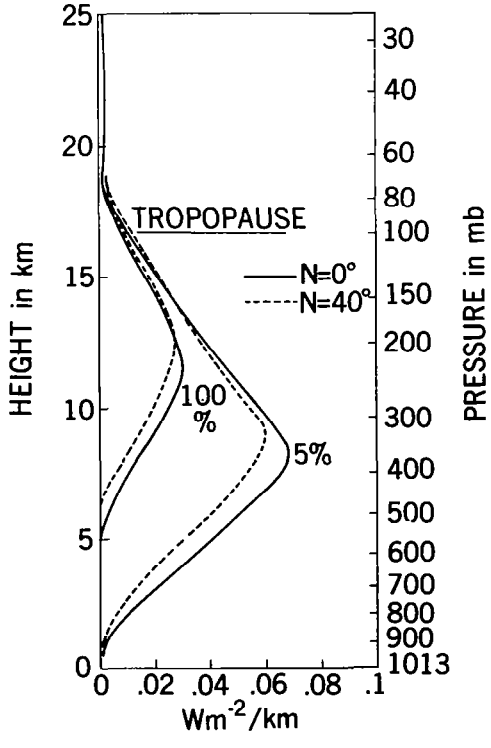

Fig.2.3: Curves

$$\int_0^\infty \phi_\nu B_\nu(\log p) \frac{d\tau_\nu(w \log p)}{d \log p} d\nu$$

vs. height for the upward going radiation in the spectral range of channel 1 in a tropical model atmosphere

Over high clouds channel 1 also measures radiation emitted from the cloud sufaces, which is determined by their temperature. The temperature can be obtained from simultaneously measured data of channel 2, assuming that the clouds are completely opaque, have no reflectivity in the infrared, and fill completely the field of view of the radiometer. It is evident that cases of partly transparent clouds lead to high mistakes of interpretation. Also different albedos of clouds in both spectral regions (DEIRMENDIJAN, 1962; HAVARD, 196o; ZIRKIND, 1965) may cause some uncertainties.

The evaluation procedure which is the only applicable one, consists in comparisons of simultaneously measured data of both channels with intensities of the emerging radiation calculated for model atmospheres. The model assumptions are: temperature profiles (COLE and KANTOR, 1963), valid for a certain climatological zone and time period (chapter 2.3); constant relative humidity in all layers of the troposphere and constant gradient of the frost point in the level of the stratosphere; constant mixing ratio of water vapor above 1oo mb of $2 \cdot 1o^{-6} g/g$ (MASTENBROOK, 1963). For calculation of the upward going radiation in the filter region of channel 1 also carbon dioxide (with o,o3 % per volume) and ozone (vertical profiles for different latitudes) were taken into account. As described above clouds were assumed to be black in the infrared. Their surface temperature was assumed to be equal that of the air adjacent above them. For the case of surface temperatures higher than those given in the atmosphere temperature profile, only the surface temperature was increased, while all other conditions were kept constant.

All calculations of radiation intensities were carried out with the computer program developed by WARK, YAMAMOTO and LIENESCH (1962). Evaluation diagrams could be drawn from the results, obtained for different cloud heights and for different values of the relative humidity. One of them is shown in Fig.2.4. It is determined only for radiation vertically emerging from a tropical model atmosphere. (See page 12)

In this diagram the pattern of isolines for equivalent black body temperature $T_{equ.}$ * shows the influence of tropospheric water vapor on the radiation within both spectral ranges. The curves for channel 1 turn with decreasing cloud height and increasing relative humidity from the vertical into horizontal direction, while those for channel 2 change only a little bit their direction. On the left hand side of the diagram, however, which is representative for measurements over very high clouds (low surface temperatures) channel 1 approximately also measures the surface temperatures of the clouds. Points of intersection between the isolines for both channels determine the desired values of the relative humidity and of the surface temperature. These intersections are not well defined in the left hand past of the diagram. In the evaluation procedure then it was assumed that the upper troposphere is nearly saturated (r.h. = 99 %) or filled with thick clouds if measurements of both channels had equivalent temperatures of less than 228°K. This assumption, in fact, seems to be very arbitrarily, because it is not possible to distinguish between measurements above a very high, dense

---

* The equivalent black body temperature $T_{equ.}$ of the intensity I of infrared radiation in a spectral interval described by the filter function ϕ_ν is defined by

$$\bar{I} = \Delta\omega \int_0^\infty \phi_\nu B_\nu(T_{equ}) \, d\nu$$

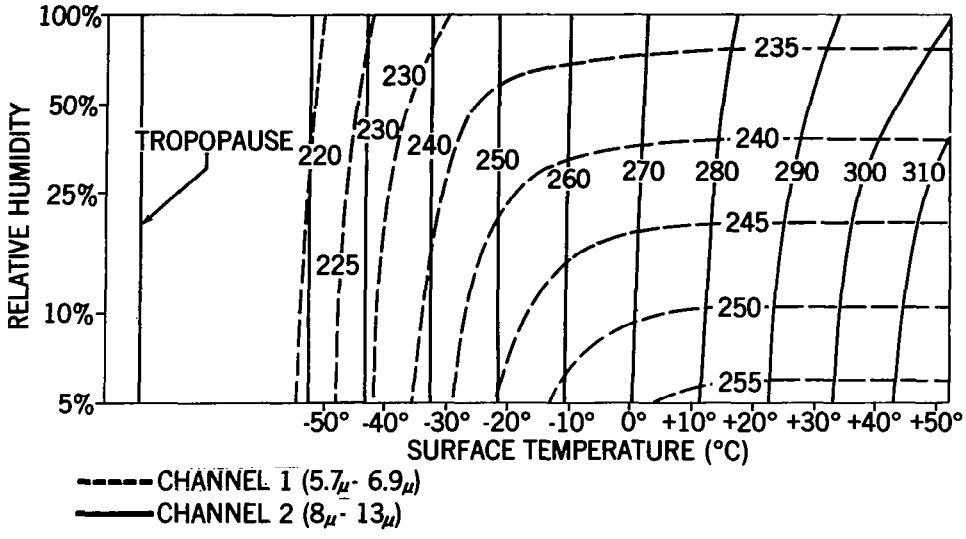

Fig.2.4: Evaluation diagram, computed for radiation emerging vertically from a tropical model atmosphere. Isolines are drawn for equivalent blackbody temperatures (in °K)

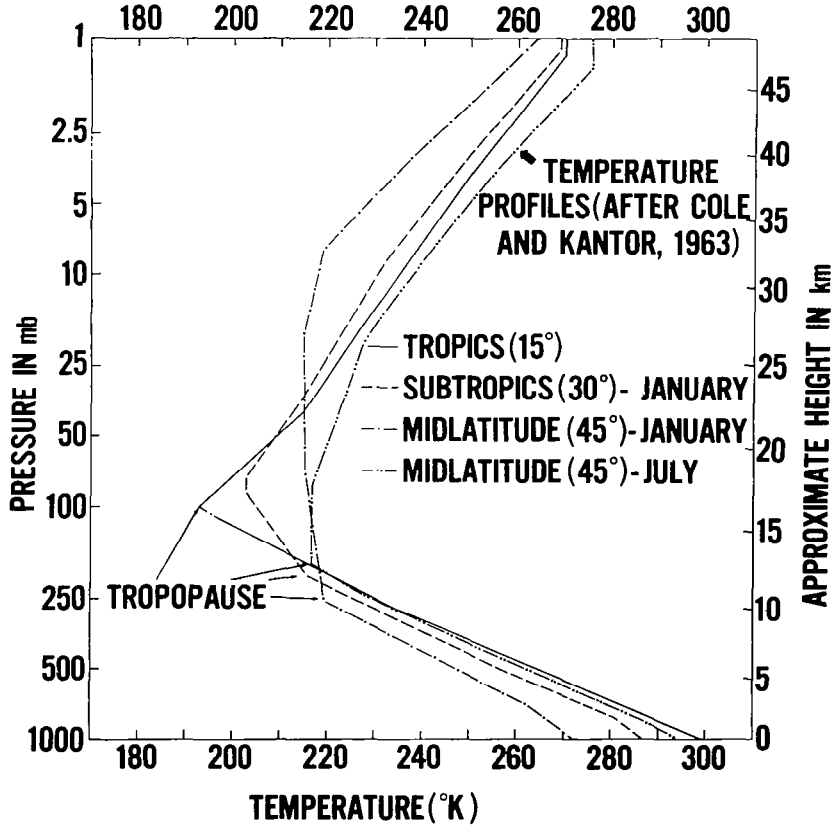

Fig.2.5: Temperature profiles

and cold, but thin cirrus layer or a lower but warmer and thicker cumulus or alto stratus layer, which fills the entire upper troposphere. In order to account for the nadir angle dependence of measurements similar diagrams were calculated for nadir angles of 30° and 40° and were used in the evaluation procedure as described below in chapter 2.3.

Due to latitudinal changes of the stratospheric temperatures and due to the temperature and pressure dependence of the absorptivity of water vapor the intensity of outgoing radiation in both channels would vary with latitude even if all other conditions (surface or cloud temperature, relative humidity etc.) would be kept constant. Evaluations of data measured at different latitudes with diagrams computed only for one model atmosphere then would lead to systematic errors. Therefore, radiation data measured in a certain latitudinal belt and calendar month were evaluated using calculations from the climatologically nearest corresponding temperature profile as shown in Fig.2.5.

The results, which will be obtained by evaluations of radiation data of both channels are now

(1) the mean relative humidity of the upper troposphere or above clouds in the upper troposphere, and
(2) an effective surface temperature.

Both of these quantities must be understood to be valid only for an ideal stratification with given temperature profile and a cloudless (and dustless) upper troposphere which is bounded below by a black emitting surface (cloud or ground). Since only one measurement within the water vapor band was available, it is not possible to define a fixed level for which the humidity

value holds. Variations of the actual atmospheric stratification, in particular transparent or broken cloud layers and colder or warmer stratospheric layers, affect errors in the results (RASCHKE, 1965), by which the validity of this simple procedure is limited.

2.3 Evaluation procedure

All evaluations of the data of TIROS IV were performed with the IBM 7o9o computer of the GODDARD SPACE FLIGHT CENTER, Greenbelt, Maryland. Fig.2.6 shows a diagram of the data flow in the computer, which in principle explains two successive steps. (See page 15)

Step 1: Averaging of data in grid fields.

Data from a single orbit (channel 1, channel 2 and also nadir angle) were averaged within grid fields given by a standard computer program (G.S.F.C., 1962) for mapping of TIROS radiation data in a Mercator Scale Map (1:4o mill.). In this program one grid field near the equator is about 5x5 degrees longitude and latitude wide.

Before averaging the radiation data were corrected according to the degradation of the sensors (chapter 3). Those measured with nadir angles $N < 45°$ were omitted. This procedure produces the data which are stored on the master grid tape.

Step 2: Evaluation.

As mentioned in chapter 2.2 the nadir angle dependence has been taken into account by evaluating data measured with nadir angles between 0 and 25 degrees (26°-35°, 36°-45°) with intensities calculated for upward going radiation at the nadir angle of 0° (3o°, 4o°). Table 2.2 shows the latitude boundaries used for each model atmo-

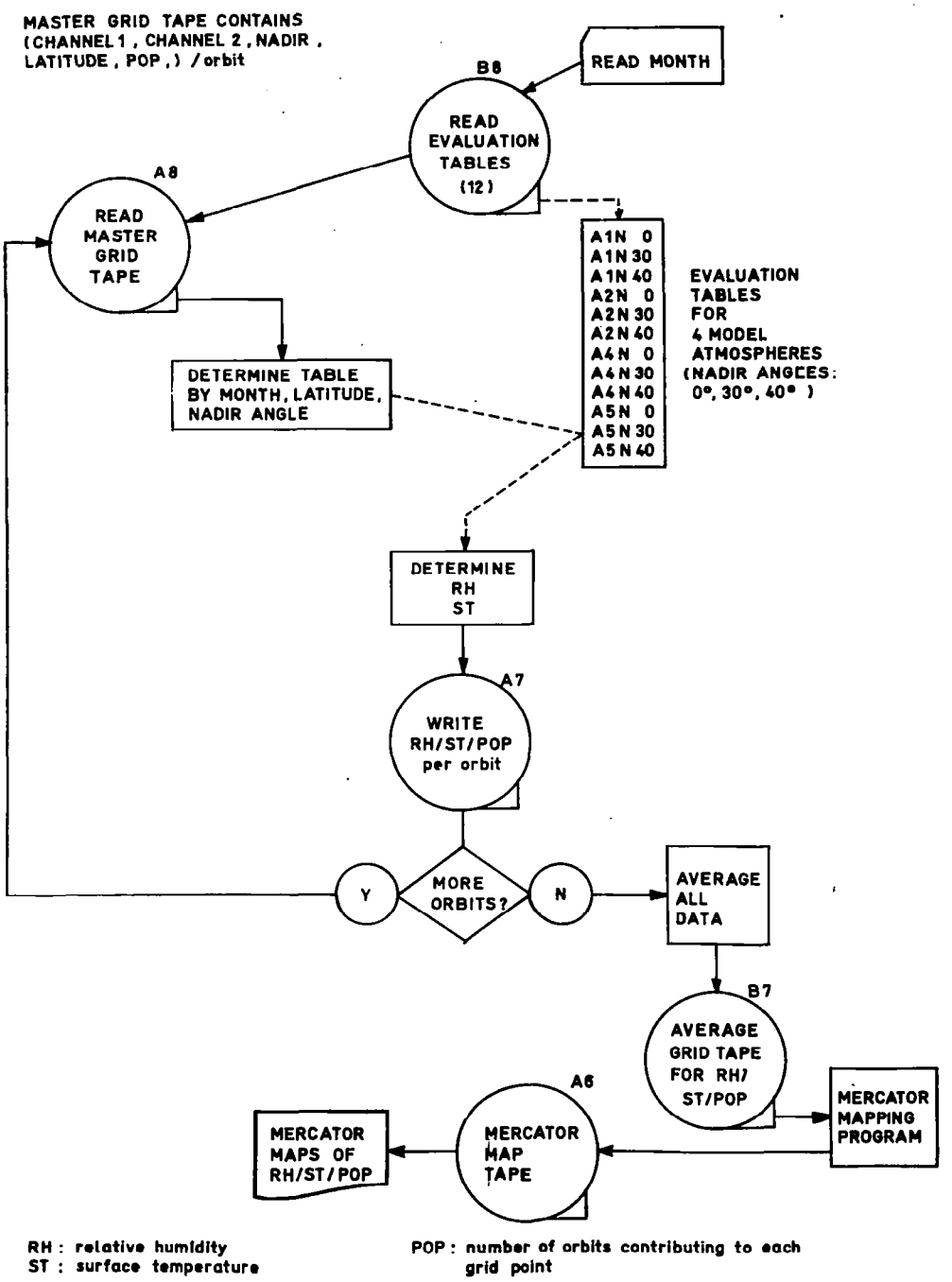

Fig.2.6: Diagram of data flow in the computer of TIROS IV infrared radiation data

Month	Model Atmosphere	latitude boundaries
February	C	60°N - 35°N
	B	34°N - 20°N
	A	19°N - 35°S
	C	36°S - 60°S
March	C	60°N - 35°N
	B	34°N - 20°N
	A	19°N - 35°S
	B	36°S - 60°S
April	B	60°N - 40°N
	D	39°N - 20°N
	A	19°N - 19°S
	C	20°S - 39°S
	B	40°S - 60°S
May	B	60°N - 40°N
	D	39°N - 20°N
	A	19°N - 19°S
	B	20°S - 39°S
	C	40°S - 60°S
June	D	60°N - 36°N
	A	35°N - 19°S
	B	20°S - 34°S
	C	35°S - 60°S

Table 2.2: Latitude boundaries for each model atmosphere and each calendar month

sphere given in Fig.2.5 which were determined by comparison with temperature profiles published by KANTOR and COLE (1965) for each calendar month and various latitudinal belts.

This evaluation procedure has been repeated with data of any orbit separately.

3.0 CORRECTION OF RADIATION DATA FOR INSTRUMENTAL RESPONSE DEGRADATION

3.1 Accuracy of measurements (without degradation)

By estimating the signal to noise ratio at "mid-range" temperatures of the radiation source (for channel 1 = 230°K, for channel 2 = 280°K) it has been found that the accuracy is about $\pm$ 5°K of the equivalent temperature of the measured intensity (G.S.F.C., 1963). These high errors do not allow a quantitative analysis of single spot values. Therefore, the averaging within grid fields of about 5x5 degrees was performed as mentioned above before the evaluation procedure although then the simultaneousness of measurements of both channels is lost, which is required in the evaluation method.

3.2 Postlaunch degradation of instrumental response

After launch the sensitivity of the instruments in TIROS IV decreased slowly with time. This degradation must be accounted for in quantitative evaluations of the measured data. Since no calibration source was aboard TIROS IV the magnitude of the degradation and its temporal changes must be determined under reasonable assumptions. These are:

(1) The sensitivity decreases slowly and steadily with time.
(2) The degradation is not dependent on the wavelength.
Then the measured intensity $\bar{W}^1$ of one channel is determined (BANDEEN et al., 1963) by:

$$\bar{W}^1 = C^F \bar{W}^F - C^W \bar{W}^W + (C^W - C^F) \bar{W}^S \qquad (2)$$

where $\bar{W}^F$ and $\bar{W}^W$ are the intensities incident into the apertures of the radiometer at floor side and wall side, respectively.

$$\bar{W}^S = \int_0^\infty \phi_\nu \; B_\nu \quad (T_s) \; d\nu \qquad (3)$$

is the intensity emitted from all components of the optical system inside the satellite, if their temperature T_s is equal. C^F and C^W give the subsequent fractional degradation, respectively, for the floor and wall sides. At the time of calibration of the sensors (and of the first orbit) it has been assumed that $C^F = C^W = 1$, although radiation data of channel 2 seemed to be about 5°K too low (chapter 3.3). Assuming, that the radiation incident from space into one side of the satellite does not have a measurable effect, Equation (2) can be written:

for wall side: $\bar{W}^1_W = C^W \bar{W}^W + (C^F - C^W) \bar{W}^S \qquad (4)$

for floor side: $\bar{W}^1_F = C^F \bar{W}^F + (C^W - C^F) \bar{W}^S$

Two different cases of degradation now must be considered:

1. $C^W = C^F \leqslant 1$ (symmetrical degradation)
2. $C^W \neq C^F \leqslant 1$ (asymmetrical degradation)

3.3 Degradation of channel 2

Radiation data of channel 2 only showed a slight asymmetrical degradation for the orbital days 130-142, which however will not be taken into account here. Therefore, it has been assumed that $C = C^W = C^F$, and from (4)

$$\bar{W}^1_W = \bar{W}^1_F = C \cdot \bar{W} \qquad (5)$$

The temporal change of C has been determined already (G.S.F.C., 1963) with the main assumption that the emitted radiant power of the entire quasiglobe between about 60°N and 60°S (derived for approximately 20 orbits) remains constant with time. From these results and from additional studies described below the curves C (v.s.orbital day) and for the corrections $\Delta T_{equ.}$ of measured equivalent temperatures have been determined, which are shown in Fig. 3.1. (See page 20)

To check the assumption made by the staff members of NASA, data measured in channel 2 over apparently cloudless subtropical oceans have been used to determine surface temperatures by our method assuming an average relative humidity of the troposphere of 25 %. The results confirmed in principle the temporal decrease of channel 2 data found by the other authors; however, the surface temperatures found for the first

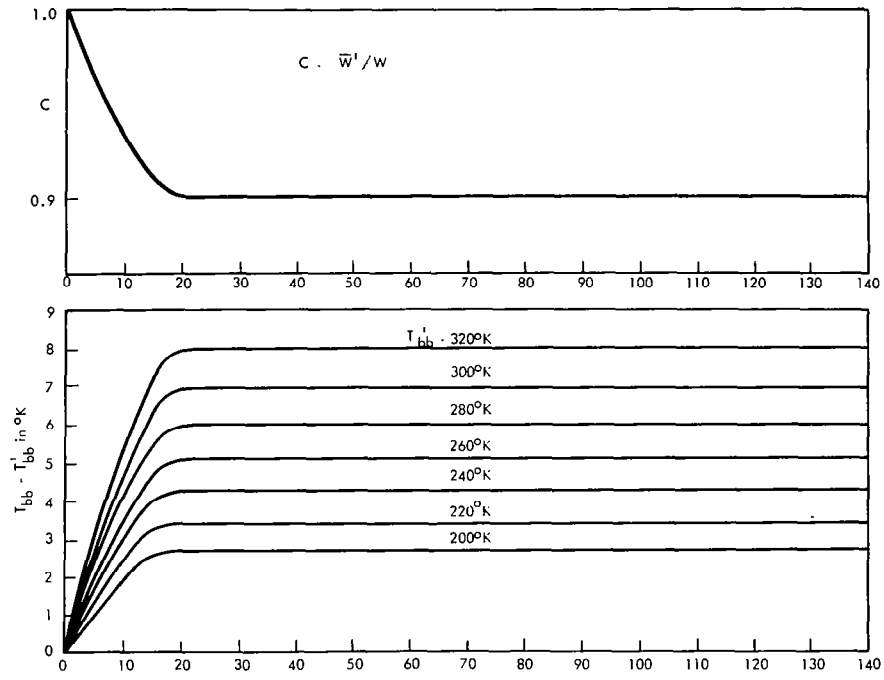

Fig.3.1: Degradation of channel 2
Upper part: Degradation factor C vs. orbital or Julian day of the satellite.
lower part: Temperatur correction $\Delta T = T_{bb} - T'_{bb}$ vs. orbital or Julian day of the satellite. A measured value T'_{bb} should be corrected by adding the ΔT value corresponding to the appropriate orbital day.

2 days were about 5-6°K lower than climatological values of the sea surface temperature. This temperature difference might have arisen by a quick degradation during the first day or by a thin cirro stratus of about 1o% absorptivity (RASCHKE, 1965). Unfortunately no reliable reports were available, whether or not such cirro stratus was present. Therefore this obvious temperature difference has not been taken into consideration here.

3.4 Degradation of channel 1

In contrast with channel 2 the optical systems in channel showed an asymmetrical degradation, which is illustrated drasticly in the scatter diagrams of Fig.3.2. In the Figure are shown frequency numbers of simultaneous measurements of both channels for wall and floor side separately. The solid curves indicate the relation of measurements of both channels in a tropical model atmosphere, as described in chapter 2.2, if the relative humidity is constant at 1oo % or 5 %. Channel 2 temperatures are corrected for degradation. The entire cloud of numbers for wall side data is shifted to lower temperatures by about 1o-16 degrees, while that for floor data seems to be shifted by 4-6 degrees to higher values both indicating the high influence of radiation emitted from all components of the instrument. The scattering of the measured values is very high at low temperatures, where both channels should measure nearly equal temperatures.

To determine the degradation factors C^W and C^F we assumed that over high clouds (channel 2 < 23o°K) the relation between equivalent temperatures of both

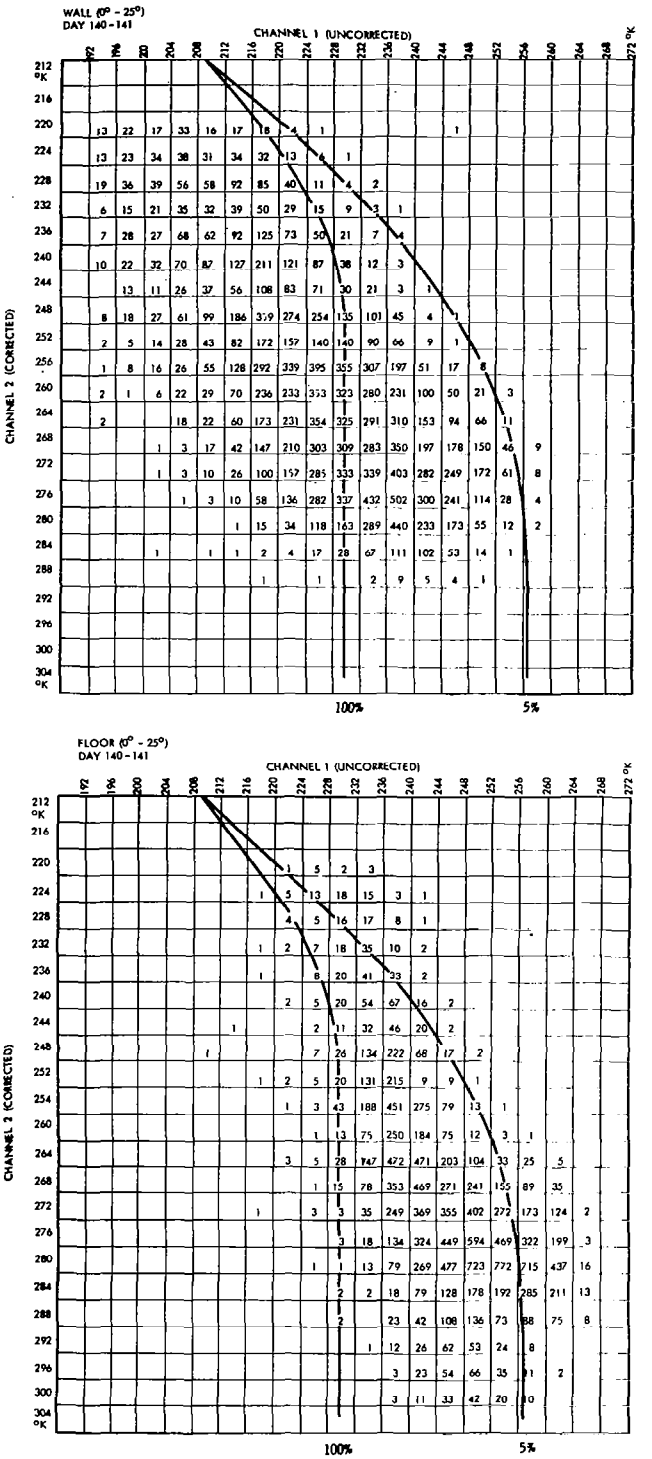

Fig.3.2: Scatter diagrams of simultaneous equivalent black body temperature measurements of channels 1 and 2 during the orbital days 14o and 141 at nadir angles N between o° and 25°.

Upper part: wall side
lower part: floor side

channels should be nearly linear, because both channels measure nearly the surface temperature of clouds. For 4°-intervals of channel 2 data (already corrected) averages of channel 1 data were determined, using only data measured with nadir angles $\leq 25°$ within 3 or 4 day periods. Curves of these averages of channel 1 measurements vs. channel 2 (upper part of Fig.3.3) then were shifted vertically until they intersect in the point: channel 1 = 226°K, channel 2 = 228°K. According to our model calculations channel 1 measures equivalent temperatures of about 226°K, over clouds with a surface temperature of 228°K while channel 2 measures $T_{equ} \sim 228°K$. From the amount of shifting the values of C^W and C^F were determined using Equations 4. The temperatures of all components of the radiometer were taken from G.S.F.C., 1963. Further, to get reasonable results it has been assumed that the floor side measurements remained undegradated during the first 25 days. (See page 24)

The lower part of Fig.3.3 shows the relation between channel 1 and channel 2 data after correction. Figs.3.4 and 3.5 show the curves for C^F and C^W and for the values T necessary for corrections of measured data. (See page 25)

It is evident that this kind of correction which seemed for us to be the only possible one, required also delicacy of feeling and some smoothing of the results. Therefore, it may be not very accurate and may still contain uncertainties.

The most important source of errors might be the noise which during the last few weeks of measurements became rather high. The results of the evaluations,

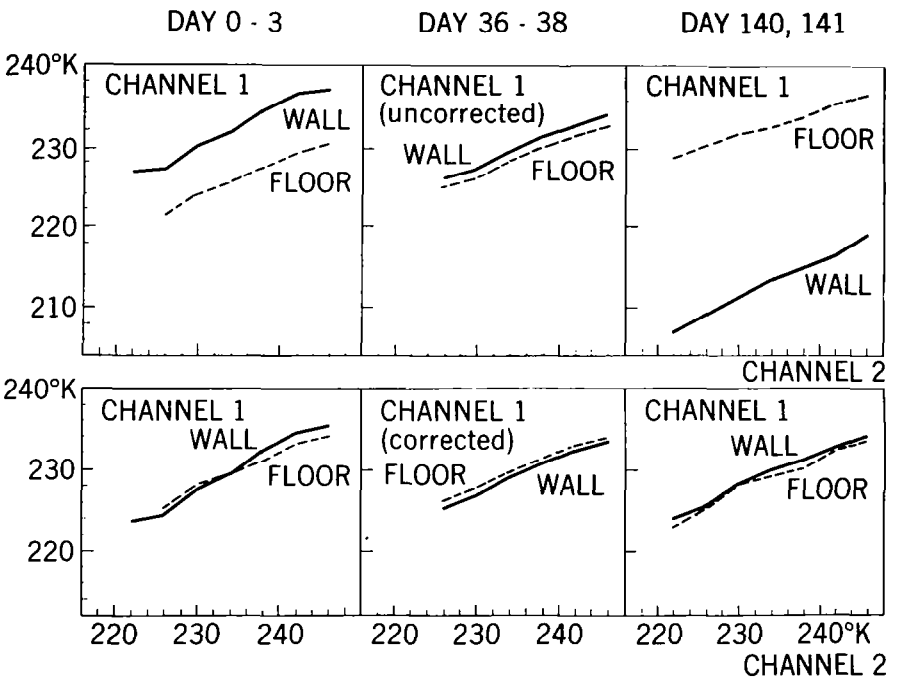

Fig.3.3: Simultaneous measurements of channel 1 (averaged) vs. those of channel 2 (corrected for degradation).
Upper part: channel 1 uncorrected
lower part: channel 1 corrected

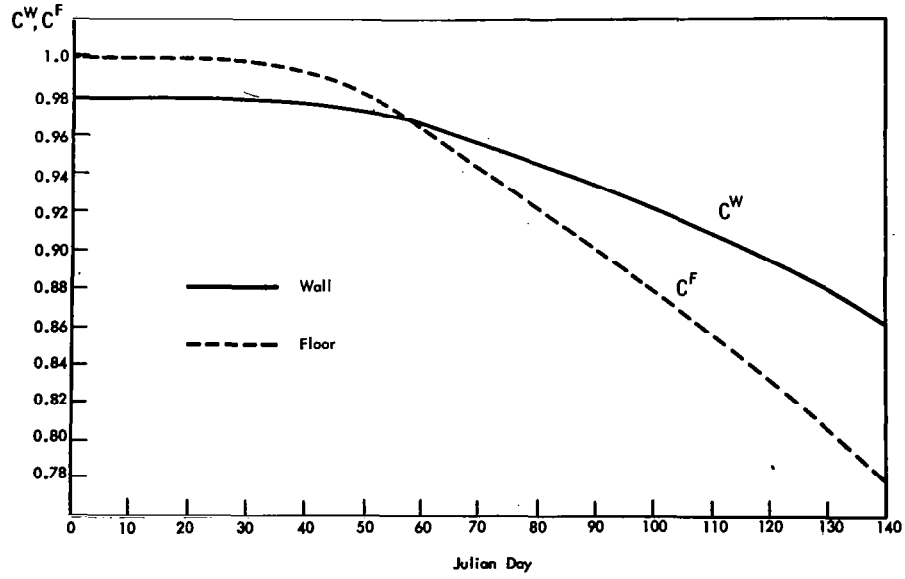

Fig.3.4: Degradation of channel 1: Degradation factors C^W and C^F vs. orbital or Julian Day of the satellite

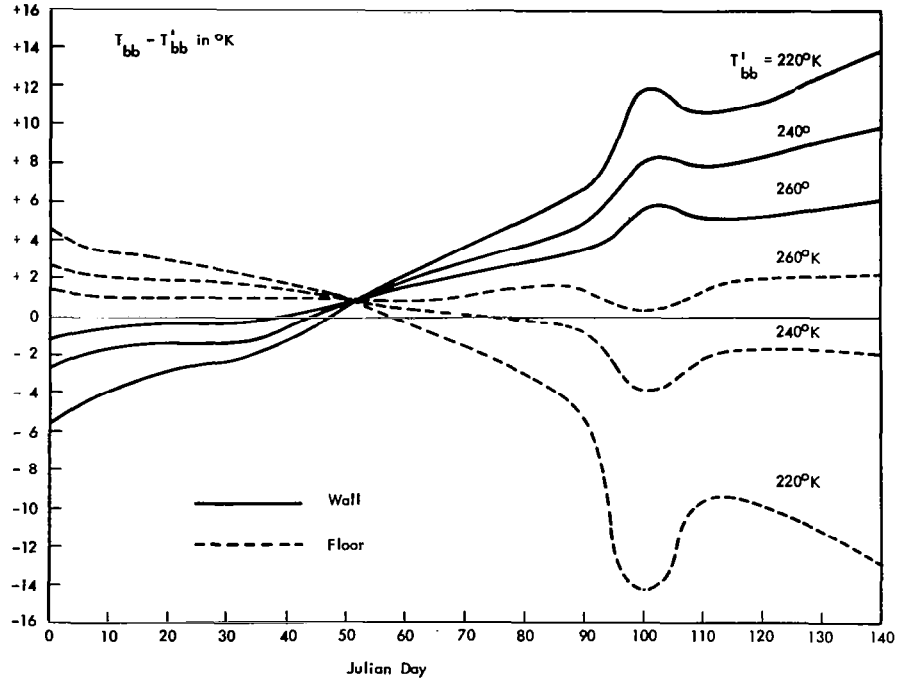

Fig.3.5: Temperature corrections $\Delta T = T_{bb} - T'_{bb}$ for channel 1.

An equivalent black body temperature measurement $T_{b'b}$ should be corrected by adding the ΔT-value corresponding to the appropriate orbital day.

the maps of the mean relative humidity etc. presented below, therefore may show the correct distribution although the quantitative data still may contain some uncertainties.

4.o MEAN RELATIVE HUMIDITY OF THE UPPER TROPOSPHERE AND SURFACE TEMPERATURE

In this chapter are shown maps of "monthly averages" of the mean relative humidity and of the surface temperature. These"monthly averages" were determined from all orbits measured during the period of one month (2.3). Corresponding maps for only 1o-day periods are shown in the Appendix A 1.

4.1 Quasi-global distributions of the mean relative humidity and of the surface temperature

The maps in Figs.4.1 - 4.1o show the horizontal distributions of the mean relative humidity of the upper troposphere and of the (effective) surface temperature on the earth between 55°N and 55°S. Isolines for the humidity were plotted for 1o, 2o, 4o, 6o and 8o %, those for the surface temperature for every 1o degrees. Stippled areas design areas over which no measurements were made from TIROS IV during each particular month.(See pages 28-37)

The isolines were plotted with the computer using a filter function which averages in a field of 3x3 grid points. By this disturbances with a "wavelength" which approximately is shorter than the distance between two grid points are attenuated. The weighting factors of the value of each grid point are given in the following matrix:

$$\begin{array}{ccc} \frac{1}{24} & \frac{1}{12} & \frac{1}{24} \\ \frac{1}{12} & \frac{1}{2} & \frac{1}{12} \\ \frac{1}{24} & \frac{1}{12} & \frac{1}{24} \end{array}$$

Here the weighting factor of the value of the central point is $\frac{1}{2}$. The sum of all factors is 1.

Generally the maps of the mean relative humidity show distributions which have been expected from the knowledge of the general circulation in the upper troposphere. Similar distributions also have been found by LONDON and TELEGADAS (1954) and by MANABE, SMAGORINSKY, and STRICKLER (1965).

Persistent moist areas (r.h. > 60%) occur in the tropics over the Western Pacific (over Malaysia and Indonesia during February and during June mainly over the monsoon areas of South and South-East Asia), over South America and over Central Africa. These areas known to be areas of high precipitation (e.g. in the maps of precipitation by MÖLLER, 1950) belong to the intertropical convergence zone. Here the upward motions of air cause upward water vapor transport and also condensation. Therefore mainly temperatures of high clouds have been measured which occur as cold areas in the maps of the surface temperatures. The latitudinal migration northward from winter to summer solstice is well recognized, particularly from April to May.

High values of the relative humidity (and low values of the surface temperature) have been found also along the polar frontal zones of both hemispheres. Both are caused by a high cloudiness in these areas.

The subtropical belts over both hemispheres occur

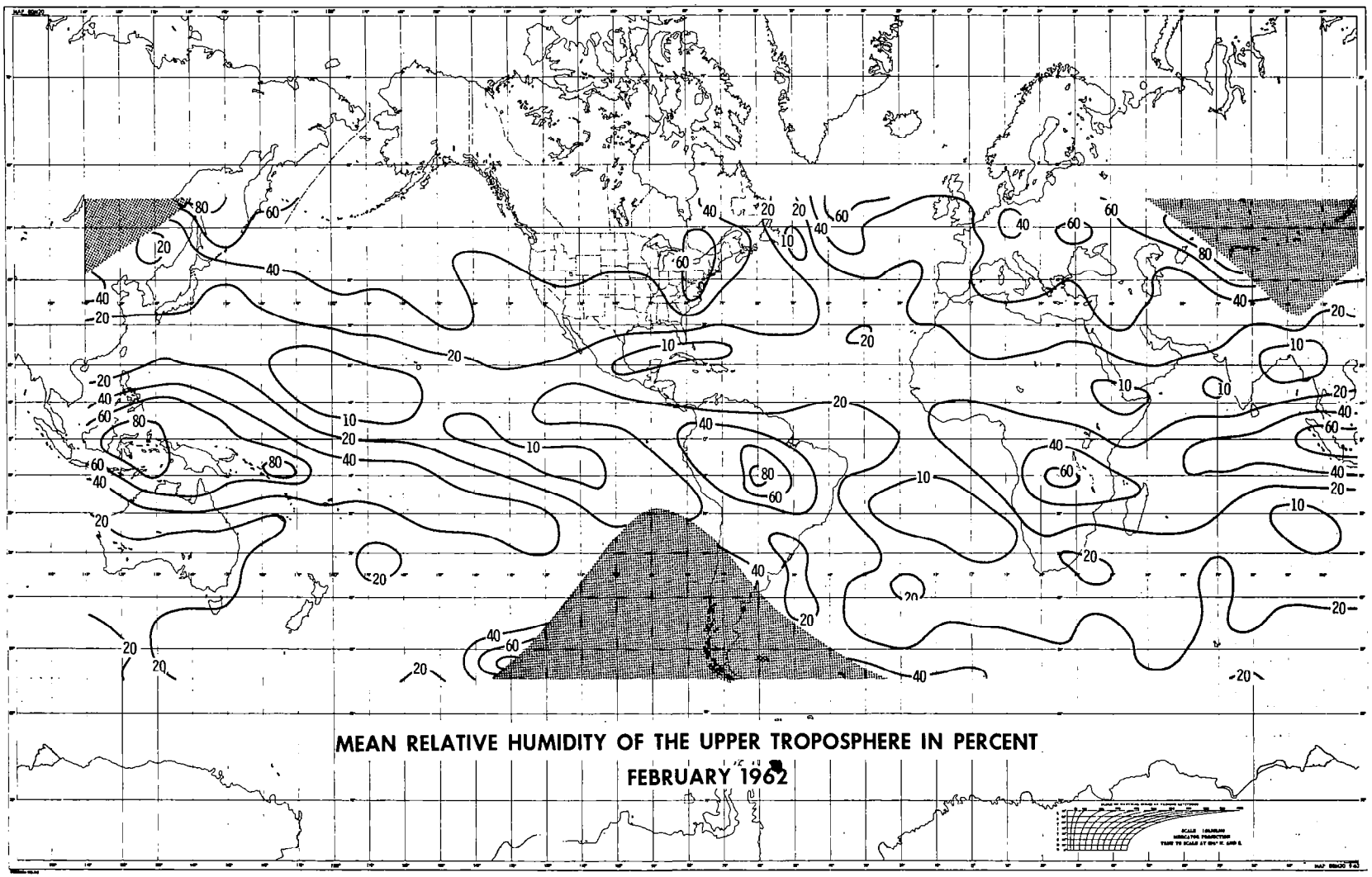

Fig. 4.1 : Quasi-global distribution of the mean relative humidity of the upper troposphere for February 1962

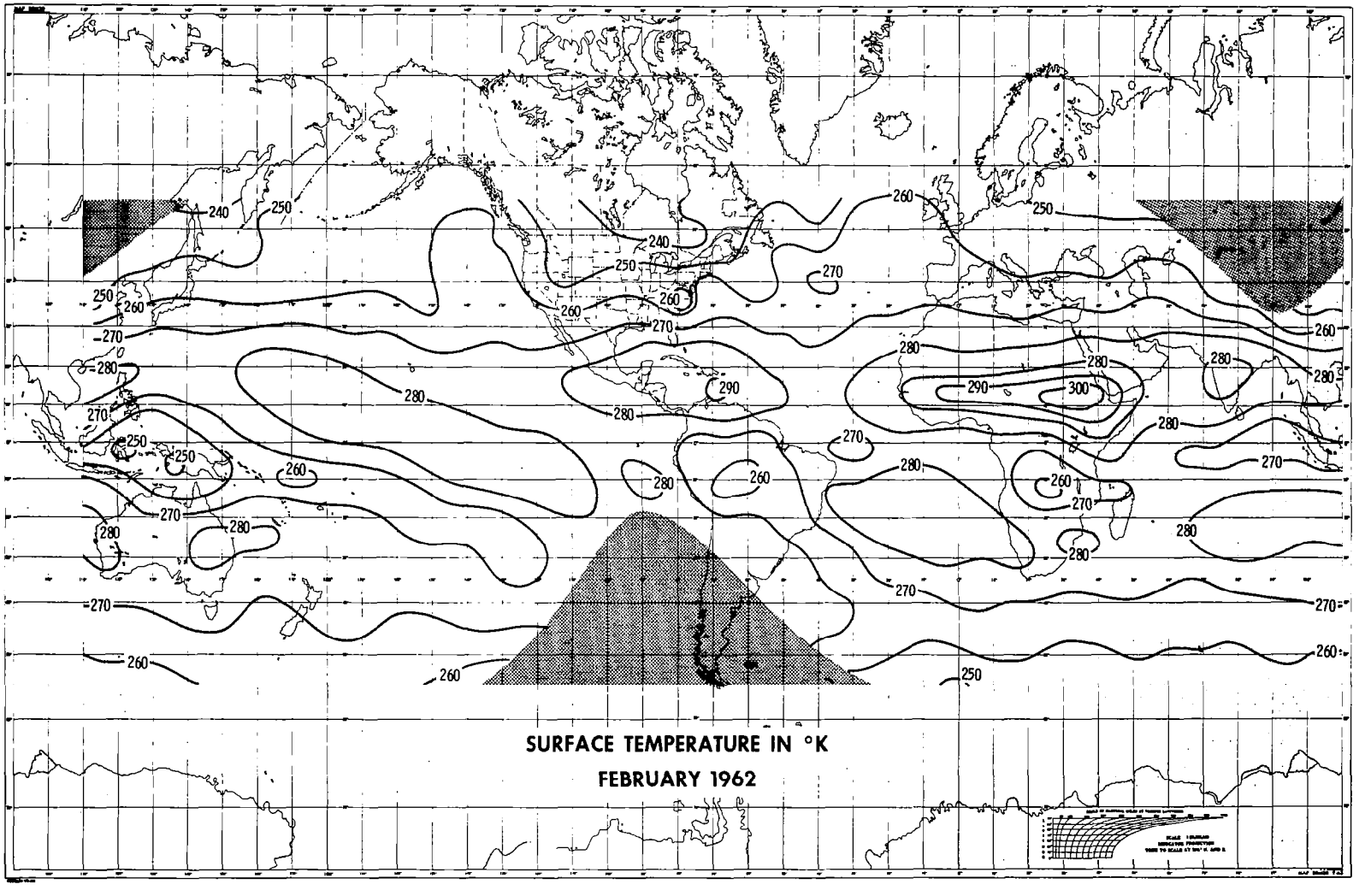

Fig. 4.2 : Quasi-global distribution of the (effective) surface temperature for February 1962.

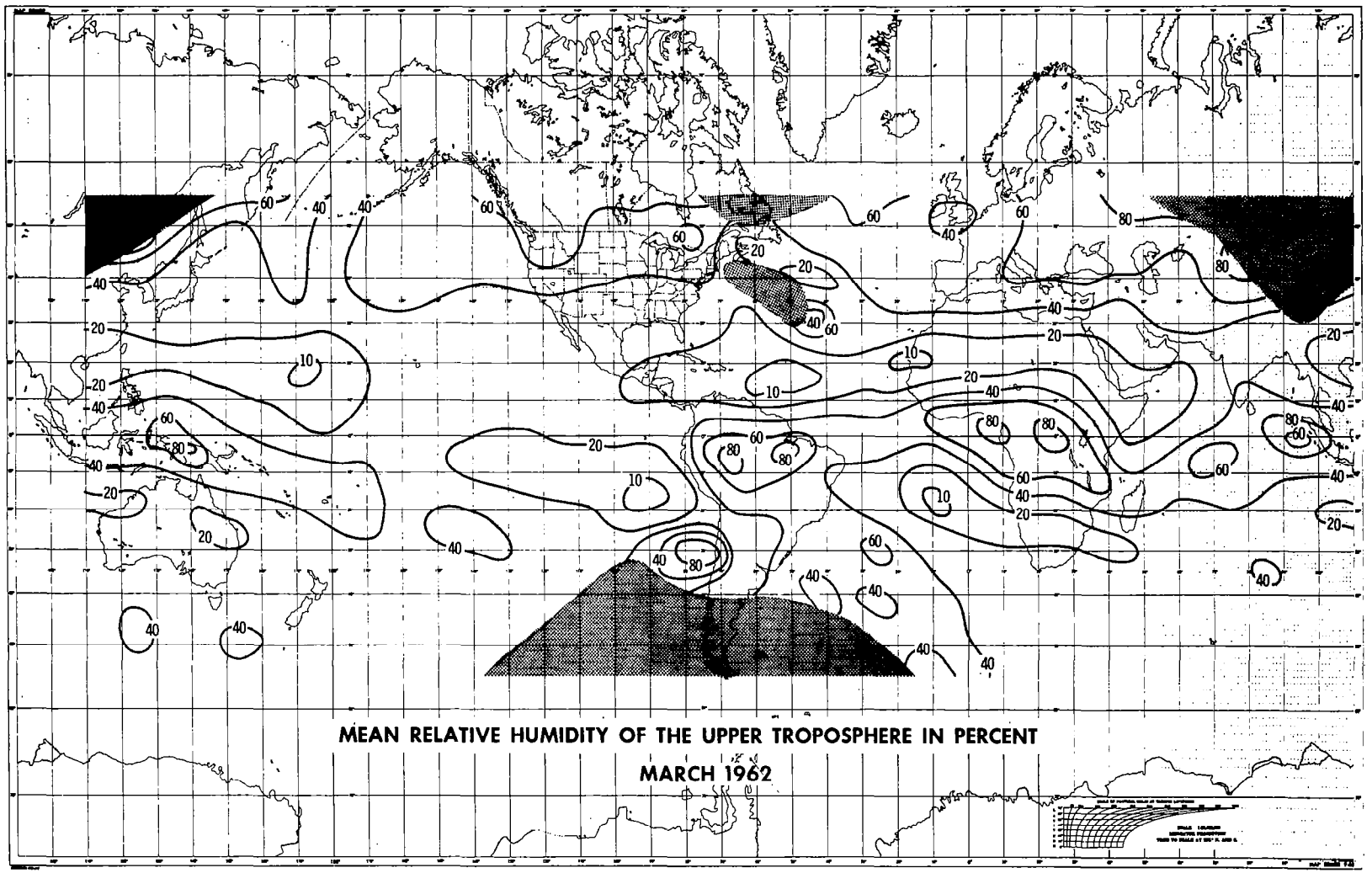

Fig. 4.3 : Quasi-global distribution of the mean relative humidity of the upper troposphere for March 1962

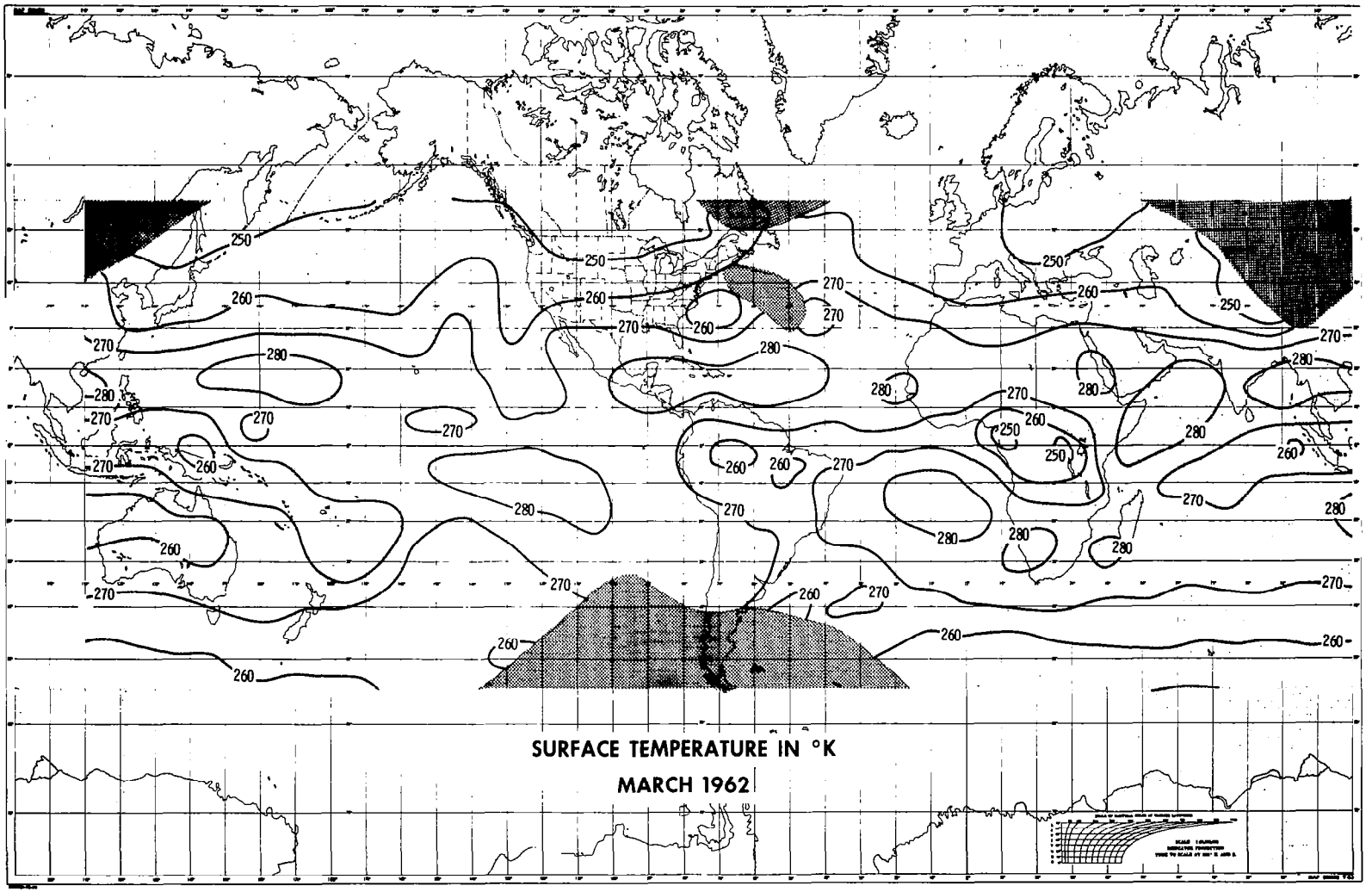

Fig. 4.4 : Quasi-global distributuon of the (effective) surface temperature for March 1962

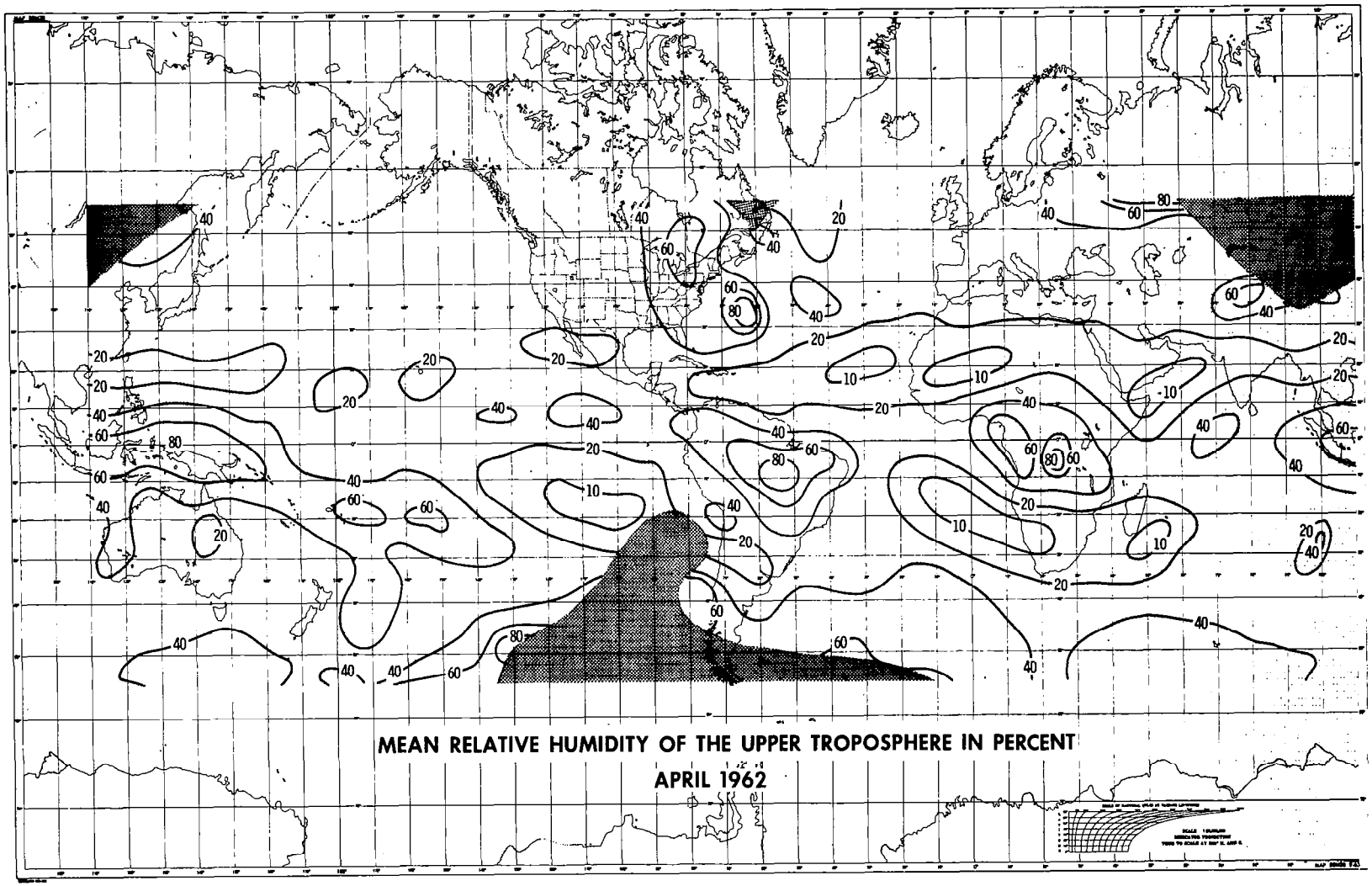

Fig. 4.5 : Quasi-global distribution of the mean relative humidity of the upper troposphere for April 1962.

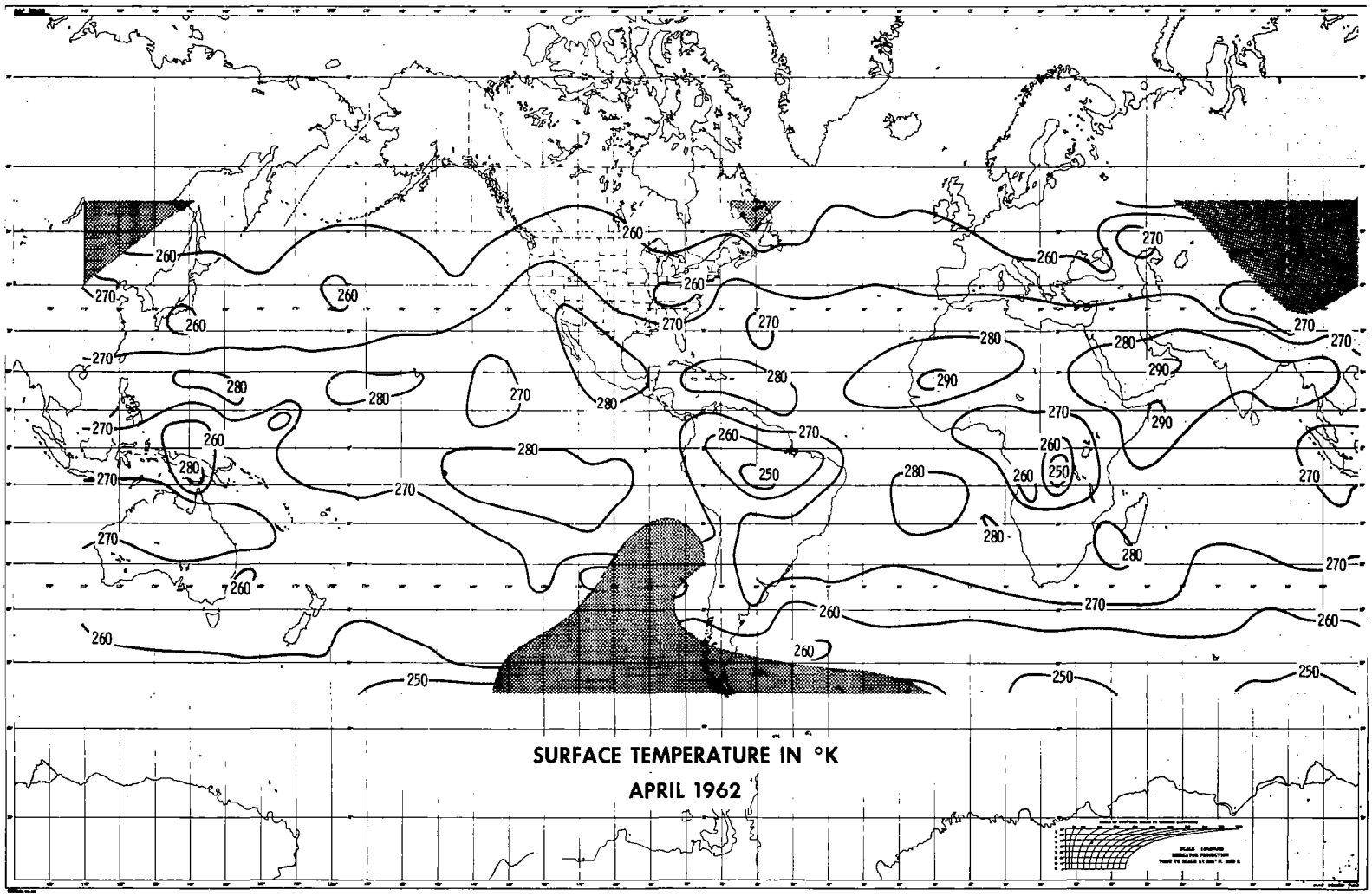

Fig. 4.6 : Quasi-global distribution of the (effective) surface temperature for April 1962.

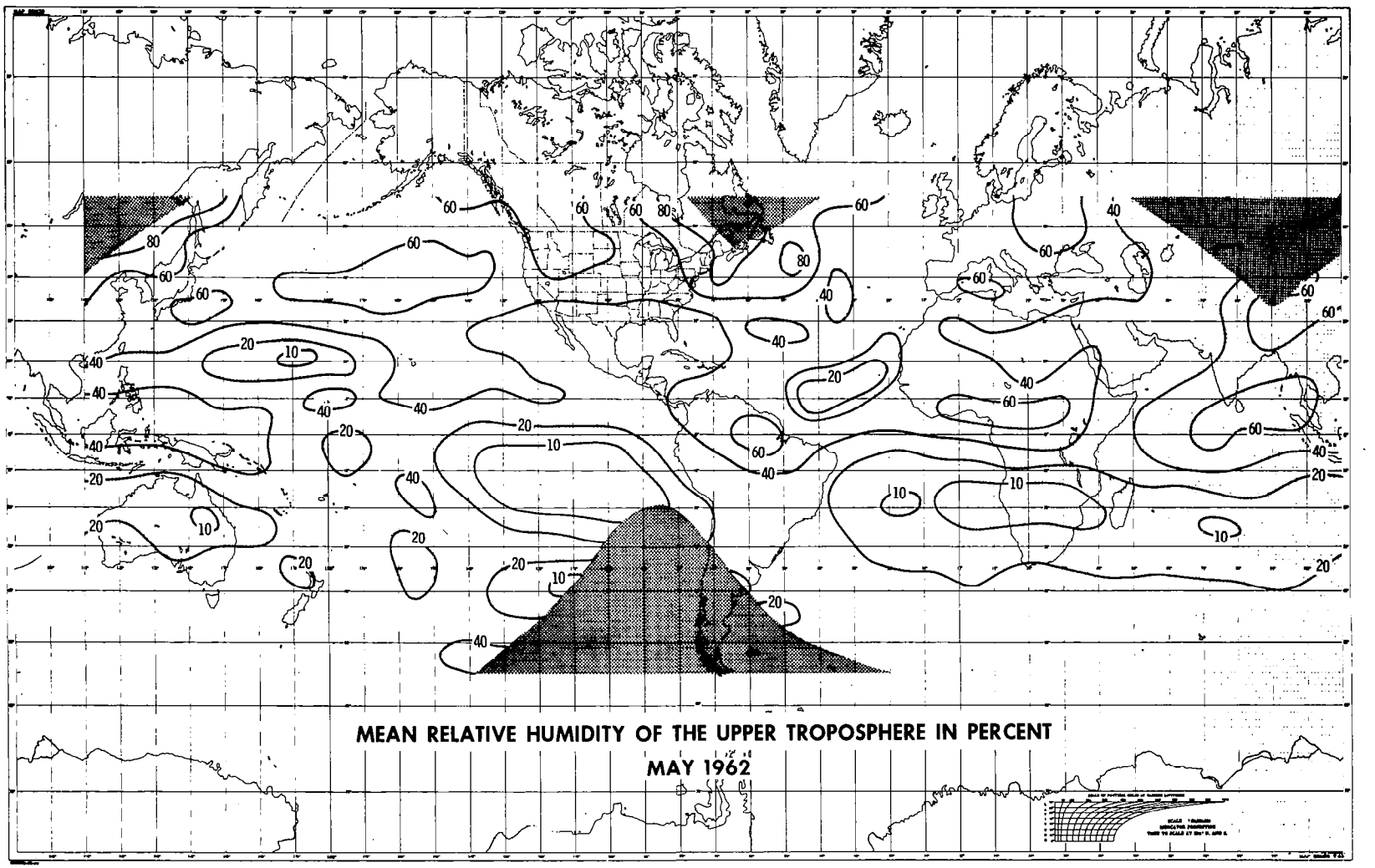

Fig. 4.7 : Quasi-global distribution of the mean relative humidity of the upper troposphere for May 1962.

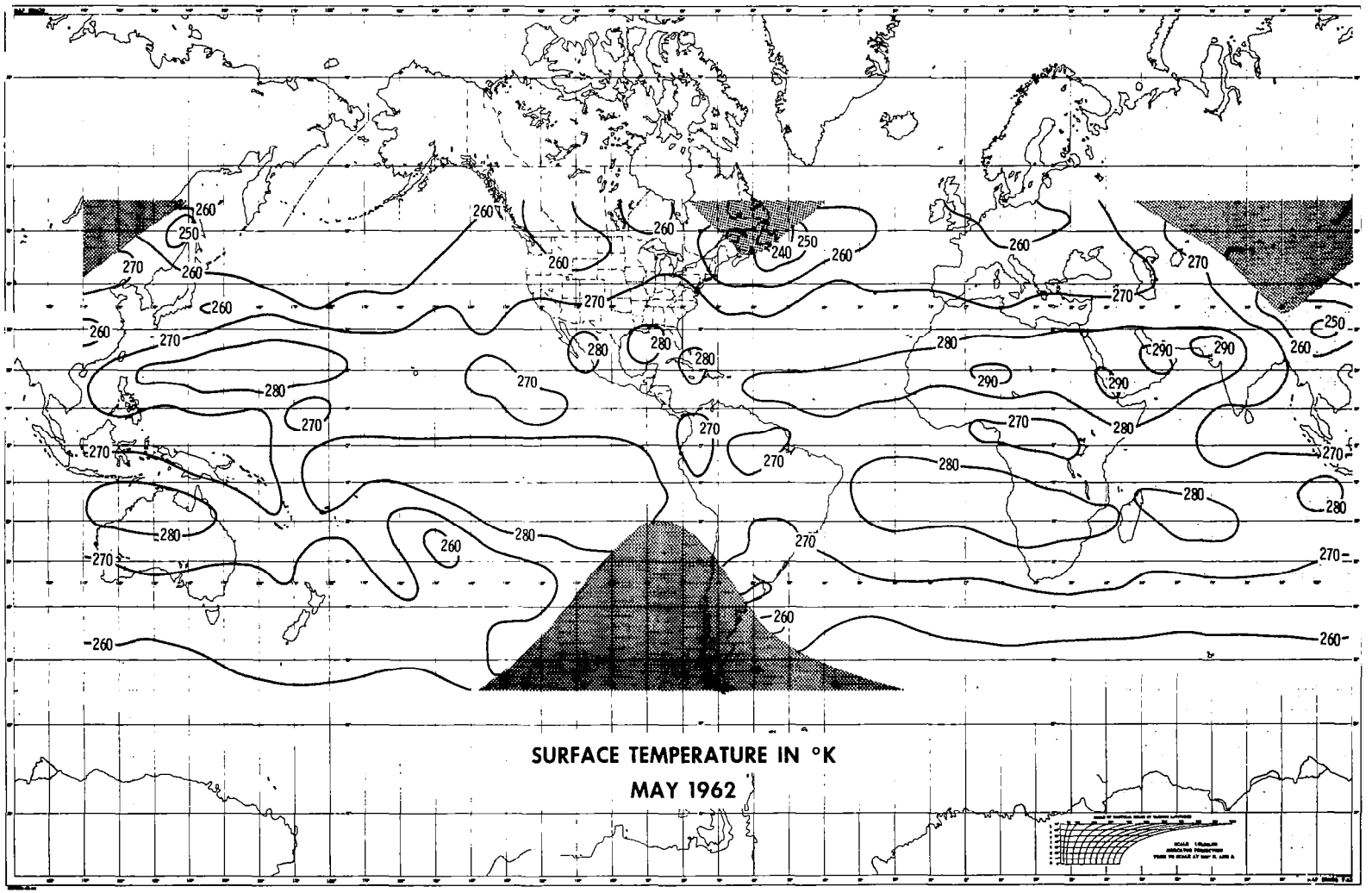

Fig. 4.8 : Quasi-global distribution of the (effective) surface temperature for May 1962.

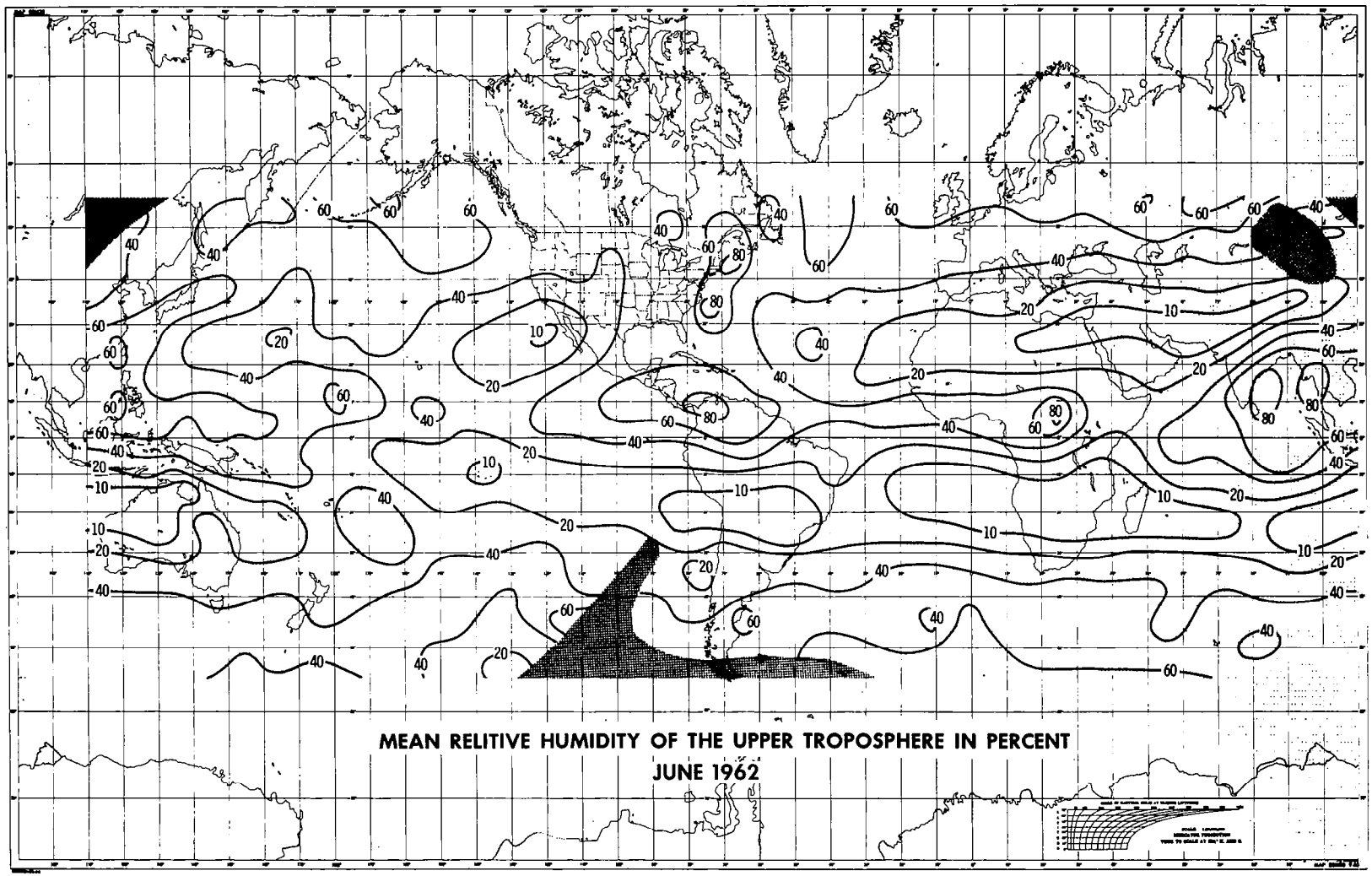

Fig. 4.9 : Quasi-global distribution of the mean relative humidity of the upper troposphere for June 1962.

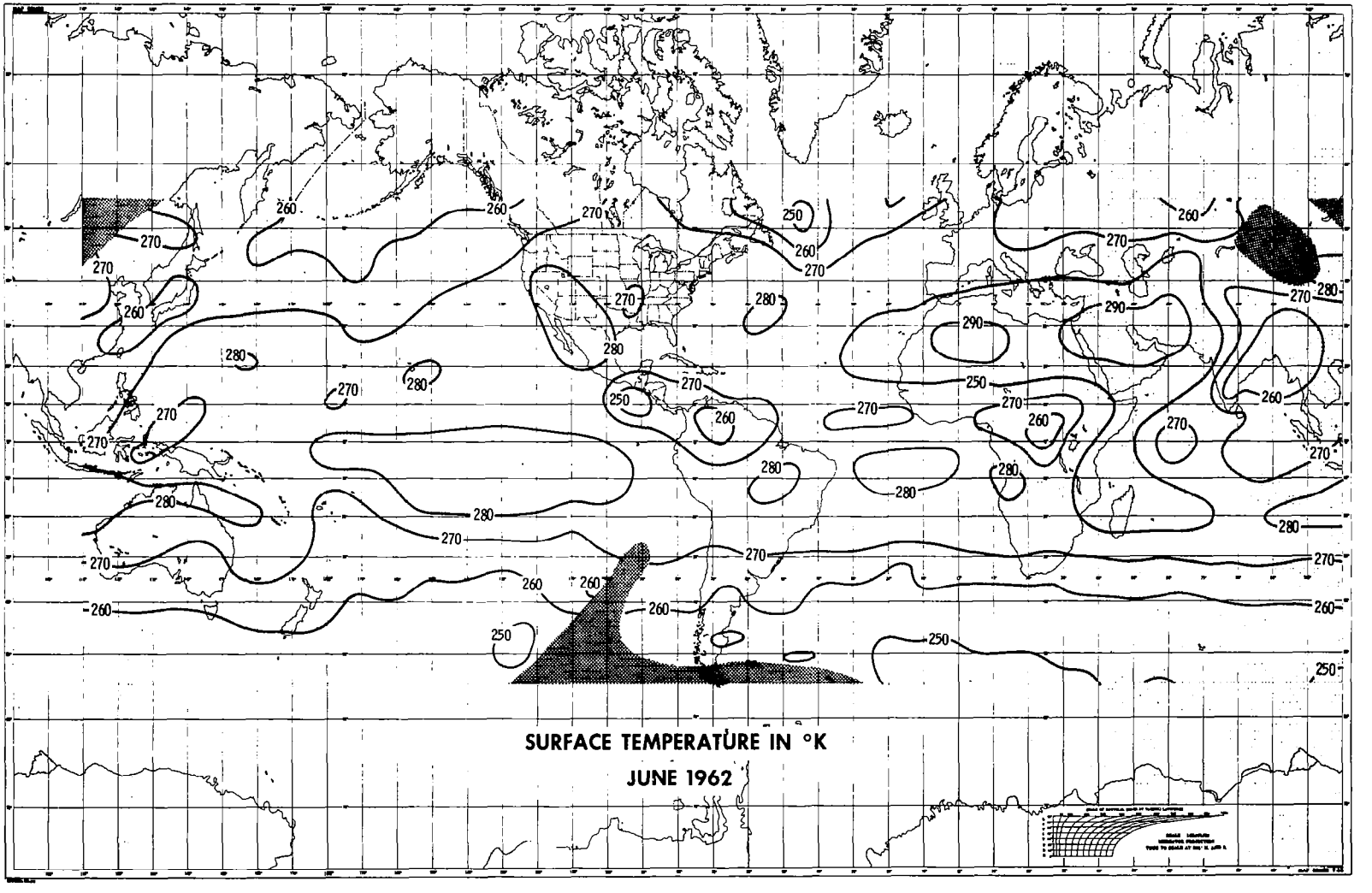

Fig. 4.1o : Quasi-global distribution of the (effective) surface temperature for June 1962.

as areas of low relative humidity. Over several areas values of less than 1o % have been found. These low values agree well with very accurate radiosonde soundings made by MASTENBROOK (1965) over the Kwajalein Atoll in November 1963. There MASTENBROOK found a very dry upper troposphere between about 3oo and 6oo mb (r.h. less than 5 %), which is that region of the upper troposphere from which channel 1 primarily receives radiation. MASTENBROOK's measurements also showed that the region close to the tropopause is nearly saturated. Since, however, channel 1 primarily measures radiation emitted in lower layers (Fig.2.3, page 9) that moist layer does not influence remarkably the upward going radiation in this spectral range.

Over the subtropics of both hemispheres surface temperatures are generally higher than those in the tropics. Over the oceans e.g. they are only about 12-17°K lower than climatological values of the water surface temperatures indicating low clouds or a small mean cloudiness during the period of one month.

Remarkable high temperatures have been found in February over Ethiopia and over the Sudan, although in other months highest values occur mainly over the deserts of North-Africa and Arabia. Probably during February TIROS IV observed the former areas mostly during day while the Sahara was observed mostly during night, thus simulating a geographic distribution from influences of the daily variation.

In order to show the temporal changes of both quantities, the relative humidity and the surface temperature, zonal averages of all data along a grid point line for ten-day periods have been calculated

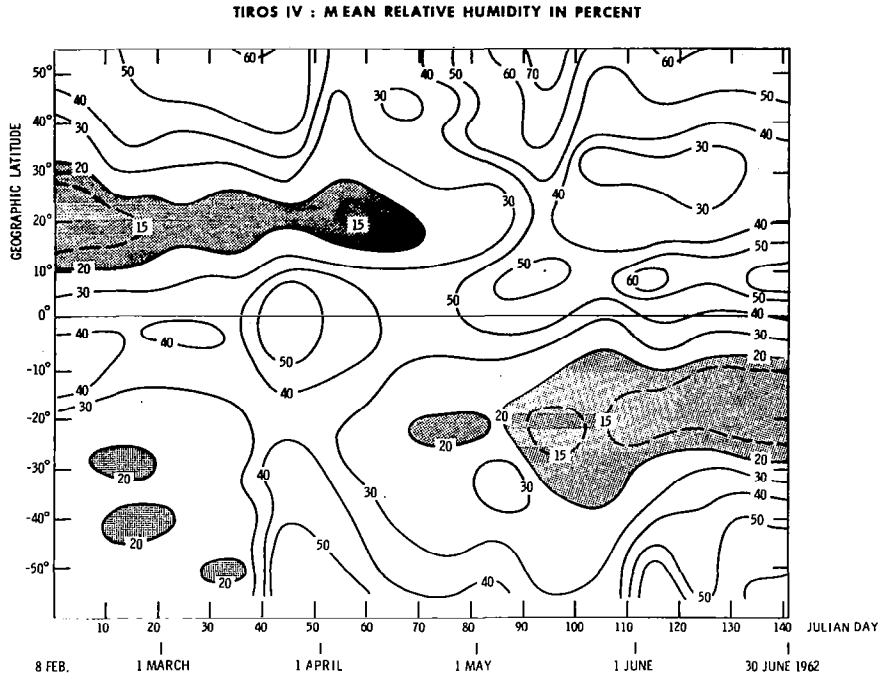

Fig.4.11: Zonal averages of the mean relative humidity for 10-day periods

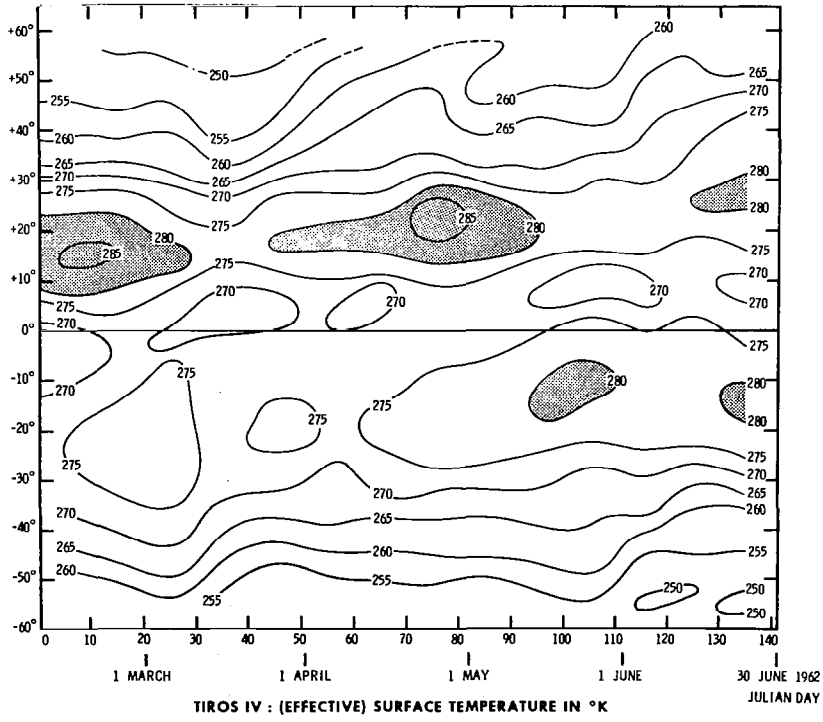

Fig.4.12: Zonal averages of the (effective) surface temperature for 10-day periods

and plotted in dependence on latitude and on time in Figs.4.11 and 4.12. In both figures the intertropical convergence zone occuring with high values of the relative humidity (4o-6o%) and low temperatures (less than 27o°K) moves in the average with season from the Southern on to the Northern Hemisphere. The subtropics over the winter hemispheres are dryer (r.h. < 15%) than over the summer hemispheres. Due to the different dimensions of land and ocean covered areas over both hemispheres the subtropics over the Northern hemisphere are about 5-8°K warmer than over the Southern hemisphere.

4.2 Discussion of the results

4.2.1 Correlation between values of the mean relative humidity and of the surface temperature

Comparisons of maps for the mean relative humidity with those for the surface temperature in the corresponding month show that in many cases areas with high relative humidity coincide with those of low temperatures and vice versa. This would suggest that generally the relative humidity of the troposphere above high clouds is high (MÖLLER and RASCHKE, 1963).

To check this the coefficient of linear correlation R has been calculated correlating both quantities, using values which were determined for each orbit separately as desribed in chapter 2.3. For all data of March 1962 R =-o.54. It is smaller (R = -o,35), if only values for lower clouds ($T_{surf.}$ - 27o°K) were accounted for, because then all measurements over high clouds (and possibly also over cirrus layers) were omitted. These small numbers show, that the correlation is smaller as

relative humidity in %	surface temperature in °K											
		LESS THAN 211	211 – 22o	221 – 23o	231 – 24o	241 – 25o	251 – 26o	261 – 27o	271 – 28o	281 – 29o	291 – 3oo	3o1 – 31o	GREATER THAN 31o
	4–1o	o	o	928	1124	1o47	1893	3855	1oo19	13661	1o96	127	o
	1o–2o	o	o	298	733	1664	4334	8499	14964	17462	1338	215	o
	21–3o	o	o	o	1188	1581	3973	6974	9136	58o9	419	56	1o
	31–4o	o	o	o	75o	1668	3825	6o58	5681	2473	218	o	5
	41–5o	o	o	o	778	1557	355o	4376	3o92	1o26	99	o	o
	51–6o	o	o	o	92o	1449	2592	2666	1979	614	31	o	1o
	61–7o	o	o	o	765	1114	2315	2322	1131	322	19	o	5
	71–8o	o	o	o	643	743	22o8	97o	948	268	21	o	o
	81–9o	o	o	o	774	958	1324	1711	8o1	98	o	o	o
	91–99	o	6	894	1268	7964	7634	3867	1139	167	15	o	o

Fig.4.13: Scatter diagram of values of the mean relative humidity and of the surface temperature (March 1962)

it might be expected by a first comparison of the maps.

In a scatter diagram (Fig.4.13) this small correlation is demonstrated again.

Although a large number of values (from 2oo, 284 grid points) were correlated the correlation coefficient still may contain uncertainties which are caused by the low accuracy of measurements. The rather high noise level may still have some influence on the scattering of the results as shown in Fig.4.13. Therefore these investigations should be repeated with more and more accurate data which might be available in a short time from the Nimbus II MRIR measurements. Comparisons with accurate simultaneous measurements of the water vapor concentration above clouds made from airplanes or other platforms are desirable.

4.2.2 Reliability of the results

To get an idea on the reliability of the results shown in Figs.4.1-4.1o, quasiglobal distributions are shown in the Figs.414-4.16 of (1) the number of orbits contributing to the "monthly average" in each grid point, and (2) variances S^2 of the mean relative humidity and of the surface temperature respectively. These quantities are presented here for March 1962.

As shown in Fig.4.14 only in a few areas the population numbers are high enough to consider the monthly averages as representative. These areas are located at mid latitudes of both hemispheres where the subsatellite paths overlap. (See page 43)

Areas close to the equator and in particular over the Atlantic Ocean, however, show populations of less than 1o. Here the averages can not be very representative.

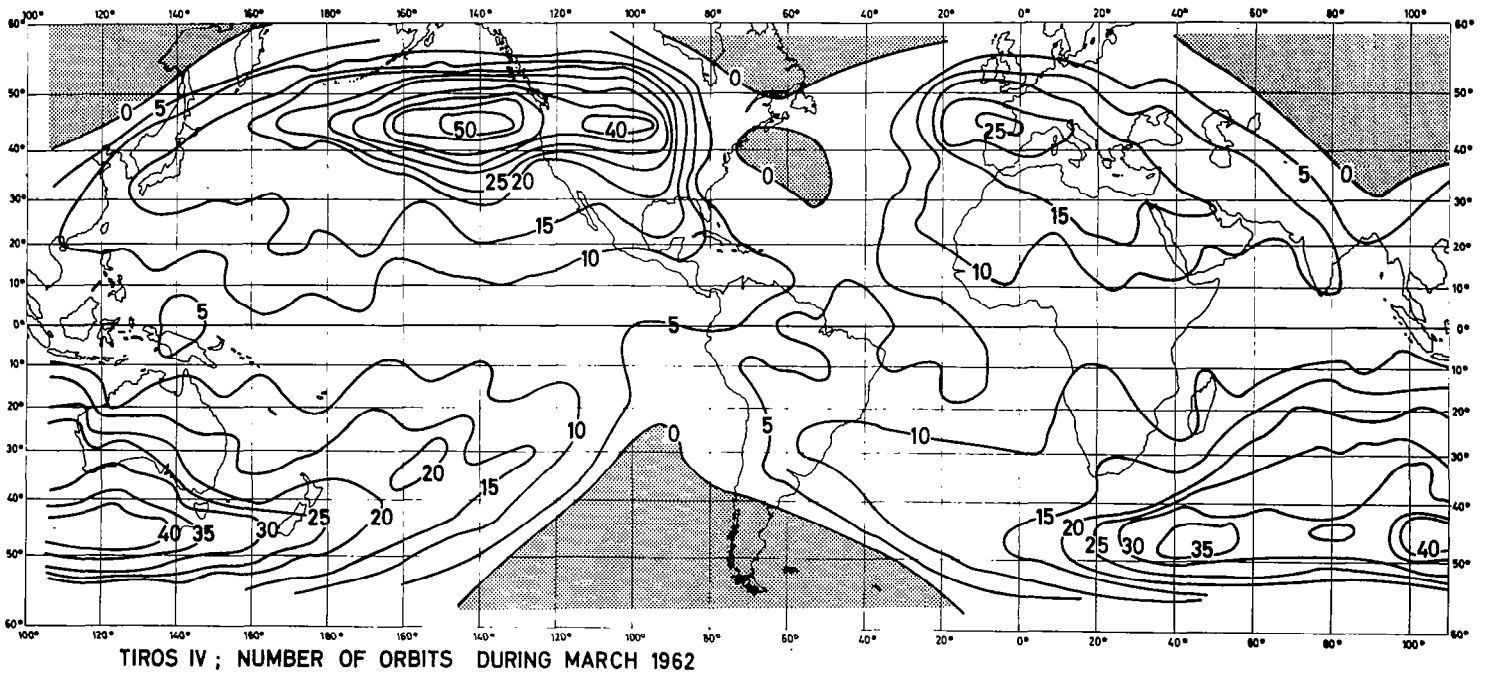

Fig.4.14: Number of orbits contributing to the monthly averages at each grid point during March 1962

Similar distributions of the population numbers of monthly maps also have been found for the other maps.

In the maps of variances S^2 (Figs.4.15 and 4.16) areas with high values of S^2 coincide once with those of high populations (Fig.4.14) but also with high relative humidity (Fig.4.2, page 23). Since the population at the grid points are not equal the interpretation of the pattern shown in Figs.4.15 and 4.16 is somewhat complicated: (see pages 45 and 46)

(1) Assuming very accurate measurements and equal populations everywhere on the maps, the variances S^2 would indicate the weather activity during March 1962 in any area. A high activity would have existed in regions close to the equator and at mid latitudes of both hemispheres. A less activity would have existed over the subtropical oceans particularly over the eastern sides of the subtropical highs in the Southern hemisphere. This can better be seen in the variance of the surface temperature than in S^2 of the relative humidity. The connection of large variance with high values of the relative humidity may also be explained purely statistically. High relative humidity does not mean that the air was permanently humid with little variance; there may have occured single cases or short periods with low humidity, too. This will result in a high variance. A very low mean humidity, however, prohibits by itself the occurance of cases with high humidity and thus a large variance.

(2) But the large values of S^2 also might be due to the large scattering of data of both channels

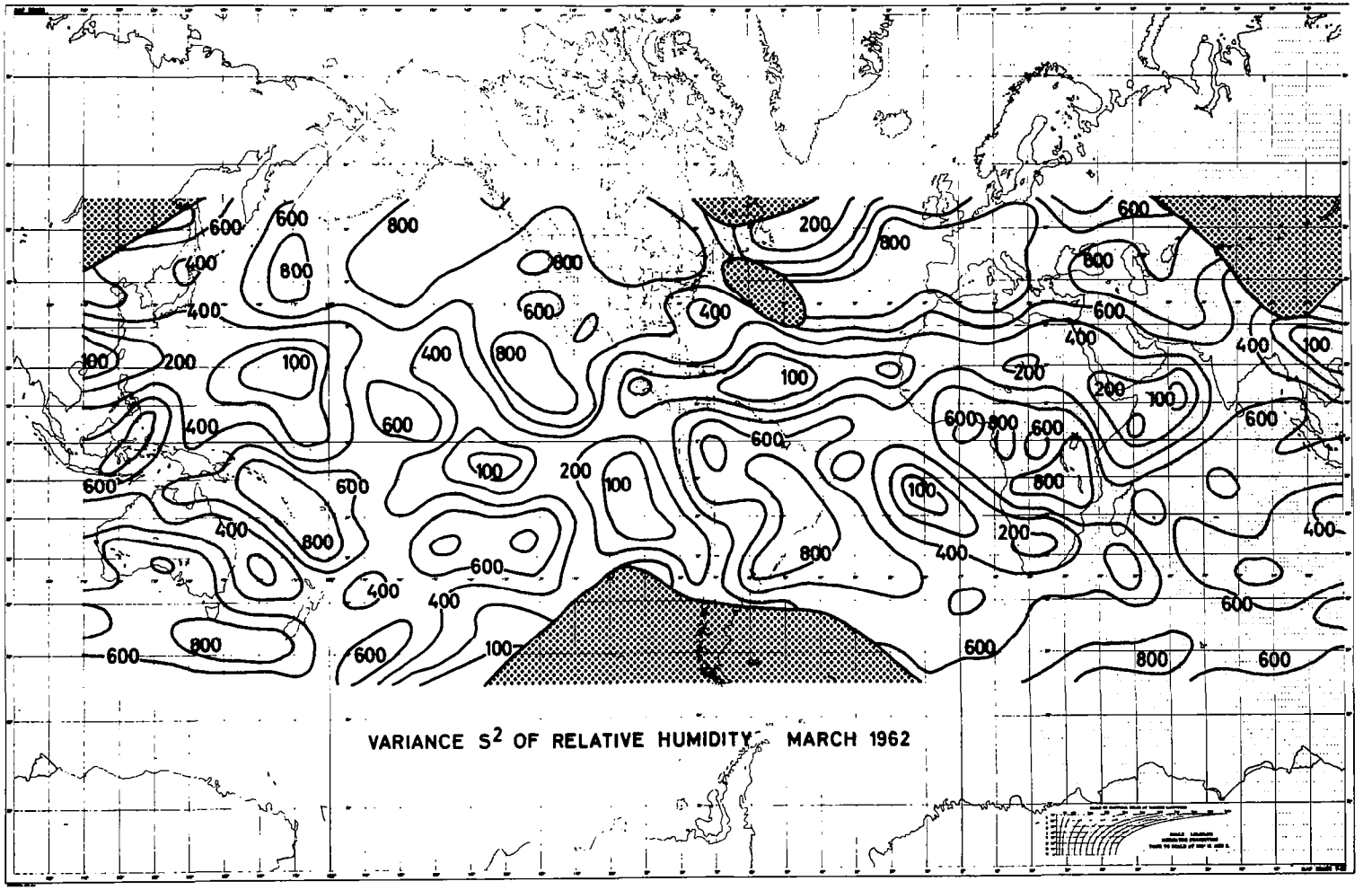

Fig.4.15: Variances S^2 (in per cent^2) of the mean relative humidity (March 1962)

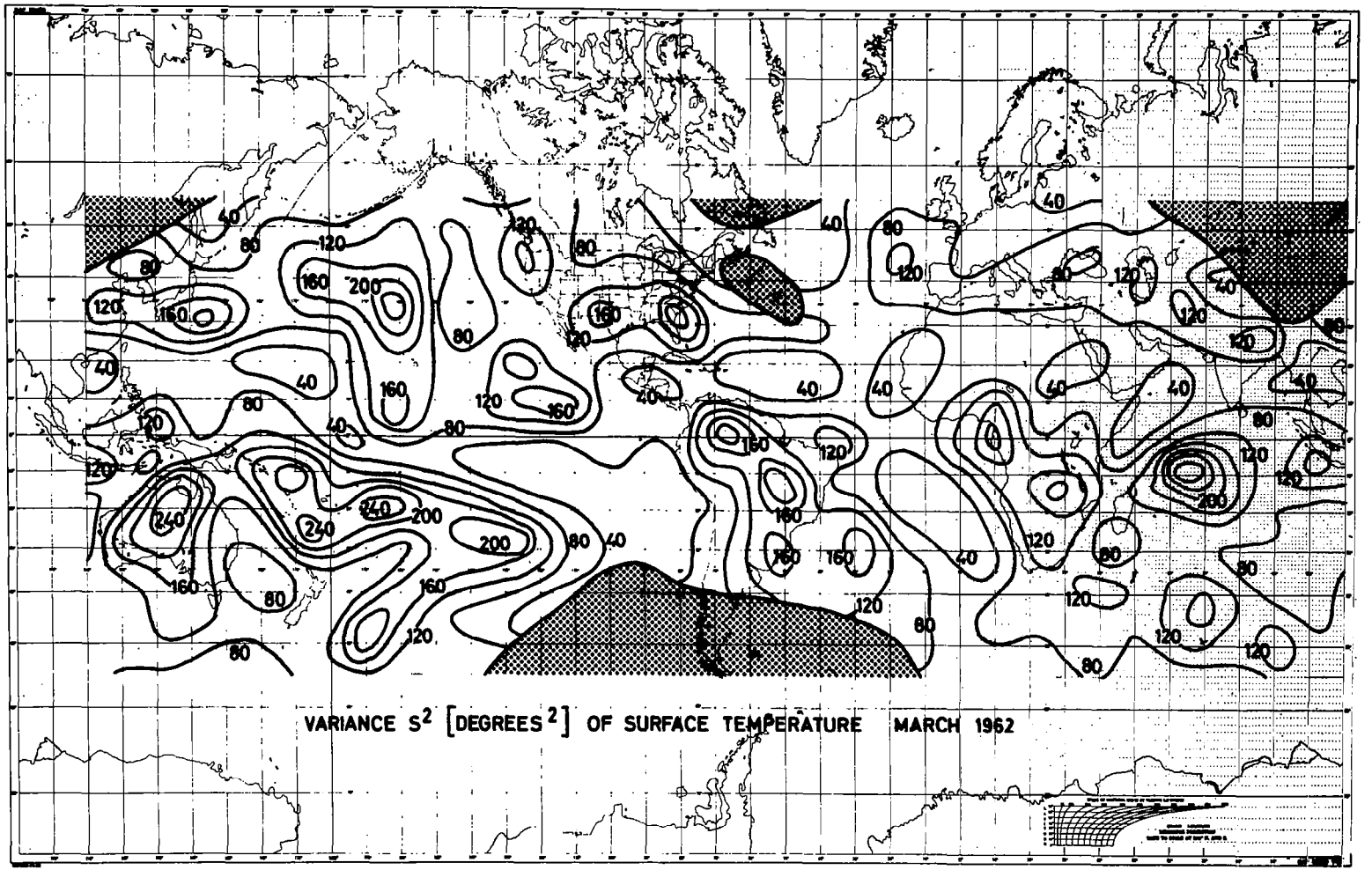

Fig.4.16: Variance S^2 (in degrees^2) of the (effective) surface temperature (March 1962)

which in particular is large at low values of equivalent black body temperature measurements. This might not yet sufficiently be smoothed out, when the averages for each gridpoint where calculated for each orbit separately (chapter 2.3). Otherwise the population numbers over most of the areas are too low to permit final conclusions. Therefore, the considerations made above should be considered to be preliminary ones.

5.o WATER VAPOR MASS ABOVE 5oo mb

5.1 Method of Determination

In the preliminary investigations in chapter 2.2 it has been shown that the values of the mean relative humidity are approximately representative for the region between about 2oo mb and 6oo mb. If the temperature profile in that layer is known the water vapor mass in columns above a certain level can be determined. But, up to now, accurate temperature profiles are not available for all grid points in a map covering the entire globe between 55°N and 55°S. Therefore only seasonable approximations given by climatological averages could be used.

In the profiles of the vertical temperature distribution by COLE and KANTOR (1963) the temperature gradient in the upper troposphere is about 5.5-7.o degrees/km. For these profiles and for the vertical water vapor distribution described in chapter 2.2 it can be shown that 9o % of the total water vapor mass in columns above the 5oo mb level are located in the layer between 2oo mb and 5oo mb. This holds also in cases of a very dry troposphere (r.h. less than 5 %). Then regardless of the profile, the total water vapor mass is a strong

function of the temperature at 5oo mb only if a constant value of the relative humidity in the troposphere prevails. In the assumed case of saturation of the troposphere this function can be expressed by the relations:

for $T \geq 253°K$ at 5oo mb:

$$\ln m = -29.24 + o.1o7 \cdot t \qquad (6)$$

for $T \leq 253°K$ at 5oo mb:

$$\ln m = -26.39 + o.o96 \cdot t$$

Here are t the temperature in °K at 5oo mb and m the water vapor mass in g cm^{-2}, ln is the logarithm of m on basis e.

There are two different relations since the vapor pressure has been determined for $T \geq 253°K$ over a water surface and for $T \leq 253°K$ over ice.

Now, from the temperature at 5oo mb the water vapor mass above 5oo mb can be determined for the case of saturation by one of the equations given above. Multiplication with a hundredth of the relative humidity yields the "correct water vapor mass". This method also has been used by BANDEEN et al. (1965).

Values of monthly averages of the temperature at 5oo mb were taken from the Monthly Climatic Data of the World (U.S.W.B.; 1962) and plotted in Figs.5.1-5.5. (see pages 49 - 53)

5.2 Maps of the water vapor mass above 5oo mb

From the monthly averages of relative humidity (Figs. 4.1 - 4.5) the distributions of water vapor mass shown in Figs.5.6 - 5.1o have been determined. Similarily

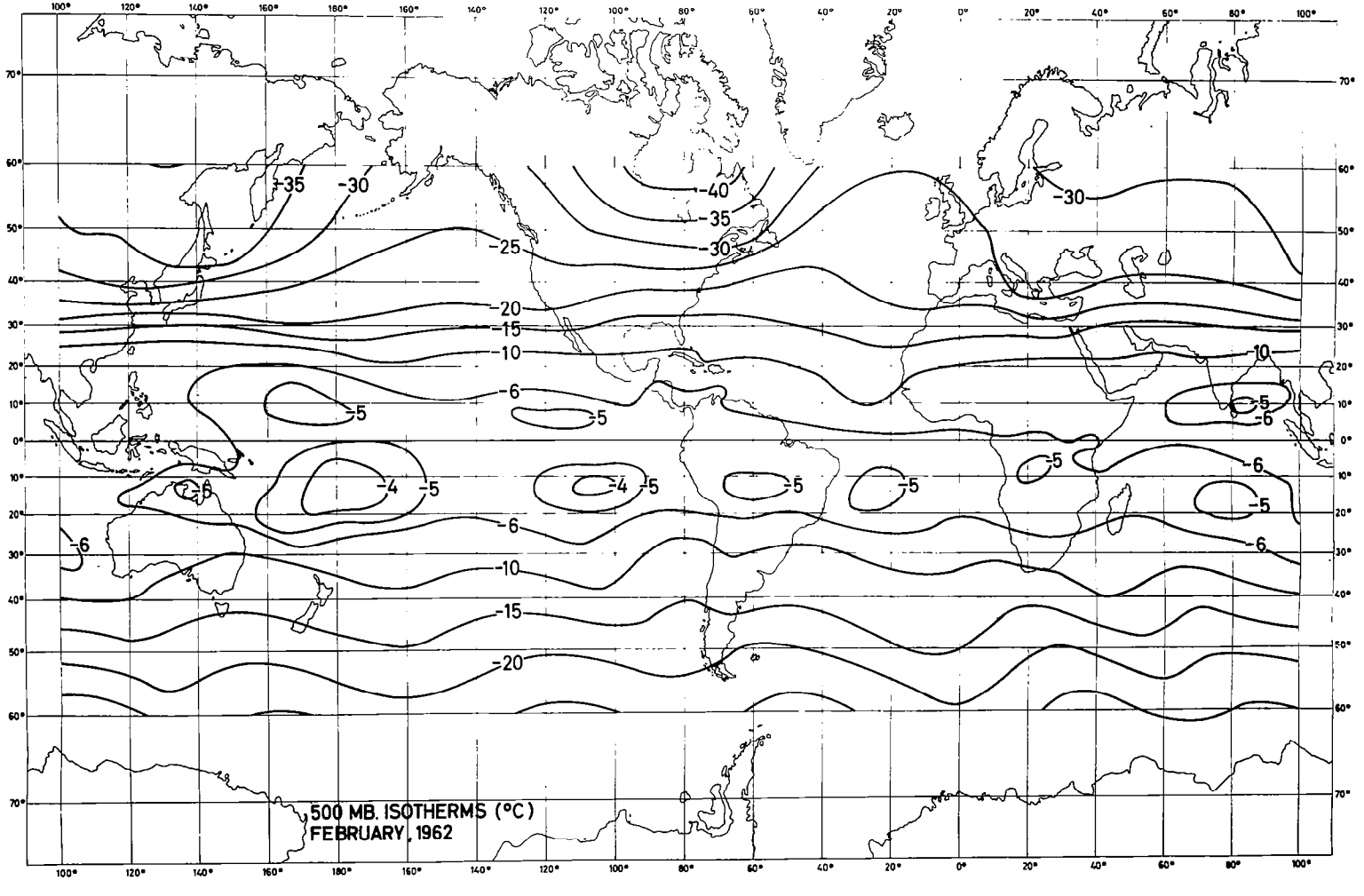

Fig.5.1: Monthly averages of the temperature at 500 mb for February 1962

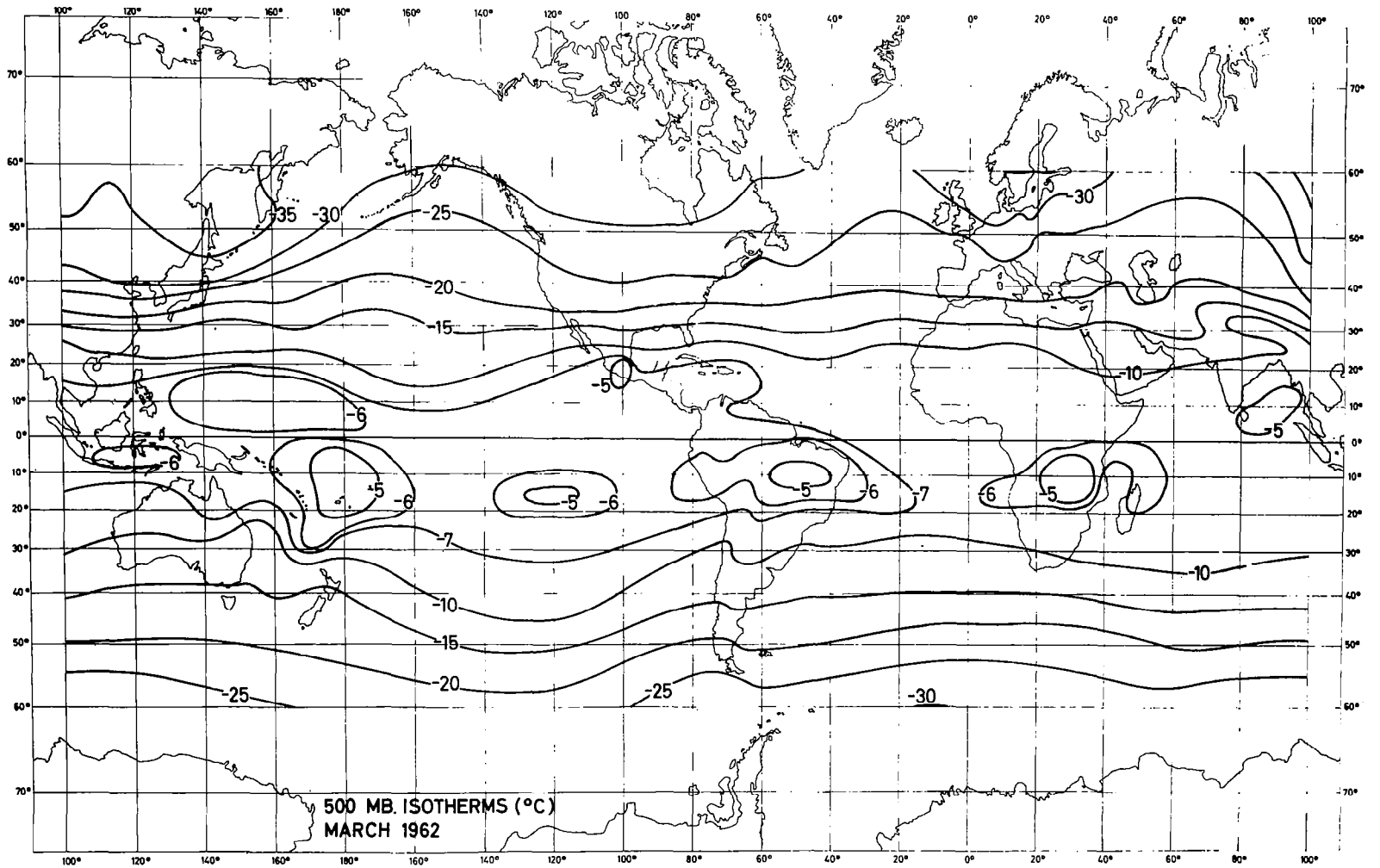

Fig.5.2: Monthly averages of the temperature at 500 mb for March 1962

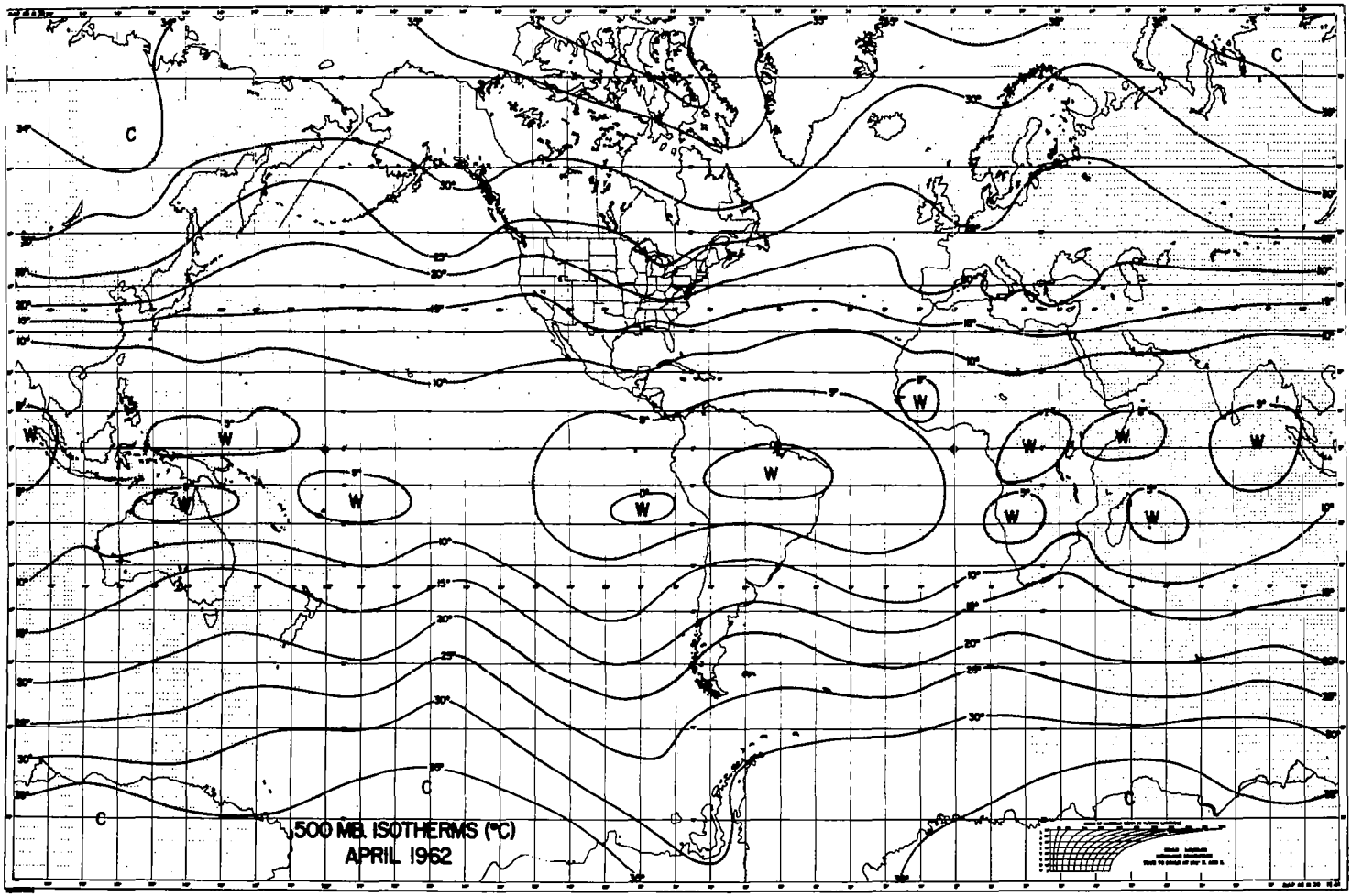

Fig.5.3: Monthly averages of the temperature at 500 mb for April 1962 (from BANDEEN et al., 1965)

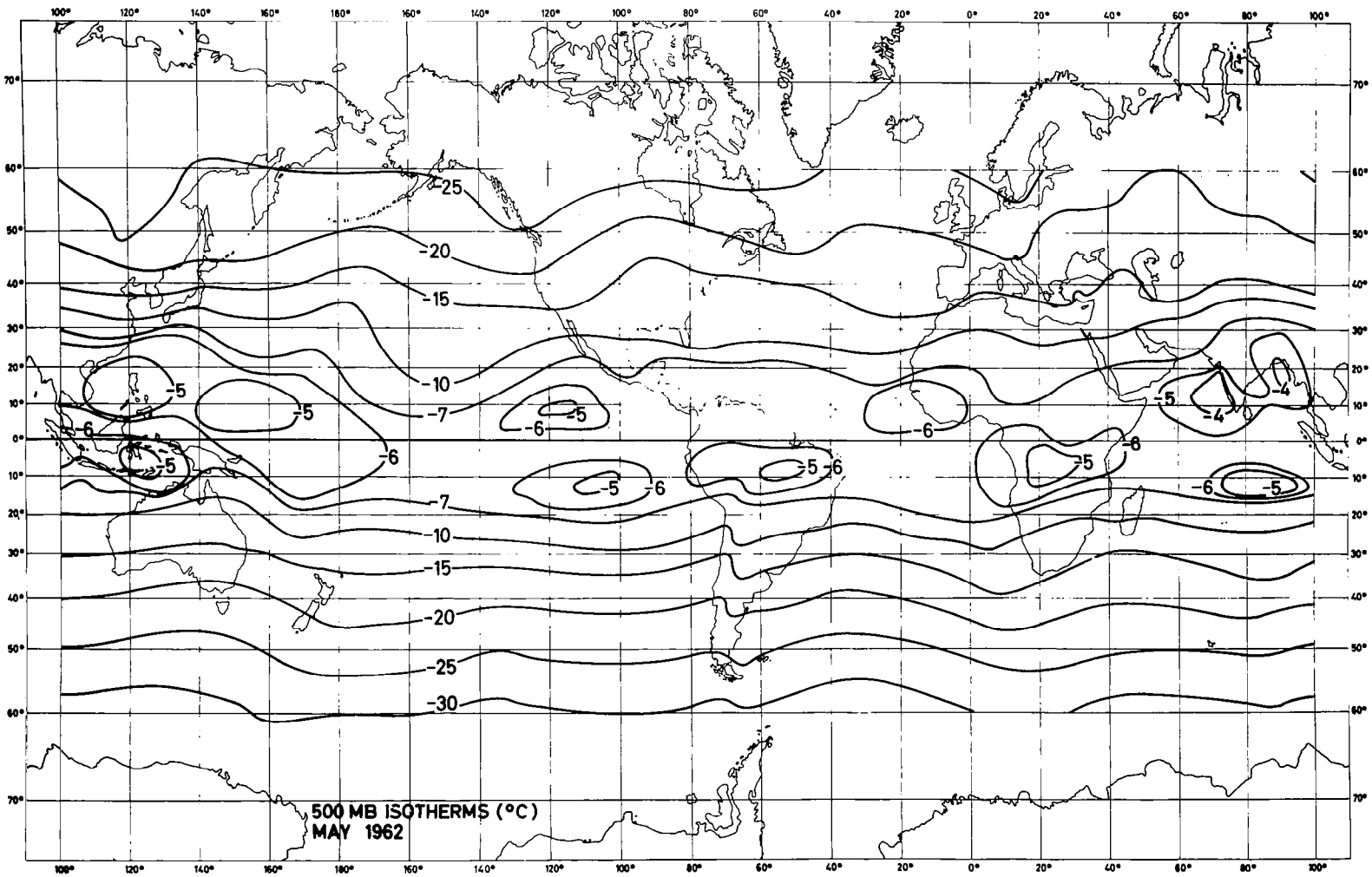

Fig.5.4: Monthly averages of the temperature at 500 mb for May 1962

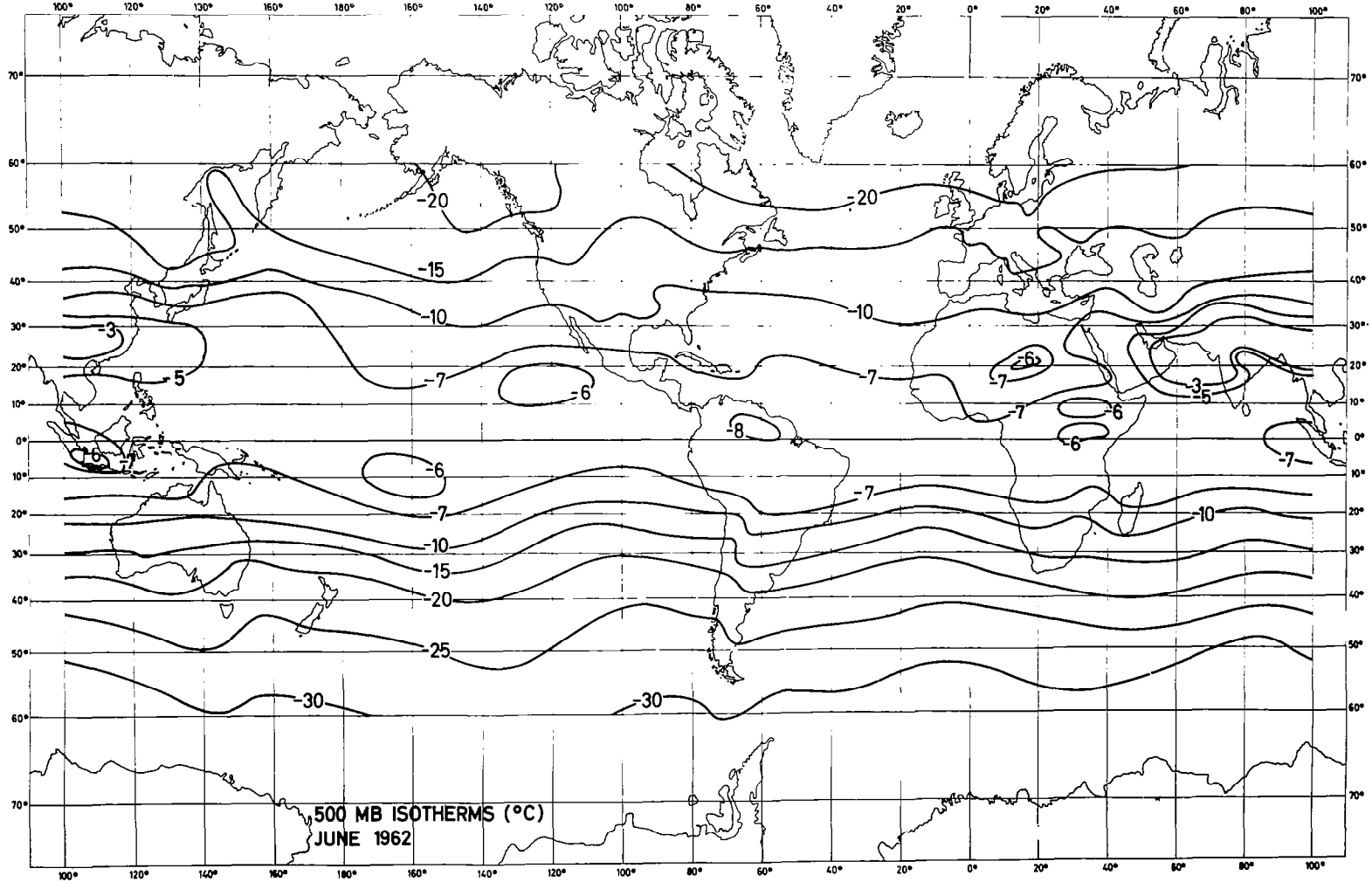

Fig.5.5: Monthly averages of the temperature at 500 mb for June 1962

also from the ten-day averages of the relative humidity (see Appendix A 1) the water vapor distribution for ten-day periods (shown in Appendix A 2) have been calculated, where, however, the monthly averages of temperature at 5oo mb must have been used, since ten-day averages were not available.

Generally the horizontal distributions of the water vapor mass in Figs.5.6 - 5.1o show a pattern which is similar to that of the temperature. Both quantities decrease from the meteorological equator in polward direction. Highest amounts of water vapor of more than o.3 g cm^{-2} have been found over regions known as such of highest precipitation. Those are South-East Asia (varying with Monsoon-period), South-America and Central Africa. (see pages 55 - 59)

Zonal averages (again for ten-day periods) also show the temporal changes of water vapor mass in each latitude. They are drawn in Fig.5.11 in dependence on the latitude and on time. (see page 6o)

BANNON and STEELE (196o) determined the water vapor mass in columns above 5oo mb from British radiosonde measurements from the years 1951-1955. Their results agree satisfactorily with those shown above.

6.o CONCLUSIONS

Based on model assumptions on the vertical distribution of water vapor, temperature and clouds (and also CO_2 and O_3) the following quantities have been determined from TIROS IV measurements of the infrared radiation in the spectral regions between 5.8 and 6.8 μ and between 8 and 13 μ:

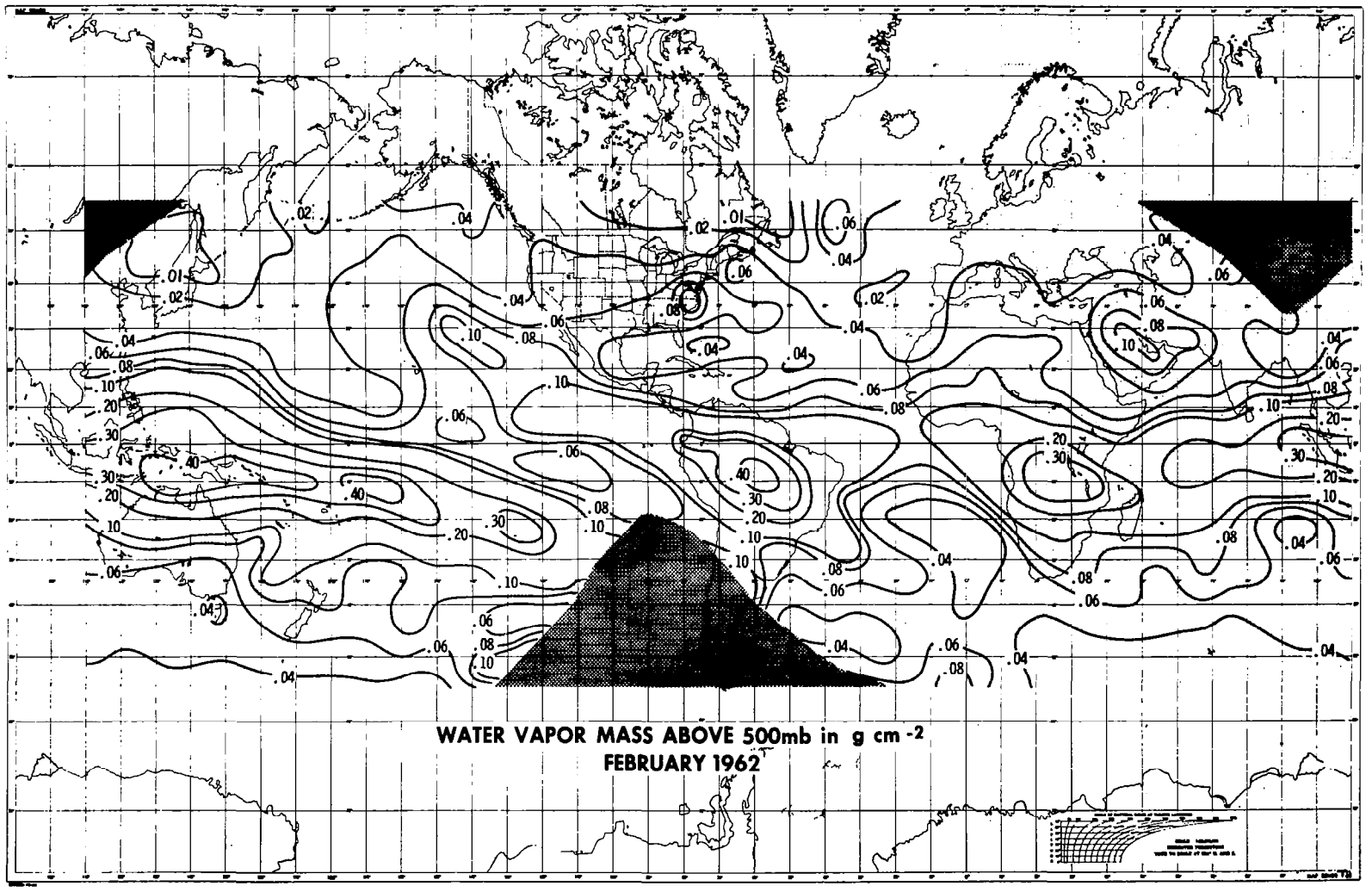

Fig.5.6: Quasi-global distribution of the water vapor mass above 5oo mb for February 1962

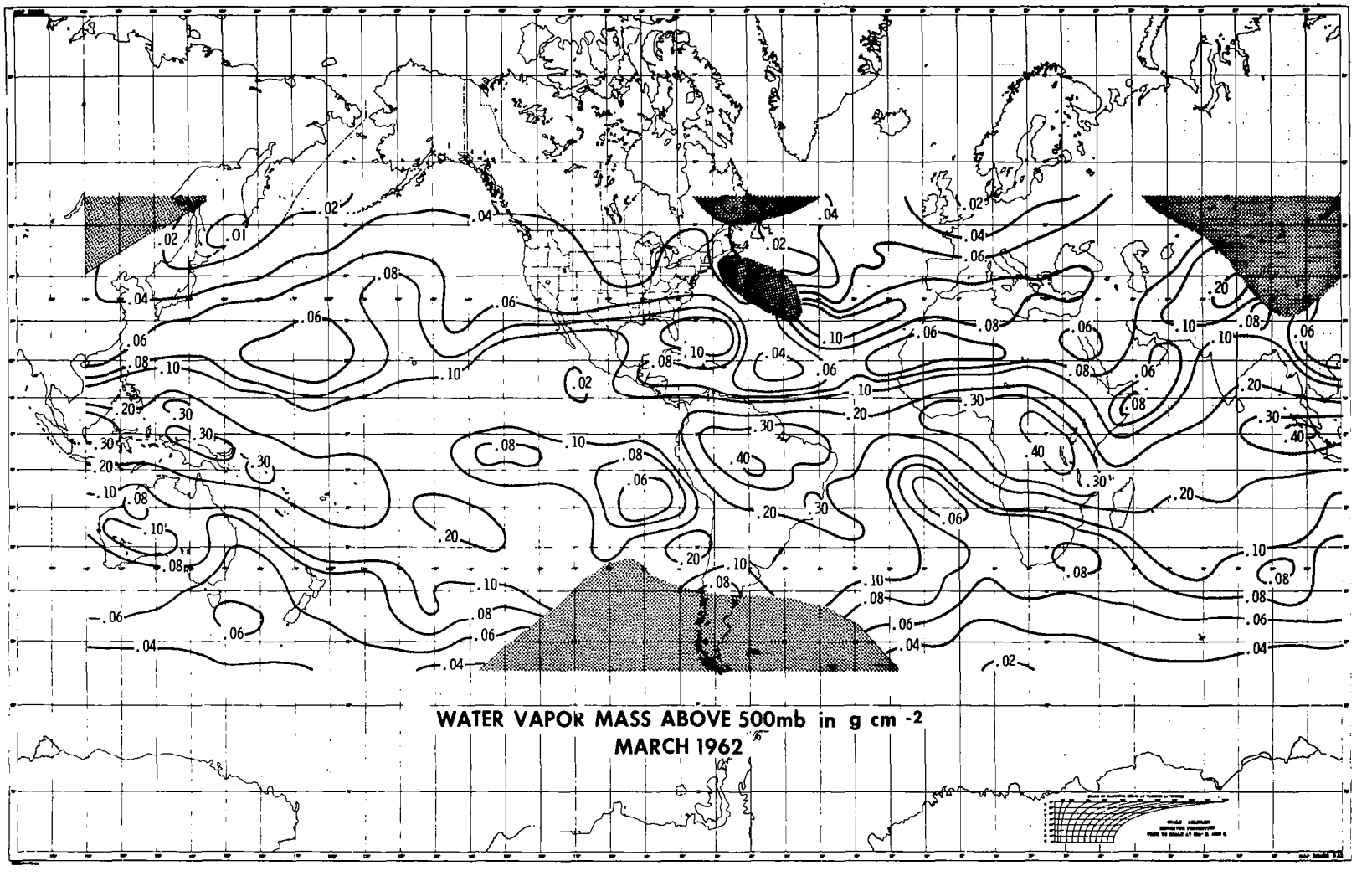

Fig.5.7: Quasi-global distribution of the water vapor mass above 5oo mb for March 1962

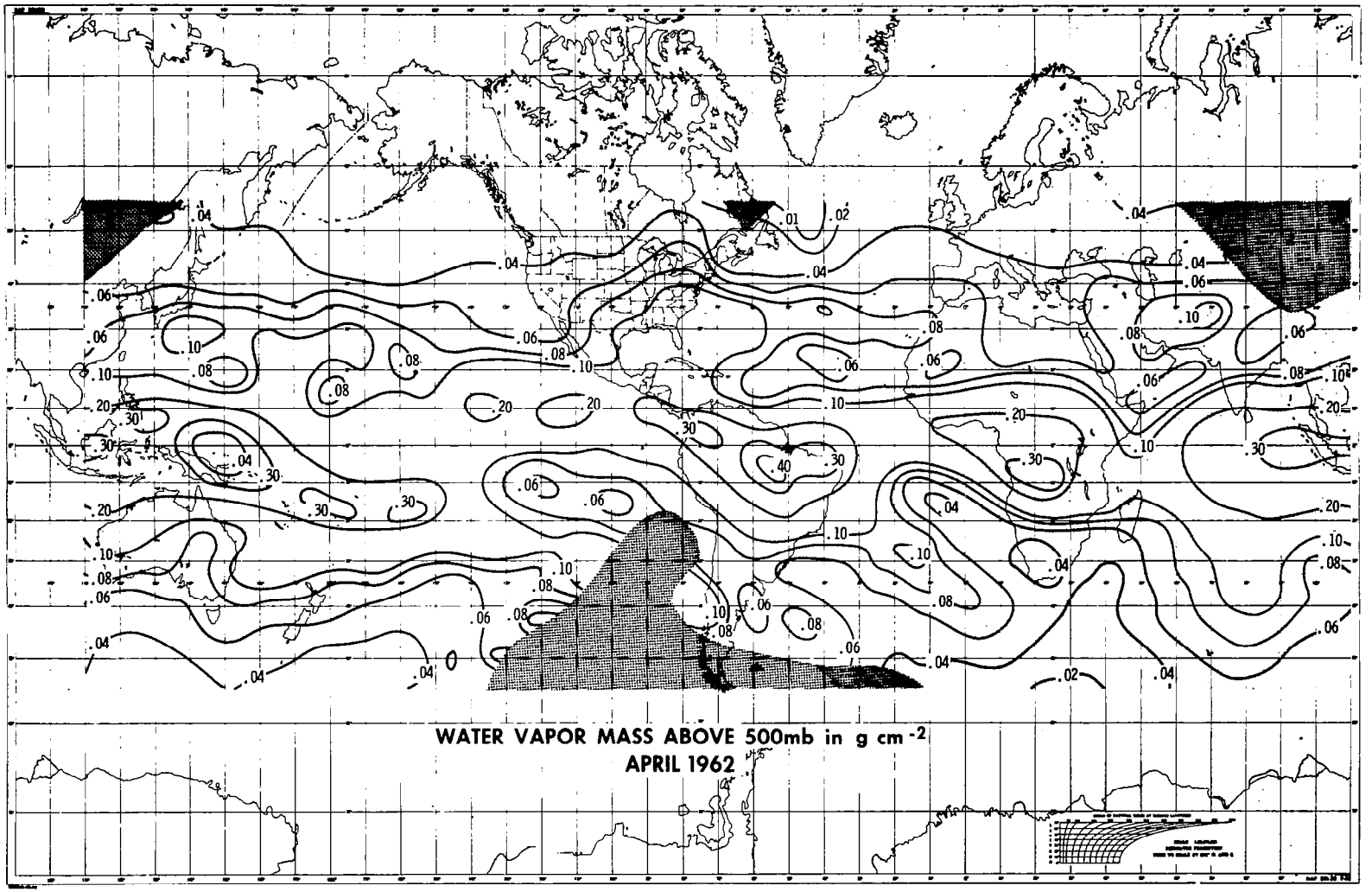

Fig.5.8: Quasi-global distribution of the water vapor mass above 5oo mb for April 1962

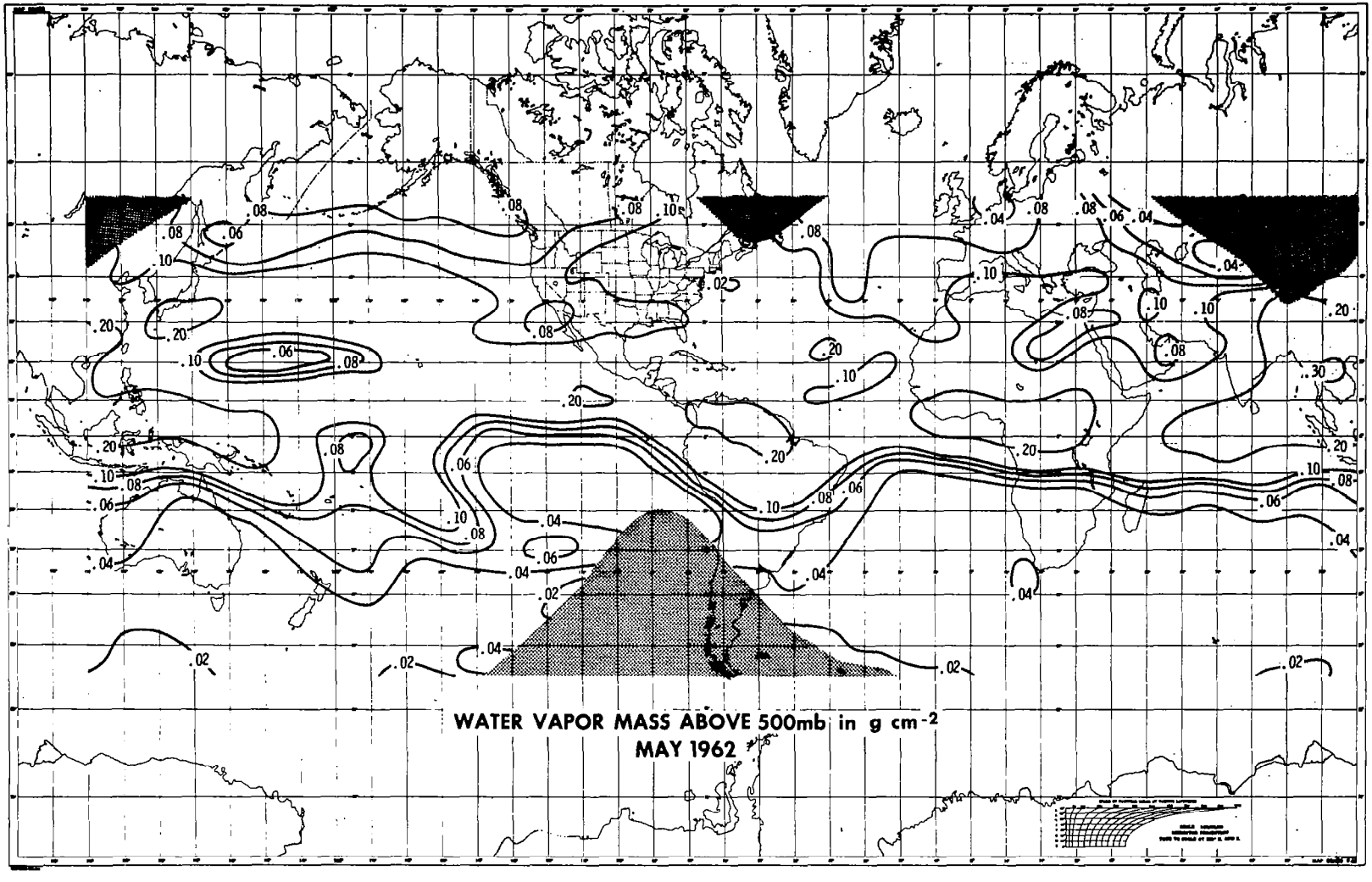

Fig.5.9: Quasi-global distribution of the water vapor mass above 5oo mb for May 1962

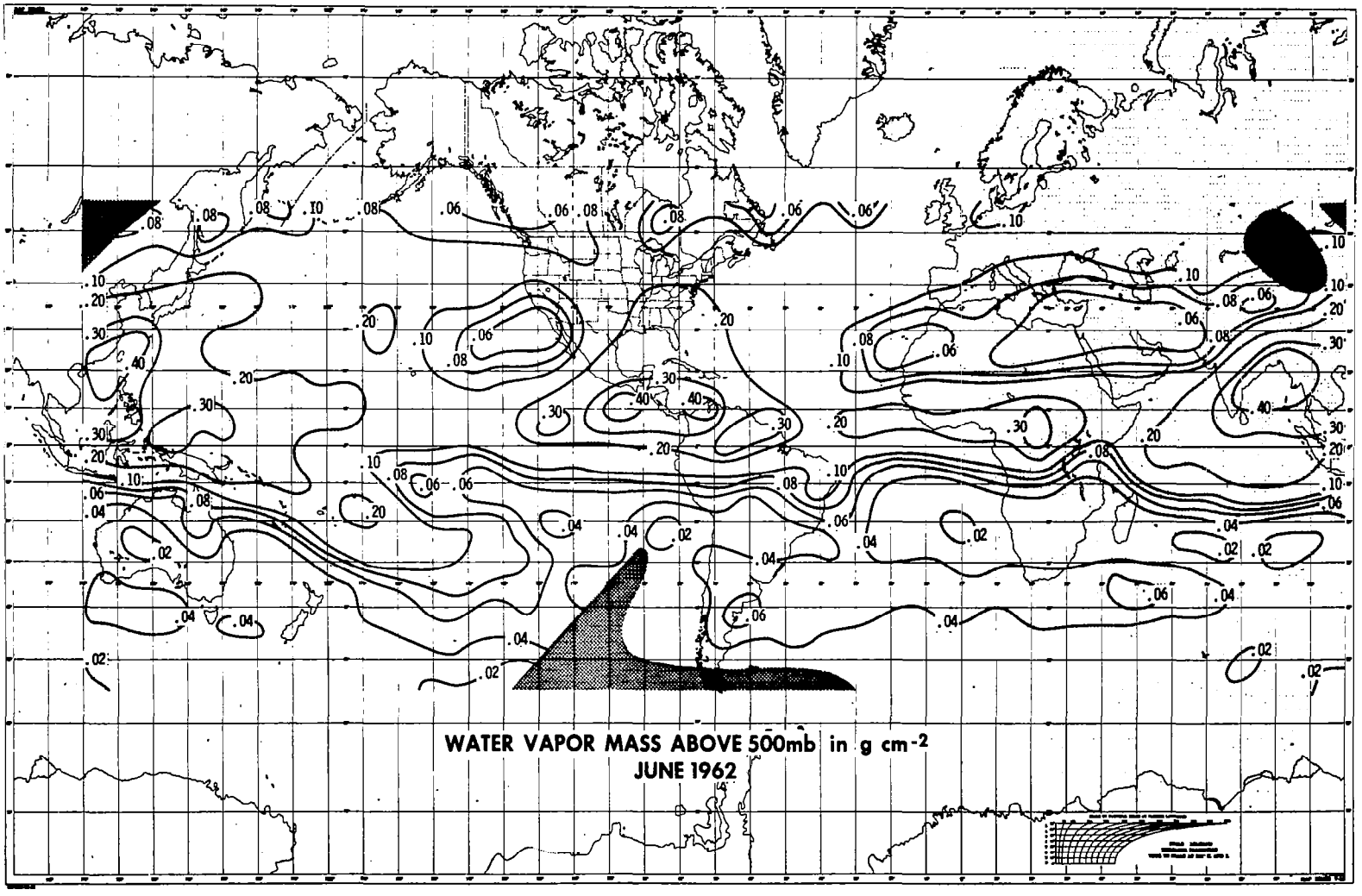

Fig.5.1o: Quasi-global distribution of the water vapor mass above 5oo mb for June 1962

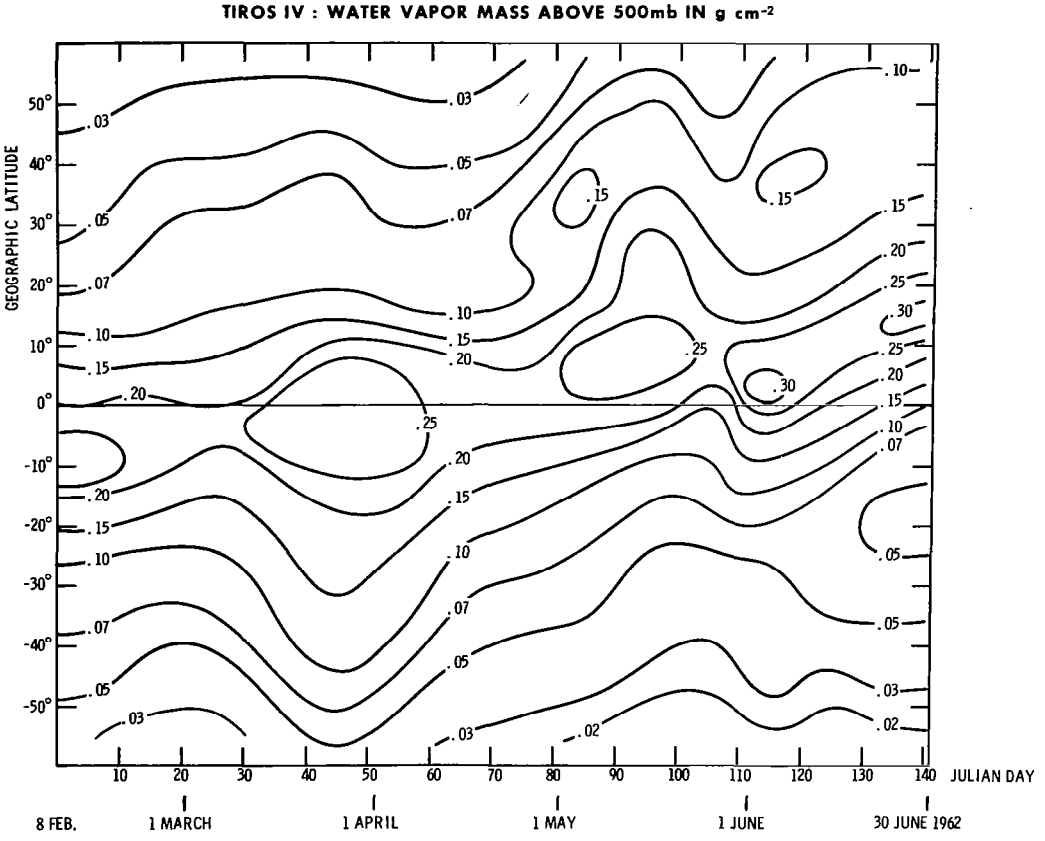

Fig.5.11: Zonal averages of the water vapor mass above 500 mb for 10-day periods

(1) The mean relative humidity of the upper troposphere,
(2) the (effective) surface temperature and
(3) the total water vapor mass above the 500 mb level using climatological values of the temperature at 500 mb.

The troposphere was assumed to be cloudless above cloud surfaces. One exception was made with the statement that the relative humidity of the upper troposphere is 99 %, when measurements are made over very high clouds (T equ. $\leq$ 228°K in both spectral regions).

The values of the mean relative humidity represent in a cloudless atmosphere a weighted average of the relative humidity between about 200 and 600 mb, or above cloud surfaces. Values of the surface temperature were determined under the assumtion of a completely black surface; therefore it should be called "effective" surface temperature.

All three quantities contain several errors which are caused mainly by deviations of the acutal stratospheric temperature and moisture from the assumed climatological averages and by the possible existence of thin but not completely transparent cloud or dust layer.

Primarily these cloud or dust layers cause errors, because their particles have optical properties which completely deviate from those of the gases. But the presence of such layers cannot be proved and their optical behavior in the spectral intervals considered here are not well known. Therefore, they could not be taken into consideration in our evaluations.

Some additional uncertainties might have arisen

by the corrections of the equivalent blackbody temperature measurements according to their degradation.

Despite the error sources discussed above (see also MÖLLER and RASCHKE, 1963) the results give some means to study the climatology and the circulation in the troposphere. This, of course, encourages further analogous evaluations of new radiation data from the Nimbus II satellite.

7.0 ACKNOWLEDGEMENT

This research was supported by a Grant (NsG - 305) of the National Aeronautics and Space Administration. The author is indebted to thank Mr. W. R. Bandeen and Dr. W. Nordberg of the Laboratory for Atmospheric and Biological Sciences of the Goddard Space Flight Center for their helpful assistance during his stay at that laboratory. Mr. A. F. Simmons and Mr. R. T. Hite prepared carefully the computer programs. Mrs. J. Minde prepared the manuscript.

8.o LIST OF REFERENCES

BANDEEN, W.R. et al.,(1965): A Radiation Climatology in the Visible and Infrared from the TIROS Meteorological Satellites. NASA TN D-2534

BANNON, J.K. and L.P.STEELE (196o): Average Water Vapour Content of the Air. Geophysical Memoirs, No.1o2, 13, London

BUETTNER, K.J.K. and C.D.KERN (1965): Determination of Infrared Emissivities of Terrestrial Surfaces. Journ.Geoph.Res., 7o, 1329-1337

COLE, A.E. and A.J.KANTOR (1963): Air Force Interim Supplemental Atmospheres to 9o Kilometers. Air Force Surveys in Geophysics, No.153. AFCRL-63-936

DEIRMENDIJAN, D. (1959): The Role of Water Particles in the Atmospheric Transmission of Infrared Radiation. Quart.Journ.R.Met.Soc.,85, 4o4-411

DEIRMENDIJAN, D. (1962): Scattering and Polarisation Properties of Poly dispersed Suspension with Partial Absorption. RAND Memorandum RM-3228-PR, July 1962

DREYFUS, M.G. and D.T.HILLEARY (1962): Satellite Infrared Spectrometer - Design and Development. Aerospace Engineering, 21, 42-45

FOW, R. (1964): Atmospheric Temperature Structure from Microwave Emission of Oxygen. Thesis at Mass.Institue of Techn.

G.S.F.C.(1962): TIROS III Radiation Data Catalog. Goddard Space Flight Center, Greenbelt, Maryland 2o771

G.S.F.C.(1963): TIROS IV Radiation Data Catalog and User's Manual. Goddard Space Flight Center, Greenbelt, Maryland 2o771

HANEL, R.A. and L. CHARNEY (1965): The Infrared Interferometer Spectrometer Experiment (IRIS), Vol.II. Meteorological Mission NASA X 65o-65-75 (unpublished Manuscript)

HAVARD, J.B. (196o): On the Raditional Characteristics of Water Clouds at Infrared Wave lengths. Thesis at University of Washington. AD 238 268

HILLEARY, D.T., D.G.WARK and D.G.JAMES (1965): An experimental Determination of Atmospheric Temperature Profile by Indirect Means. Nature, 2o5, 489-491

HOUGHTON, J. (1961): Meteorological Significance of Remote Measurements of Infrared Emission from Atmospheric Carbon Dioxide. Quart.Journ.R.Met. Soc., 87, 1o2-1o4

KANTOR, A.J. and A.E.COLE (1965): Monthly Atmospheric Structure, Surface to 8o km. Journ.Appl.Met., 4, 228-237

KAPLAN, L.D.(1959): Inference of Atmospheric Structure from Remote Radiation Measurements. J.O.S.A.,49, 1oo4-1oo7

KATZ, Y.H.(editor),(1963): The Application of Passive Microwave Technology to Satellite Meteorology: A Symposium. RAND Corp.-Memorandum 34o1 (NASr-21(o7))

KING, J.I.F.(1958): The Radiative Heat Transfer of Planet Earth. Scientific Uses of Earth Satellites, Second Revised Edition, edited by J.A.van Allan, Univ.of Mich.Press, Ann.Arbor.

KING, J.I.F.(1963): Meteorological Inferences from Satellite Radiometry, I. Journ.Atm.Sci.,2o,245-25o

KING, J.I.F.(1964): Inversion by Slabs of Varying Thickness. Journ.Atm.Sci.,21, 324-326

KONDRATIEV, K.Ya.(1961): Some Problems of Actinometry in the Free Atmosphere. Paper presented at the Symposium of the Radiation Commission in Vienna

LEUPOLT, A. (1965): Bestimmung der Kontinuum-Absorption im Spektralbereich von o.5 bis 2.5 µm. Inaugural-Dissertation, Universität München, Meteorologisches Institut

MANABE, S., J.SMAGORINSKI and R.F.STRICKLER (1965): Simulated Climatology of a General Circulation Model with a Hydrologic Cycle. Monthly Weather Rev., 93, 769-799

MASTENBROOK, H.J.(1963): Frost-Point Hygrometer Measurements in the Stratosphere and the Problem of Moisture Contamination; Humidity and Moisture, Vol.2, Reinhold Public.

MASTENBROOK, H.J.(1965): The Vertical Distribution of Water Vapor over Kwajalein Atoll, Marshall Islands. NRL-Report 6367

McCLATCHEY, R.A.(1965): The Use of the 4.3-Micron CO_2 Band to Sound the Temperature of a Planetary Atmosphere. Paper presented at the Symposium on Electromagnetic sensing of the Earth from Satellites, Miami, Nov.1965

MEEKS, M.L. and A.E.LILLEY (1962): The Microwave Spectrum of Oxygen in the Earth's Atmosphere. Journ.of Geoph.Res.,68,1683-1703

MÖLLER, F.(1951): Vierteljahreskarten des Niederschlages für die ganze Erde. Petermanns Geographische Mitteilungen, 1.Quartalsheft, 1-7. Verlag Julius Perthes, Gotha

MÖLLER, F.(1961): Atmospheric Water Vapor at 6-7 Microns from a Satellite. Planet.Space Sci.,5, 202-206

MÖLLER, F.(1962): Einige vorläufige Auswertungen der Strahlungsmessungen von TIROS II. Arch.Meteor. Geophys.Biokl., Serie B, 12, 78-93

MÖLLER, F. and E.RASCHKE (1963): Evaluation of TIROS III Radiation Data. Interims Report No.1, Meteorologisches Institut der Universität München. NASA-Grant NsG 305 (also in NASA CR-112)

RASCHKE, E.(1965): Auswertungen von infraroten Strahlungsmessungen des meteorologischen Satelliten TIROS III. Beitr.zur Physik d.Atm.,38, 97-120, 153-187

RASCHKE, E. und I.TANNHÄUSER (1965): Investigation of Atmospheric Properties based upon Evaluation of Infrared Radiation Data obtained from TIROS Satellites. Final Report. Meteorologisches Institut der Universität München. NASA-Grant NsG-305

SZAVA-KOVATS, J. (1938): Verteilung der Luftfeuchtigkeit auf der Erde. Ann.d.Hydr.u.Marit.Met.,60, 373-378

ROBINSON, E.D.(1962): Absorption of Solar Radiation by Atmospheric Aerosol, as Revealed by Measurements at Ground. Arch.Met.Geophys.Biokl., B, 12, 19

RODGERS, C.(1965): Satellite Infrared Radiometer - The Inversion Problem. Clarendon Laboratory Memorandum No.65.9,20 p.

SMITH, S.D. and C.R.PIDGEON (1964): Application of Multiple Beam Interferometric Methods to the Study of CO_2 Emission at 15 μ. Mém.de la Soc.R.d.Sc.de liège, Ser.5,9, 336-349

STARR, V.P. et al.(1958): On the Meridional Flux of Water Vapor in the Northern Hemisphere.Geofisica Pura e Applicata, 39, pp.174-185

TELEGADAS, K. and J.LONDON,(1954): A Physical Model of the Northern Hemisphere Troposphere for Winter and Summer. N.Y.Univ.,Coll.of Eng.,Sci-Rep.1, AF 19(122)-165

U.S.W.B.(1962): Monthly Climatic Data of the World (1962). U.S.Weather Bureau

WARK, D.Q., G.YAMAMOTO and J.H.LIENESCH (1962): Methods of Estimating Infrared Flux and Surface Temperature from Meteorological Satellites. J.Atm.Sci.,19,369-384

WARK, D.Q. and H.E.FLEMING (1966): Indirect Measurements of Atmospheric Temperature Profiles from Satellites: I. Introduction. Manuscript - submitted for Publication to Monthly Weather Review

YAMAMOTO, G.(1965): Determination of Precipitable From TIROS Radiation Measurements. J.Quart.Rept., Contract CWB-10788

ZDUNKOWSKI, W. et al.(1965): The Influence of Haze on Infrared Radiation Measurements Detected by Space Vehicles. Tellus, 17

ZIRKIND, R.(1965): The Near, Medium J.R.Earth Albedo; Its Use for Cloud Height Determination. Planet. Space Sci, 13, 377-390

9.o APPENDIX A 1

Maps of the mean relative humidity of the upper troposphere and of the (effective) surface temperature for periods of 1o-days covering the period from February 8, 1962 to June 3o, 1962.

(pages 68 - 95)

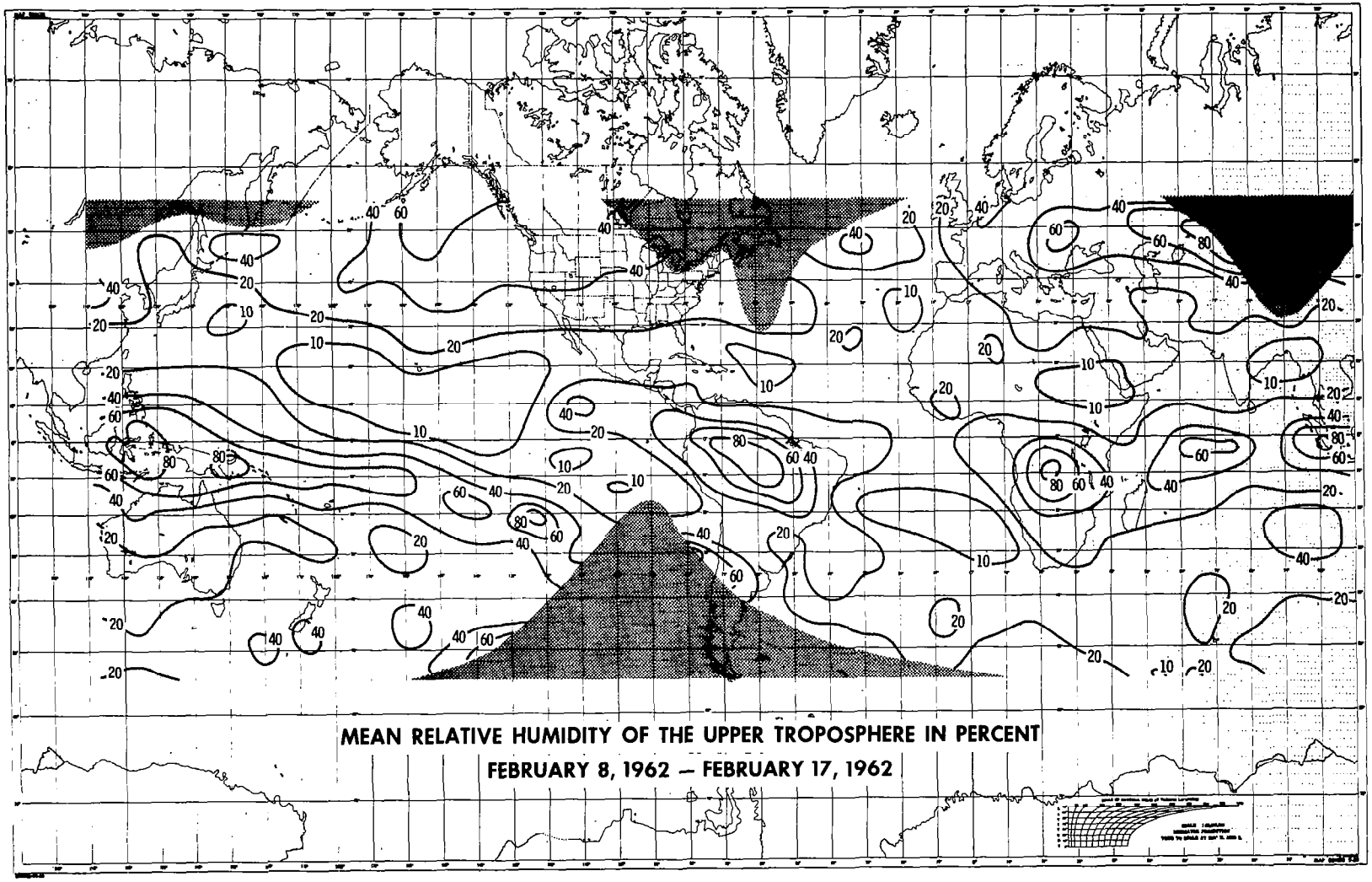

MEAN RELATIVE HUMIDITY OF THE UPPER TROPOSPHERE IN PERCENT

FEBRUARY 8, 1962 — FEBRUARY 17, 1962

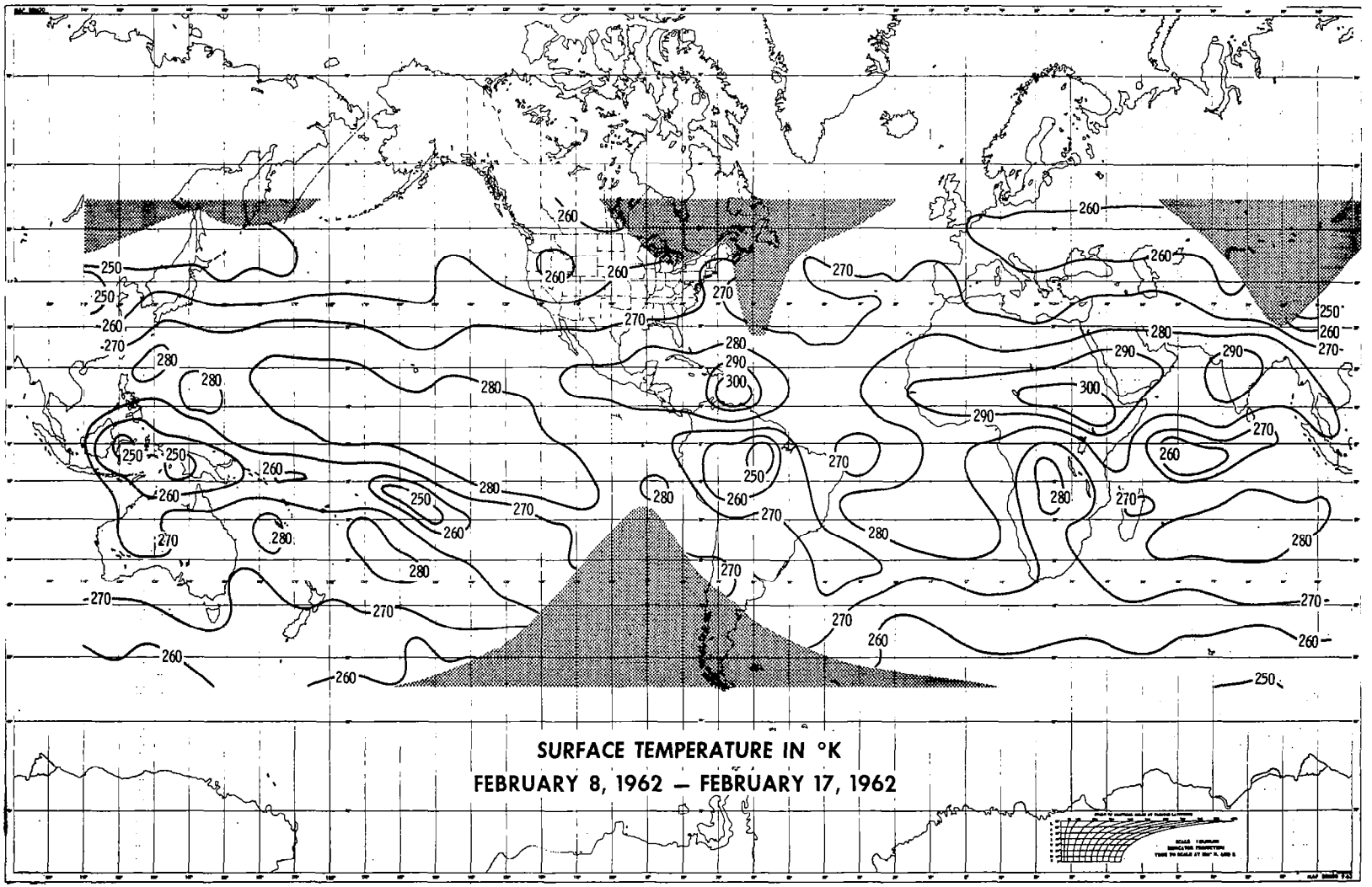
SURFACE TEMPERATURE IN °K
FEBRUARY 8, 1962 — FEBRUARY 17, 1962

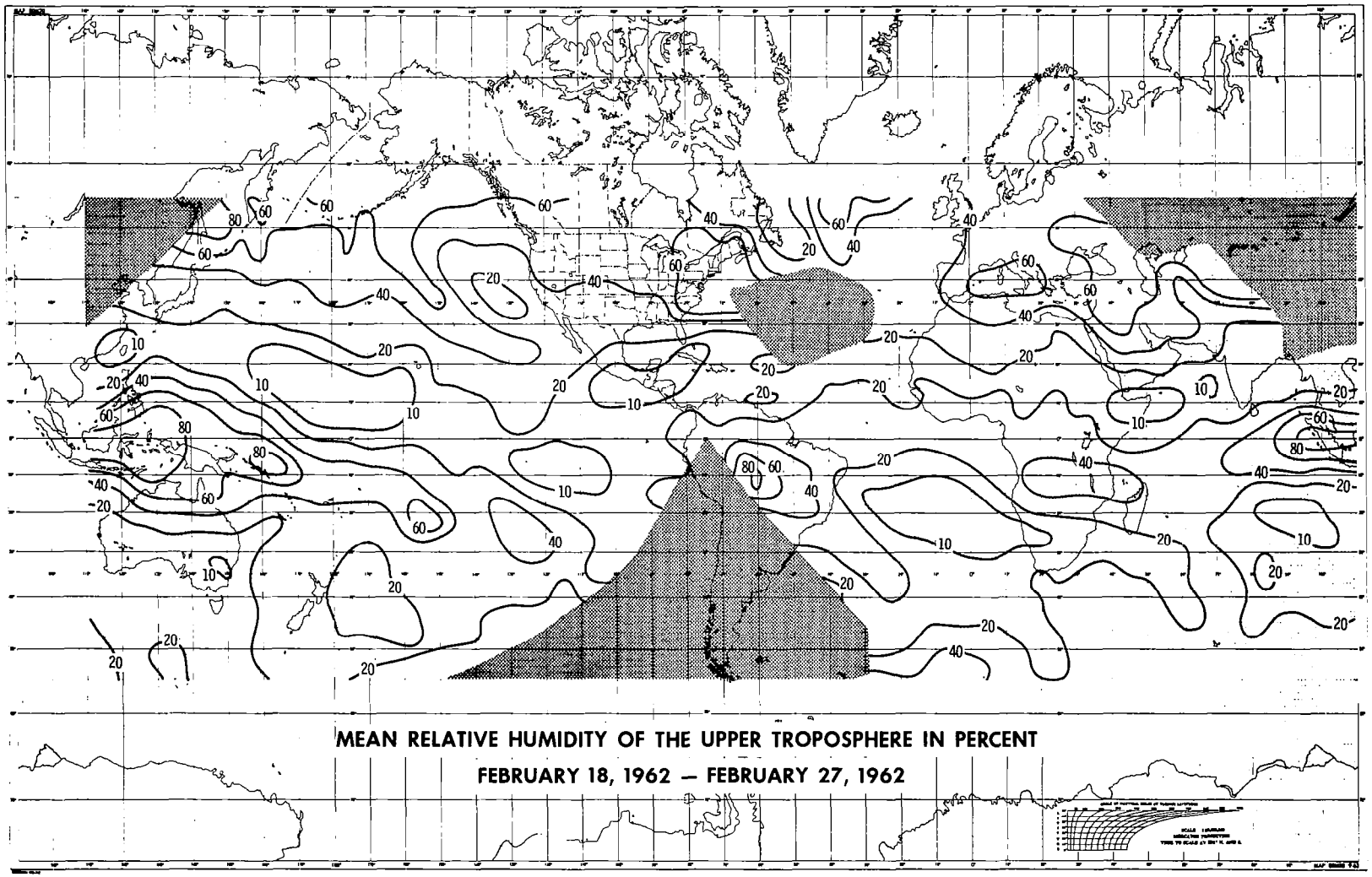
MEAN RELATIVE HUMIDITY OF THE UPPER TROPOSPHERE IN PERCENT
FEBRUARY 18, 1962 — FEBRUARY 27, 1962

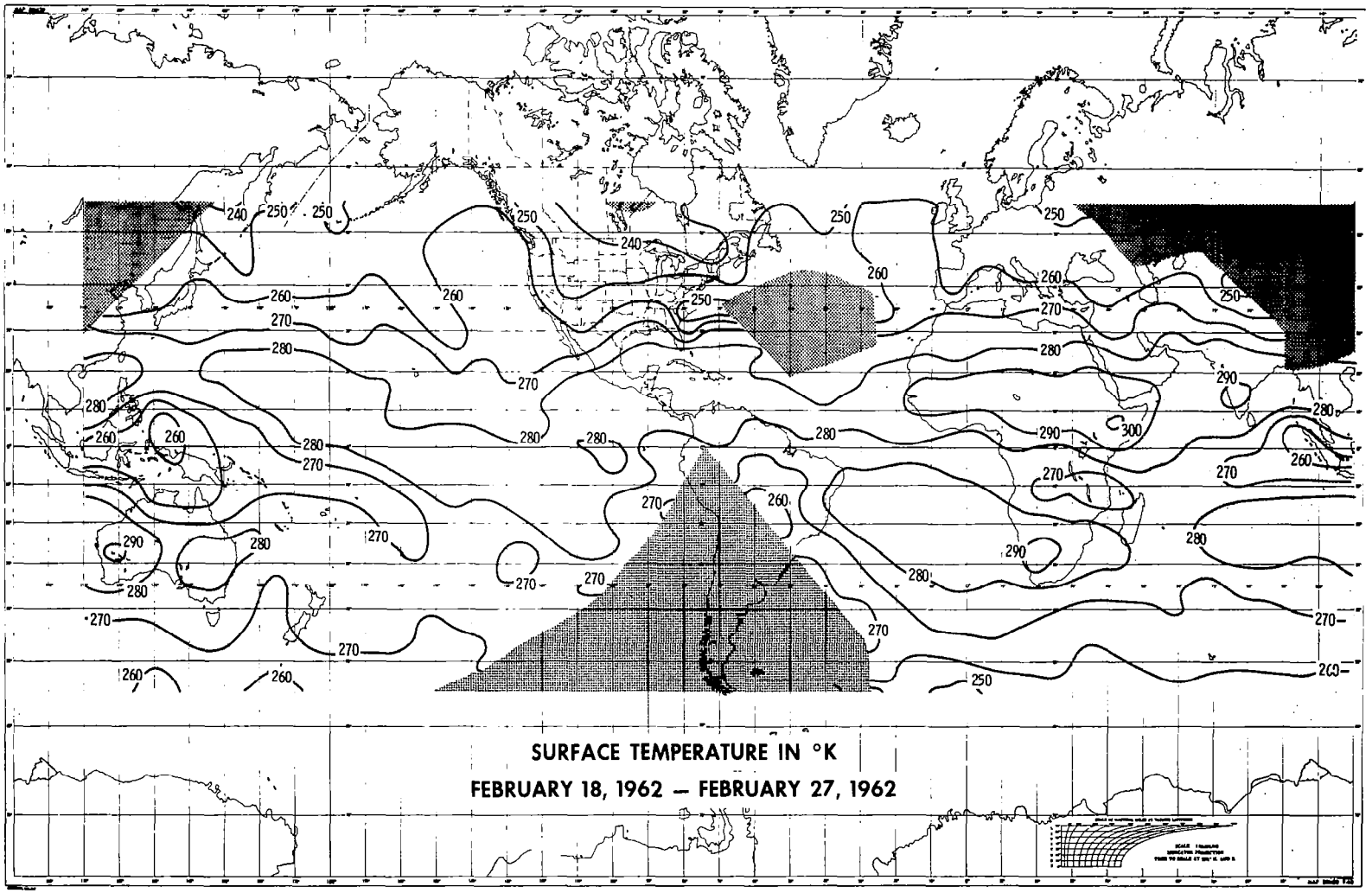

SURFACE TEMPERATURE IN °K

FEBRUARY 18, 1962 — FEBRUARY 27, 1962

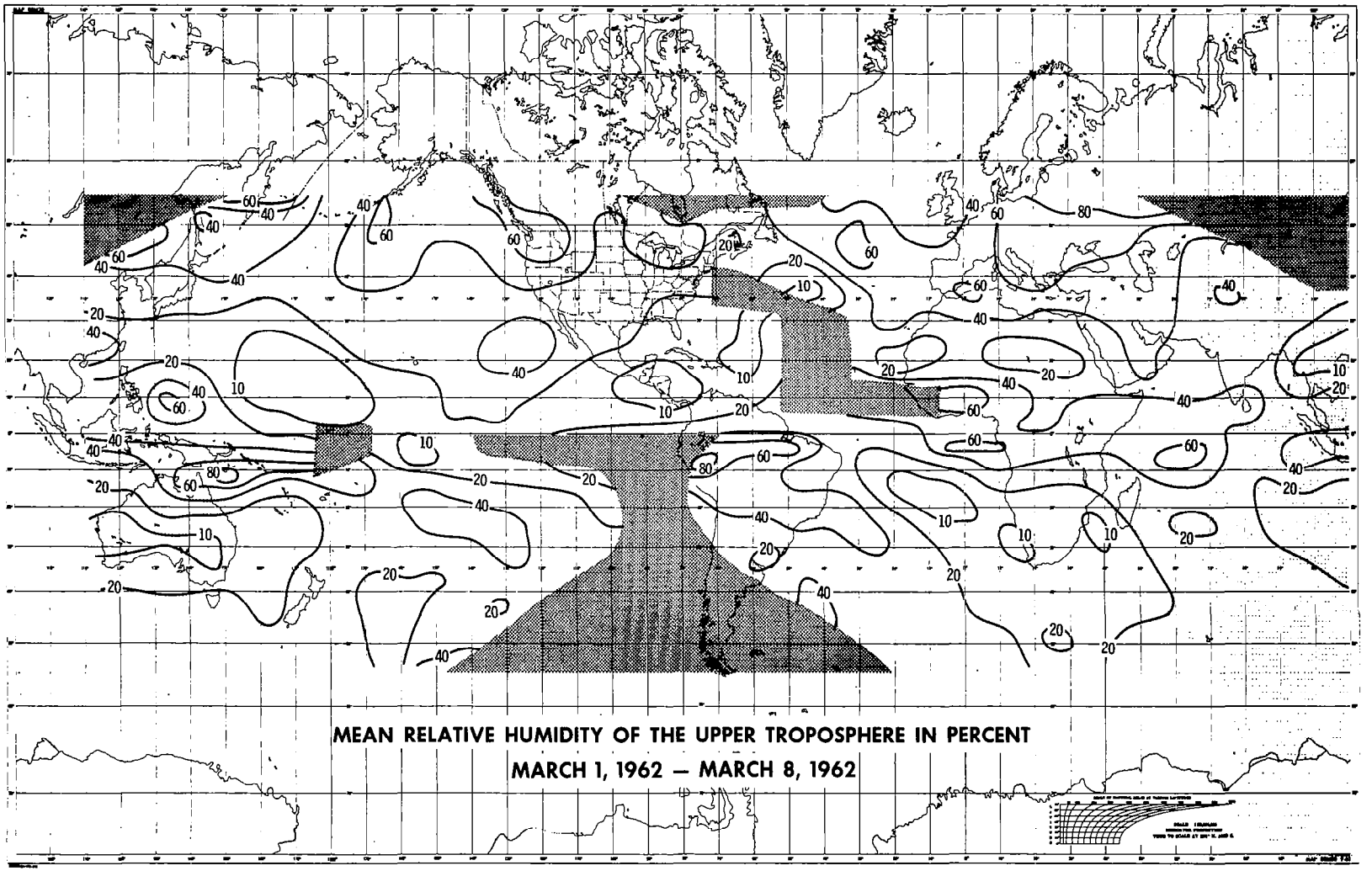
MEAN RELATIVE HUMIDITY OF THE UPPER TROPOSPHERE IN PERCENT
MARCH 1, 1962 — MARCH 8, 1962

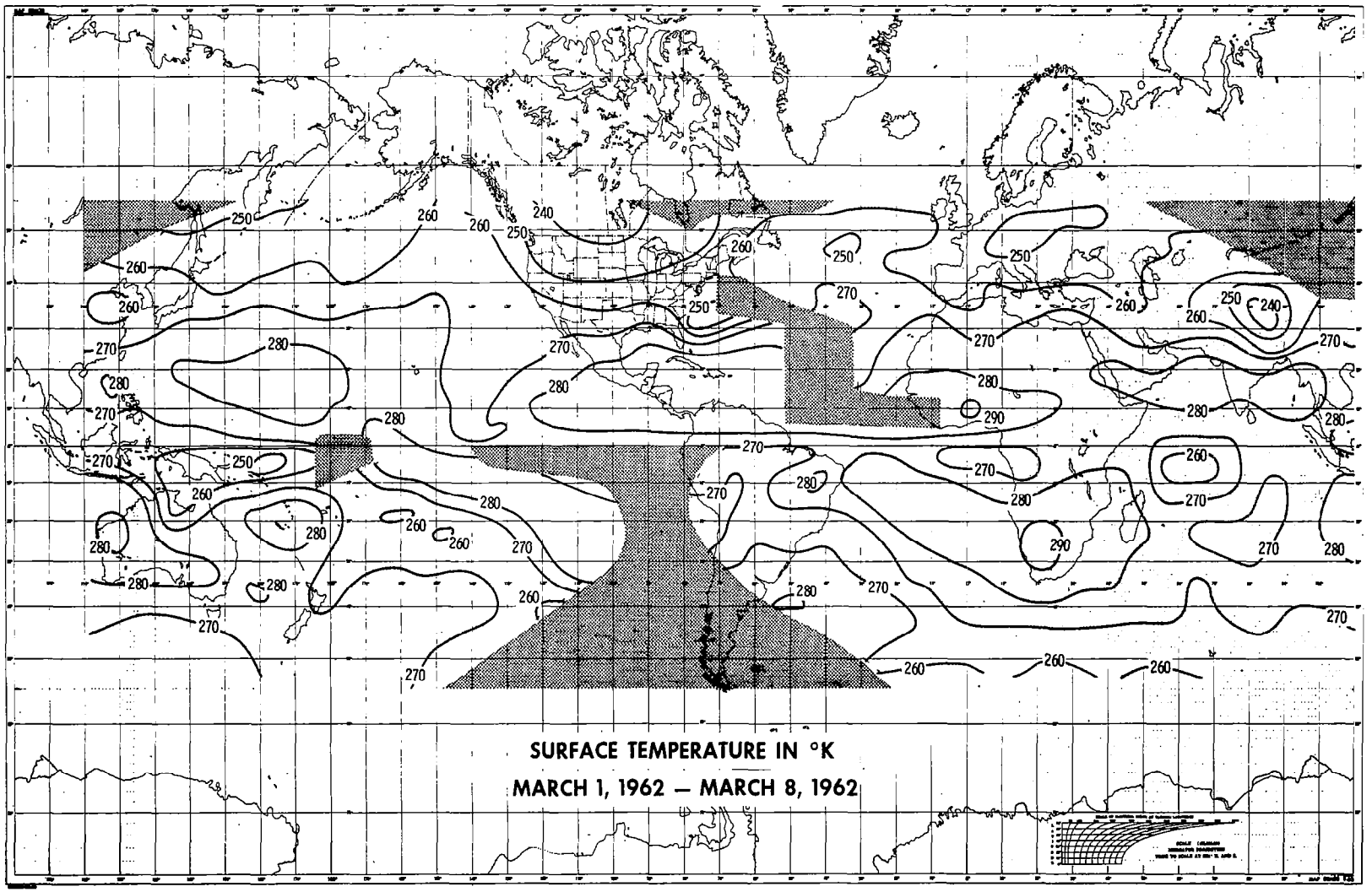
SURFACE TEMPERATURE IN °K
MARCH 1, 1962 — MARCH 8, 1962

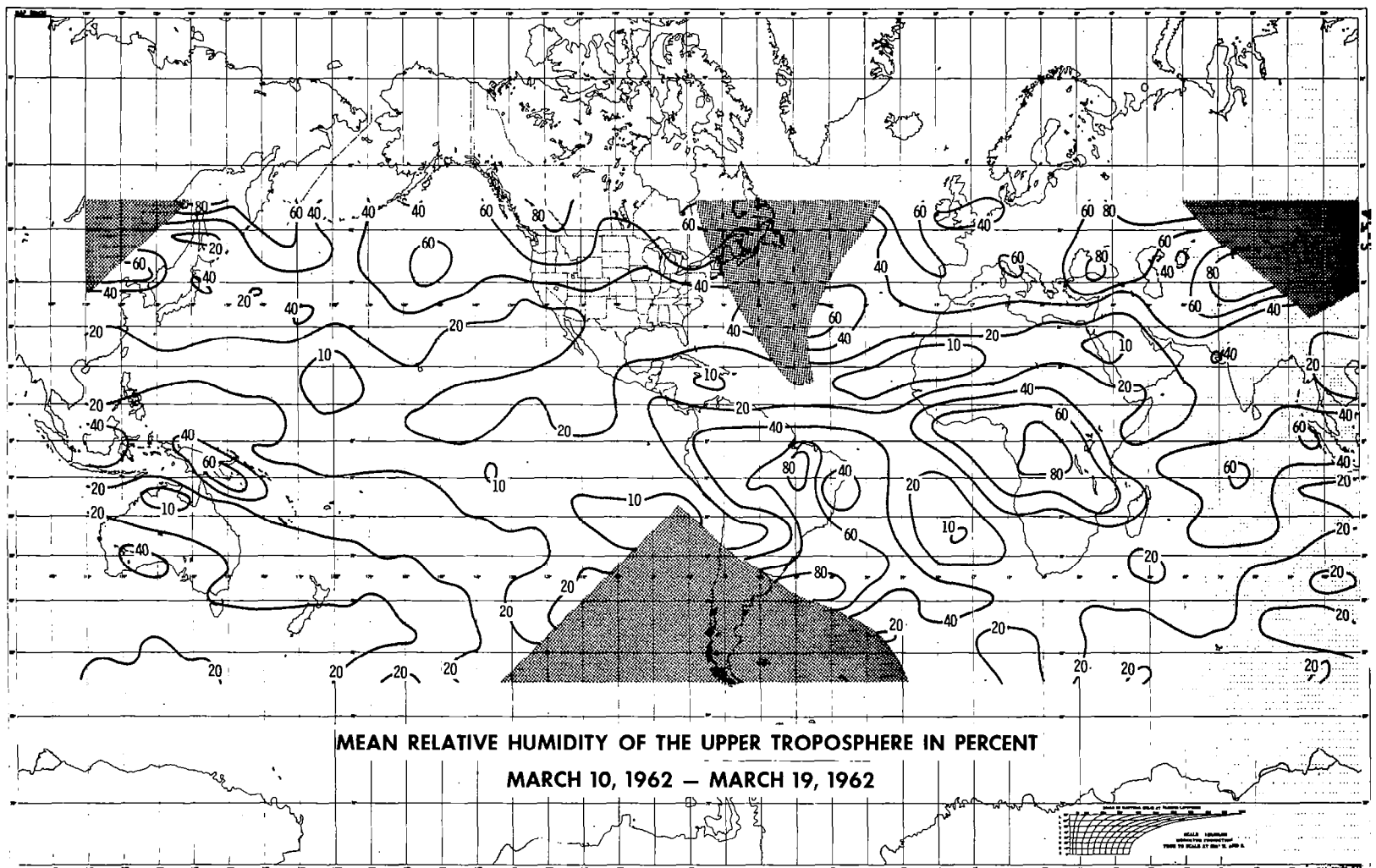
MEAN RELATIVE HUMIDITY OF THE UPPER TROPOSPHERE IN PERCENT
MARCH 10, 1962 — MARCH 19, 1962

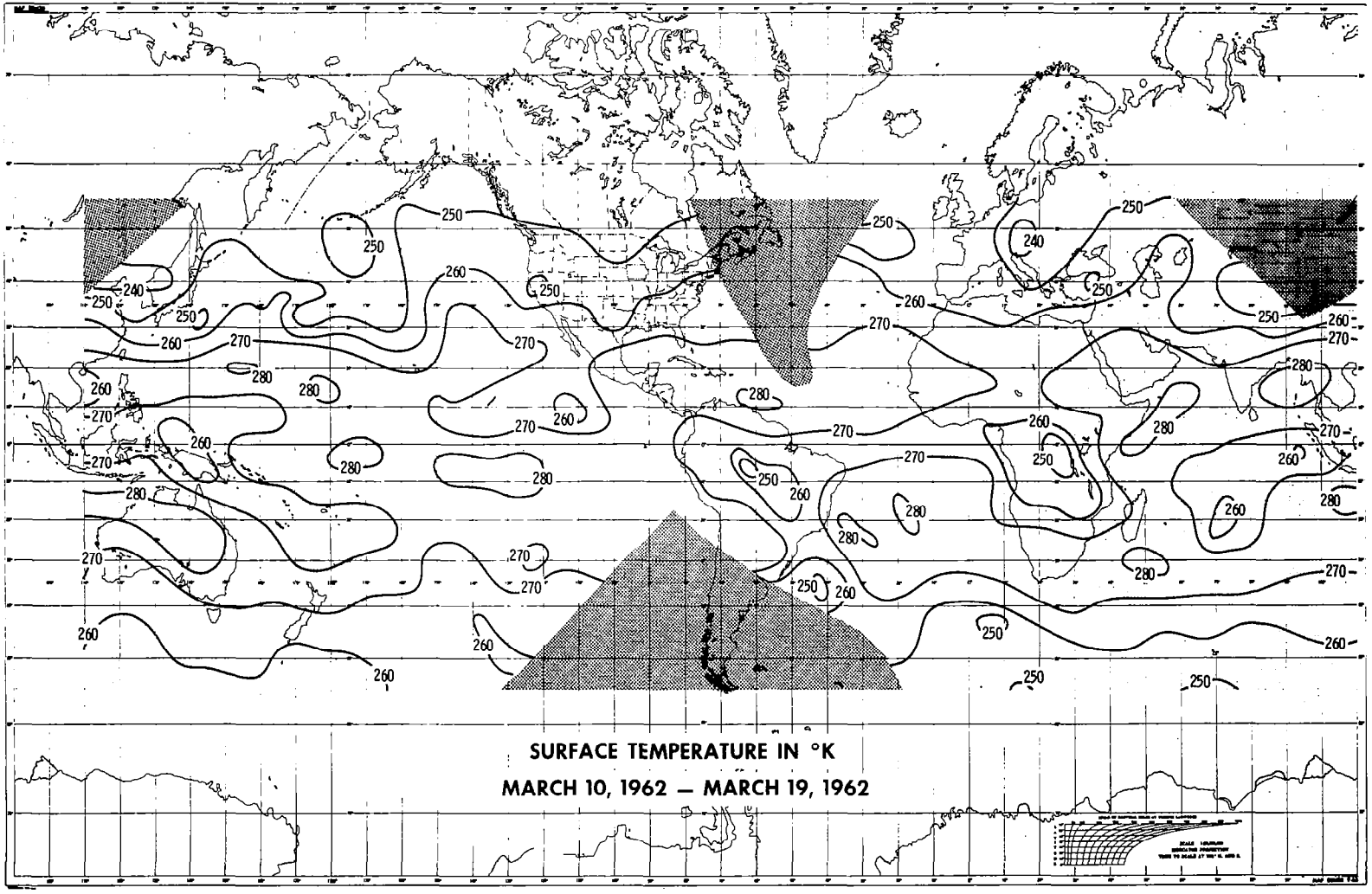
SURFACE TEMPERATURE IN °K
MARCH 10, 1962 — MARCH 19, 1962

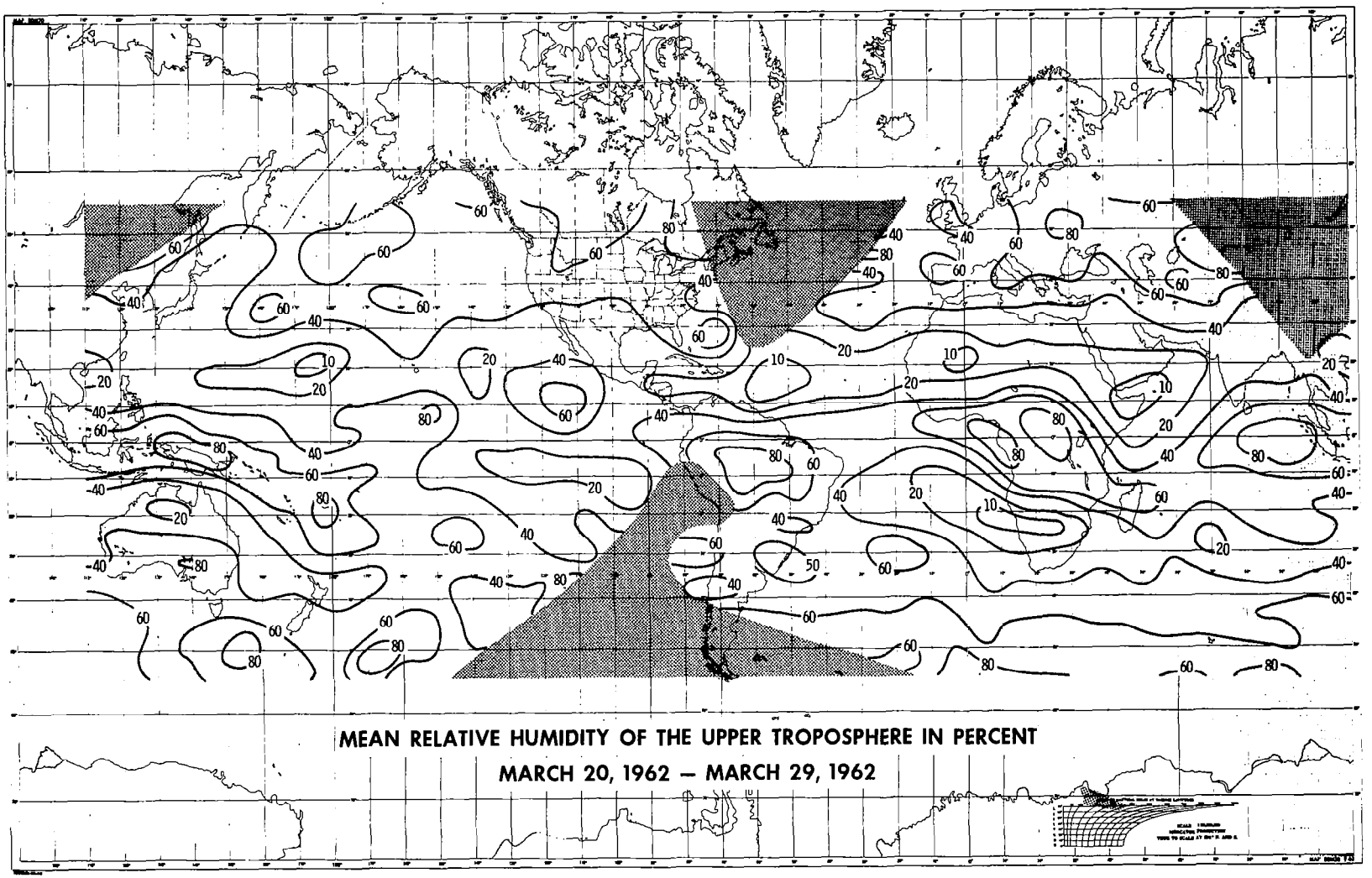

MEAN RELATIVE HUMIDITY OF THE UPPER TROPOSPHERE IN PERCENT

MARCH 20, 1962 — MARCH 29, 1962

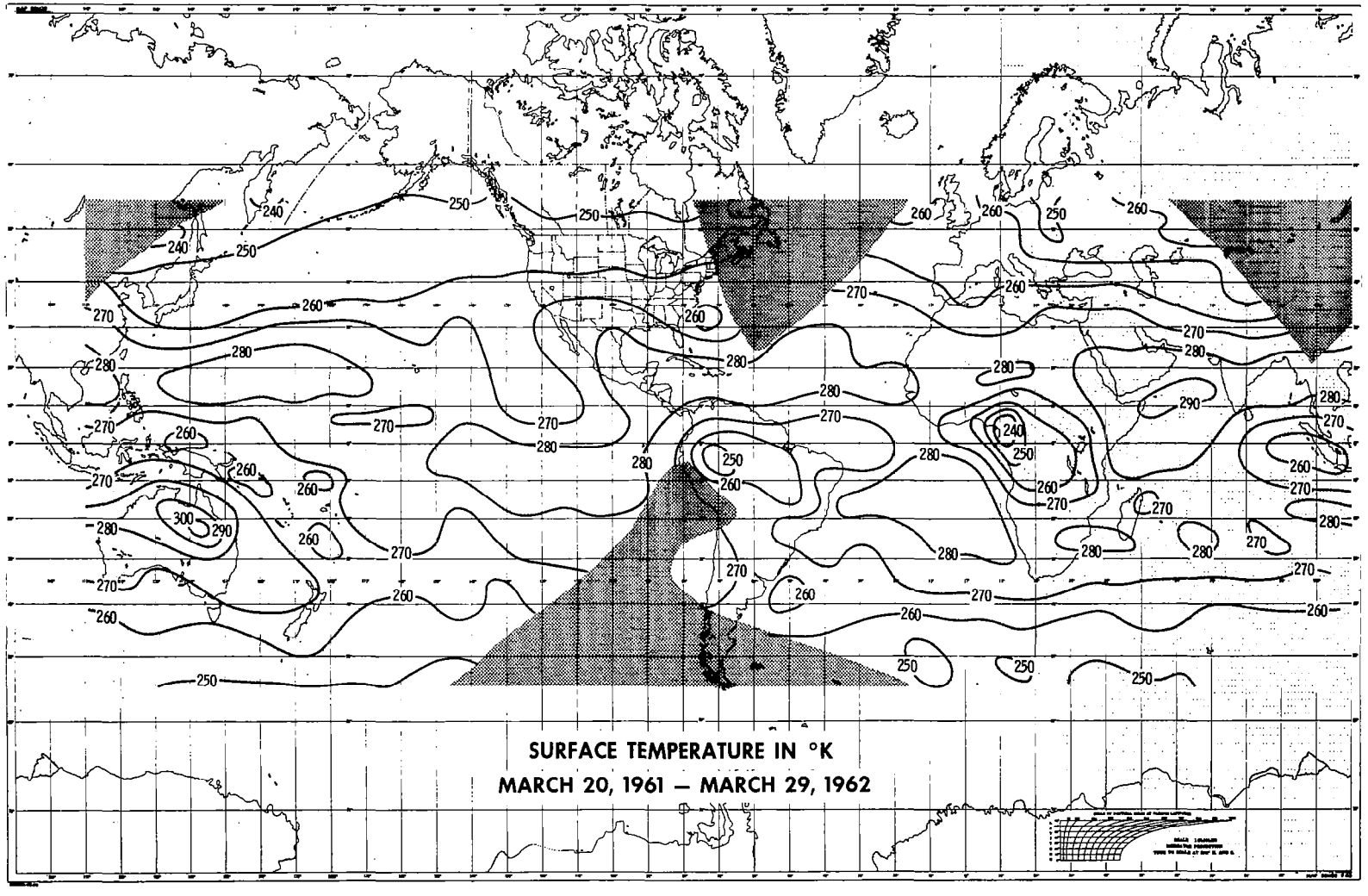
SURFACE TEMPERATURE IN °K
MARCH 20, 1961 — MARCH 29, 1962

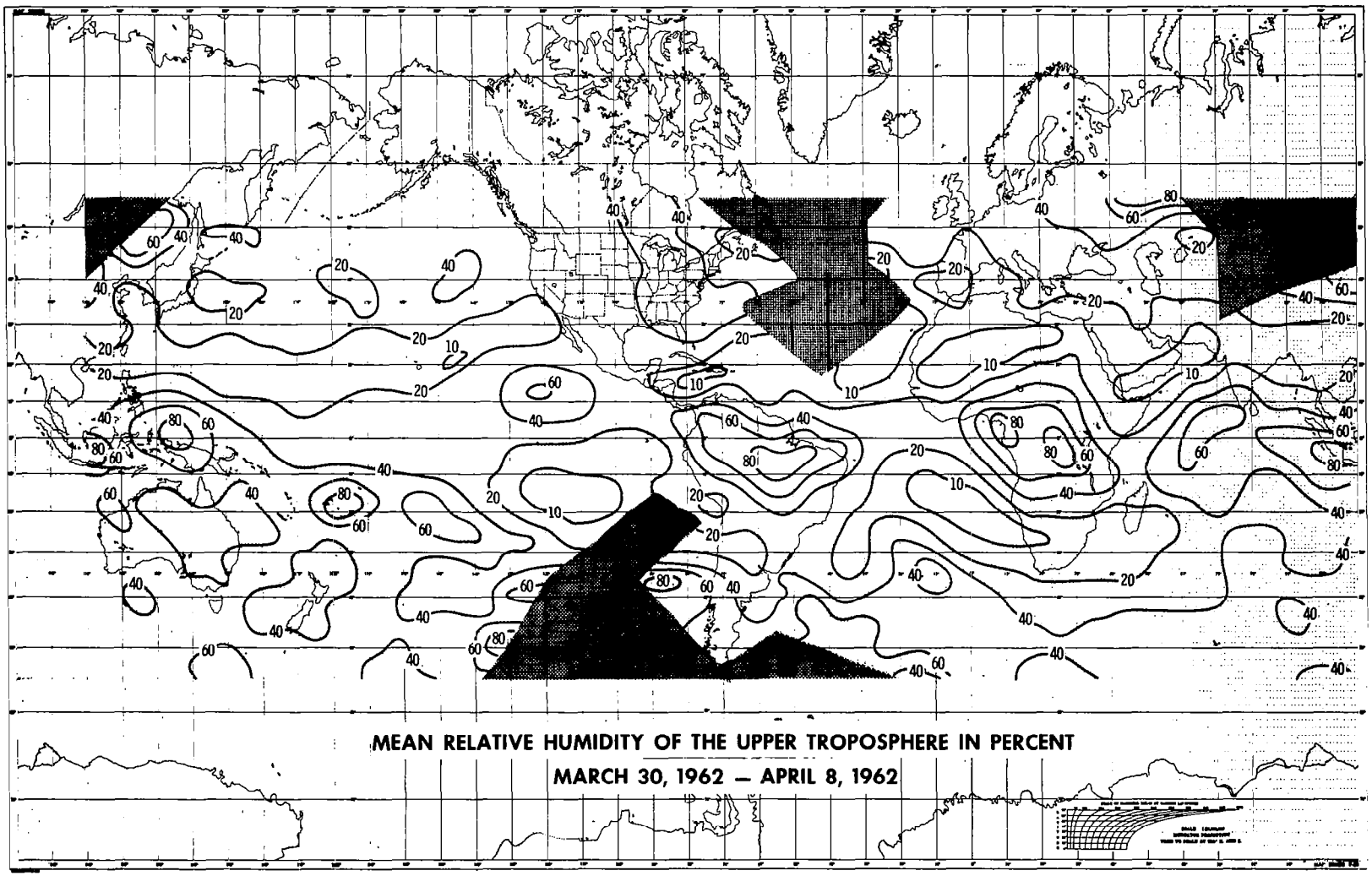
MEAN RELATIVE HUMIDITY OF THE UPPER TROPOSPHERE IN PERCENT
MARCH 30, 1962 — APRIL 8, 1962

SURFACE TEMPERATURE IN °K
MARCH 30, 1962 — APRIL 8, 1962

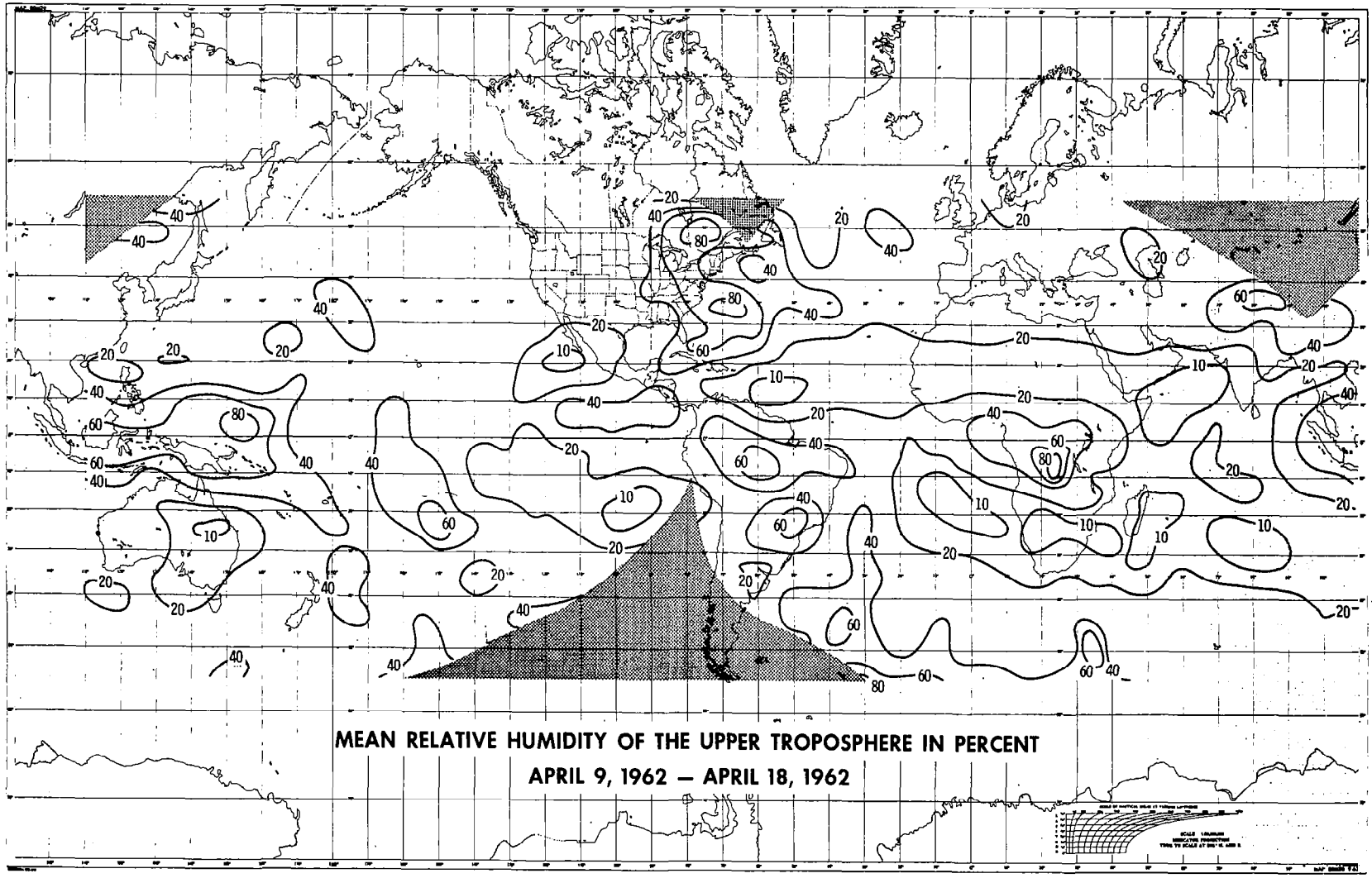
MEAN RELATIVE HUMIDITY OF THE UPPER TROPOSPHERE IN PERCENT
APRIL 9, 1962 — APRIL 18, 1962

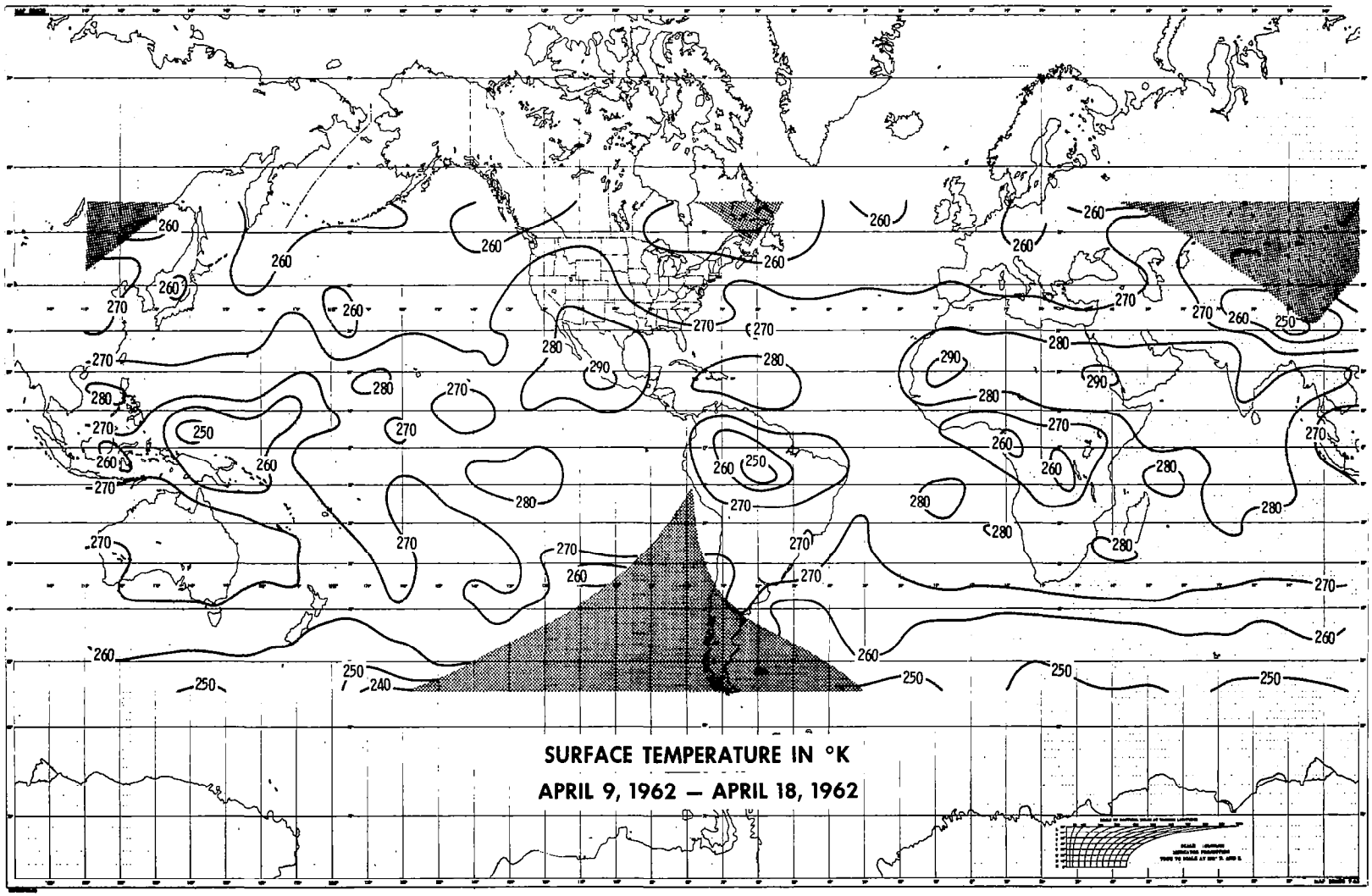
SURFACE TEMPERATURE IN °K
APRIL 9, 1962 — APRIL 18, 1962

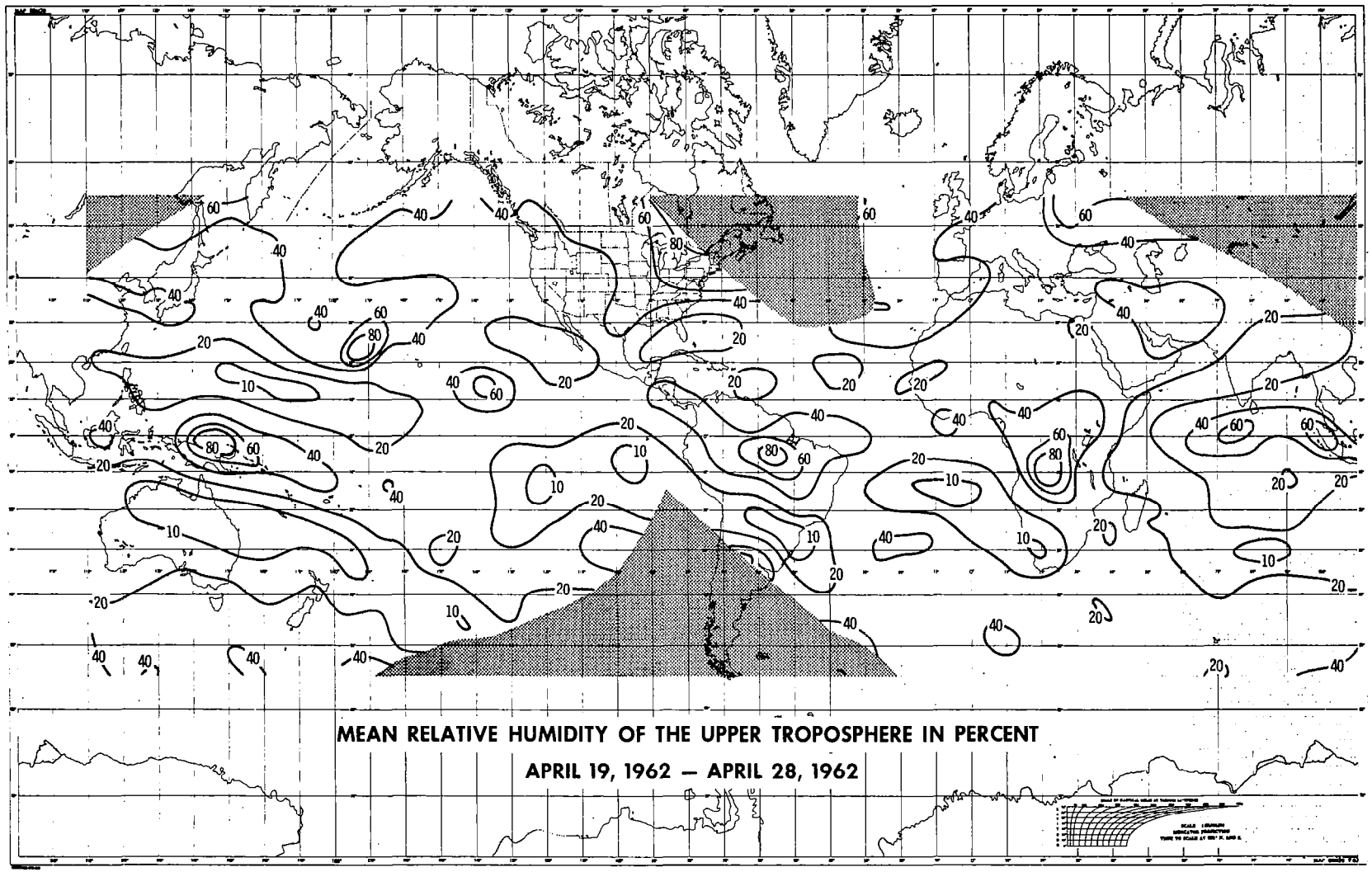
MEAN RELATIVE HUMIDITY OF THE UPPER TROPOSPHERE IN PERCENT
APRIL 19, 1962 — APRIL 28, 1962

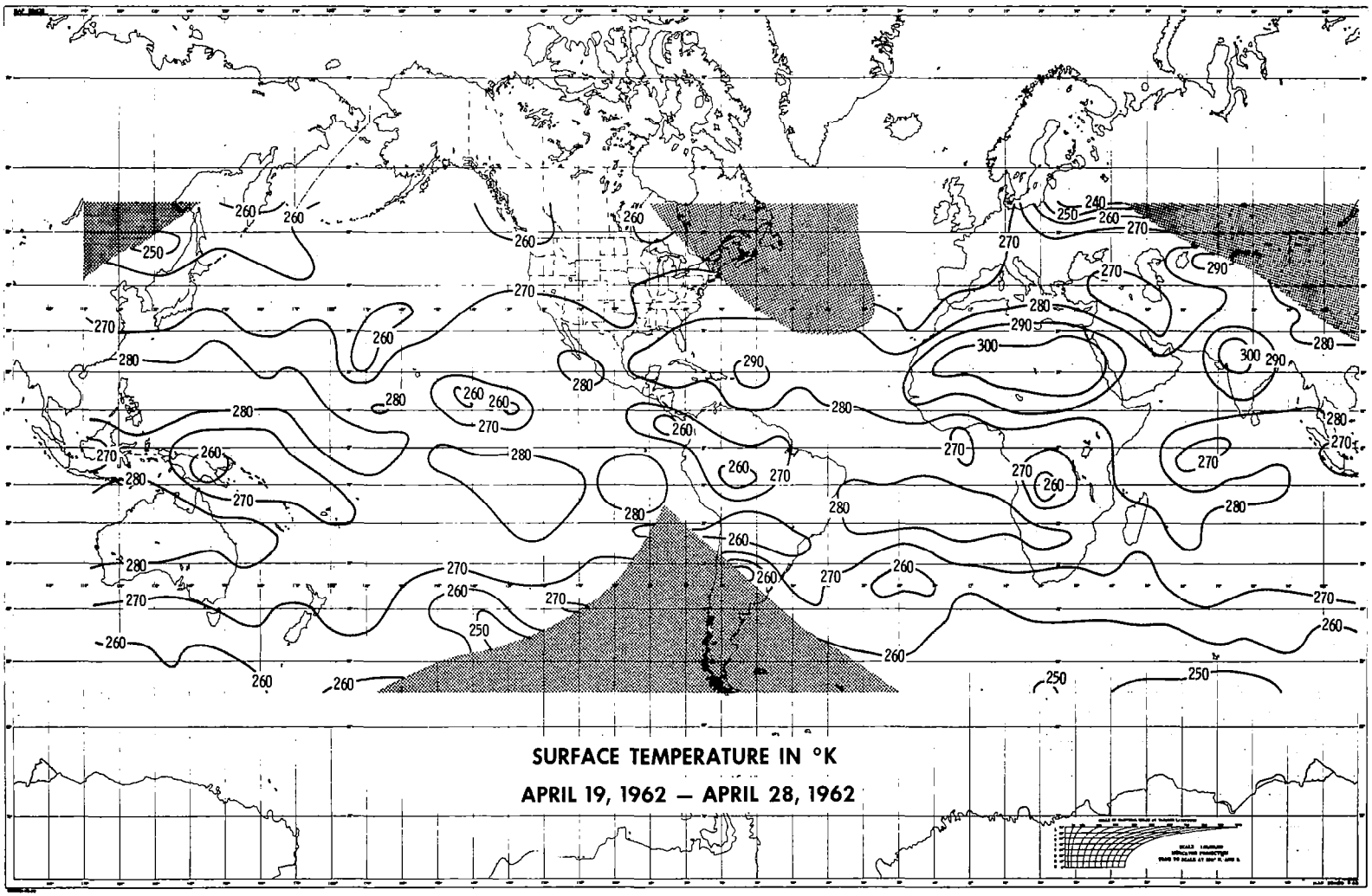
SURFACE TEMPERATURE IN °K
APRIL 19, 1962 — APRIL 28, 1962

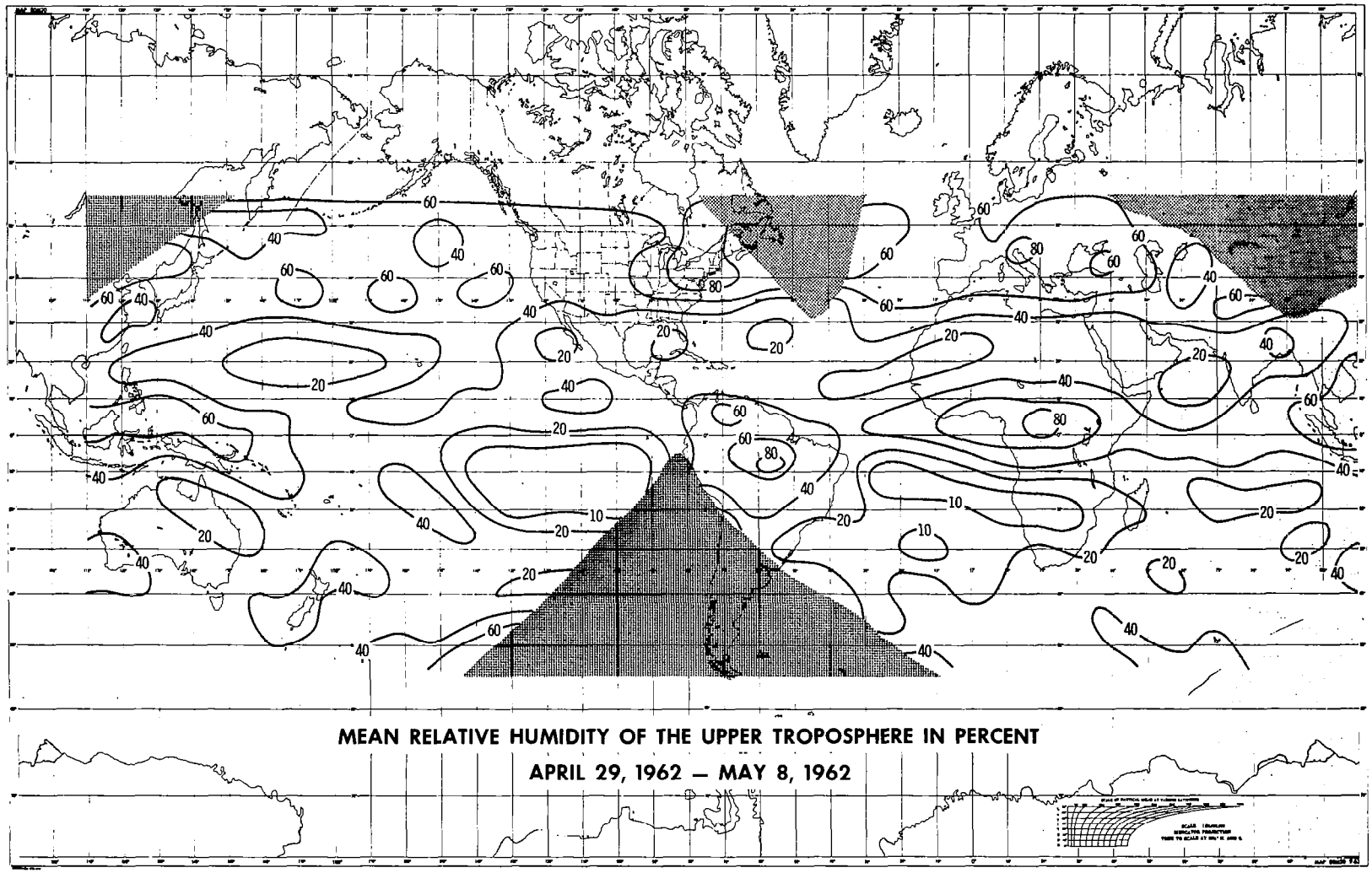
MEAN RELATIVE HUMIDITY OF THE UPPER TROPOSPHERE IN PERCENT
APRIL 29, 1962 — MAY 8, 1962

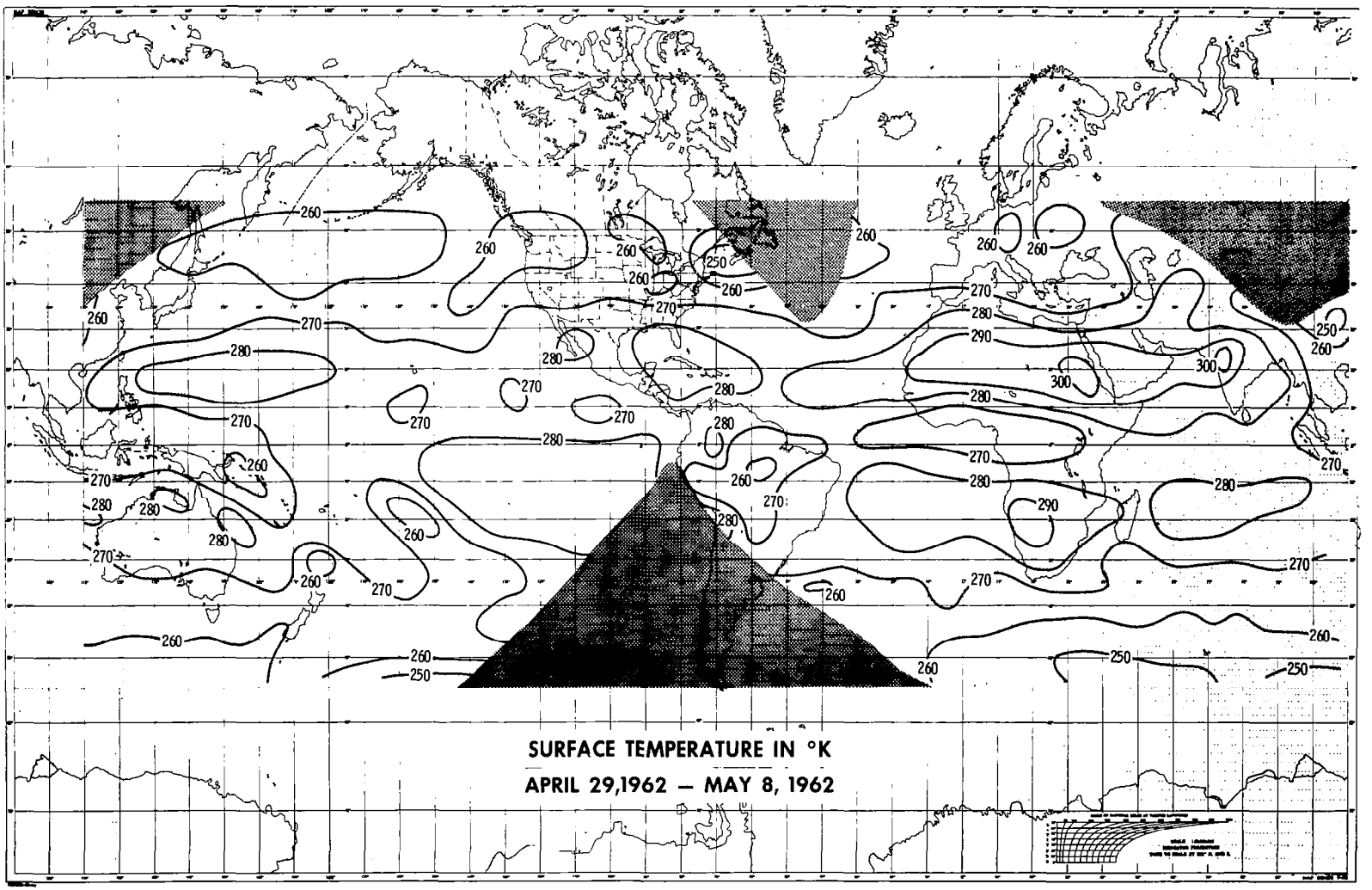
SURFACE TEMPERATURE IN °K
APRIL 29,1962 — MAY 8, 1962

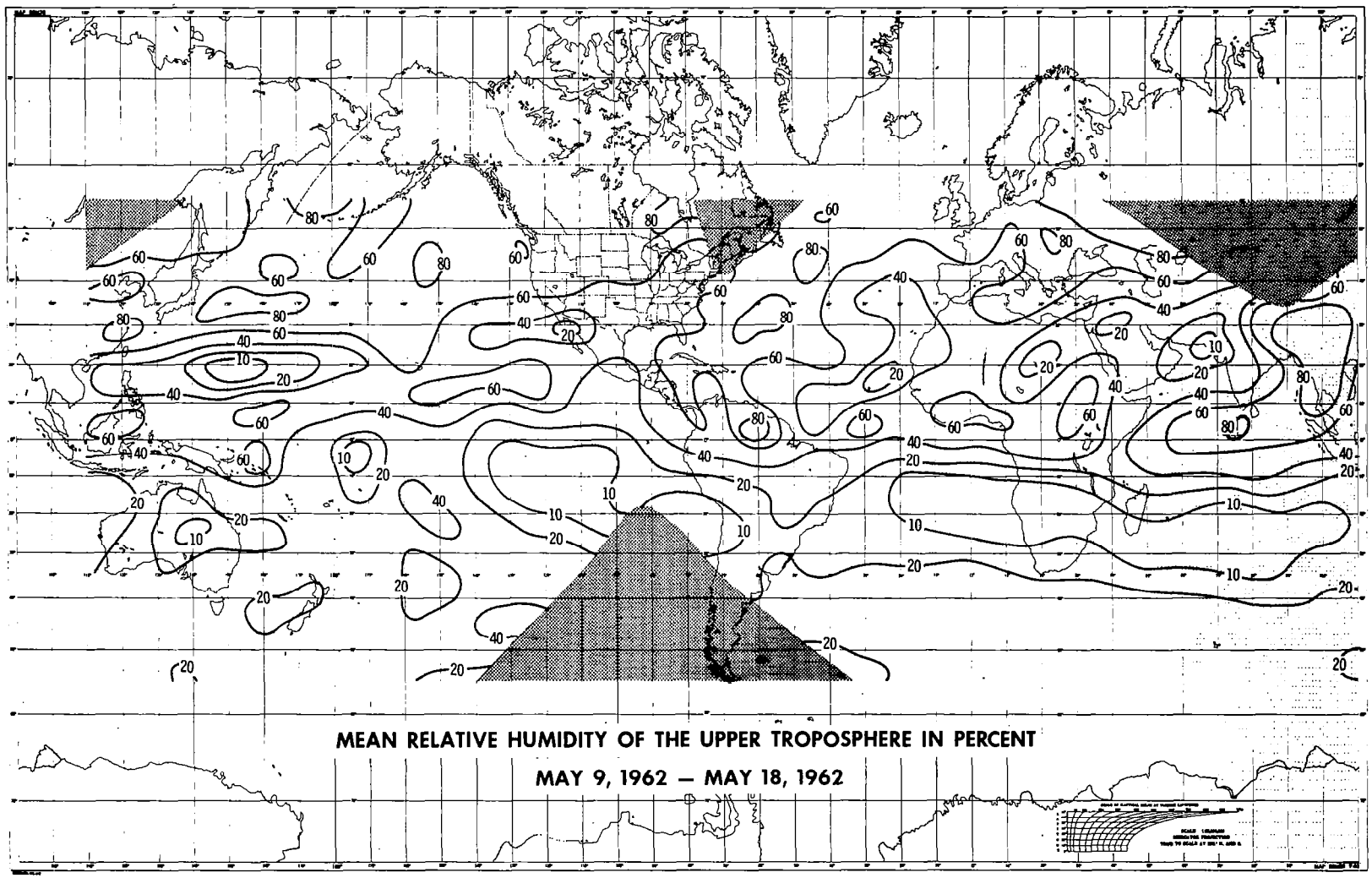
MEAN RELATIVE HUMIDITY OF THE UPPER TROPOSPHERE IN PERCENT
MAY 9, 1962 — MAY 18, 1962

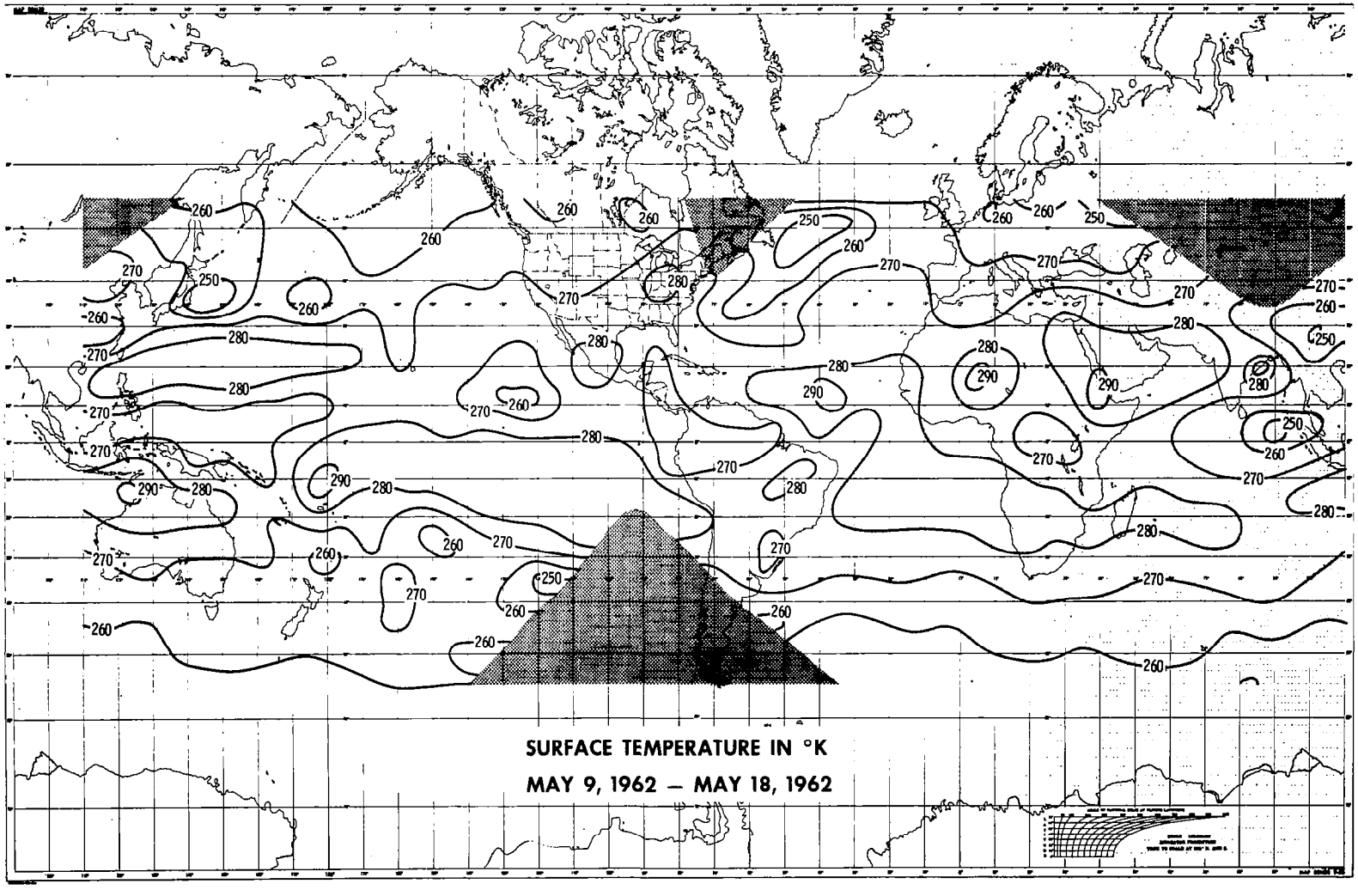
SURFACE TEMPERATURE IN °K
MAY 9, 1962 – MAY 18, 1962

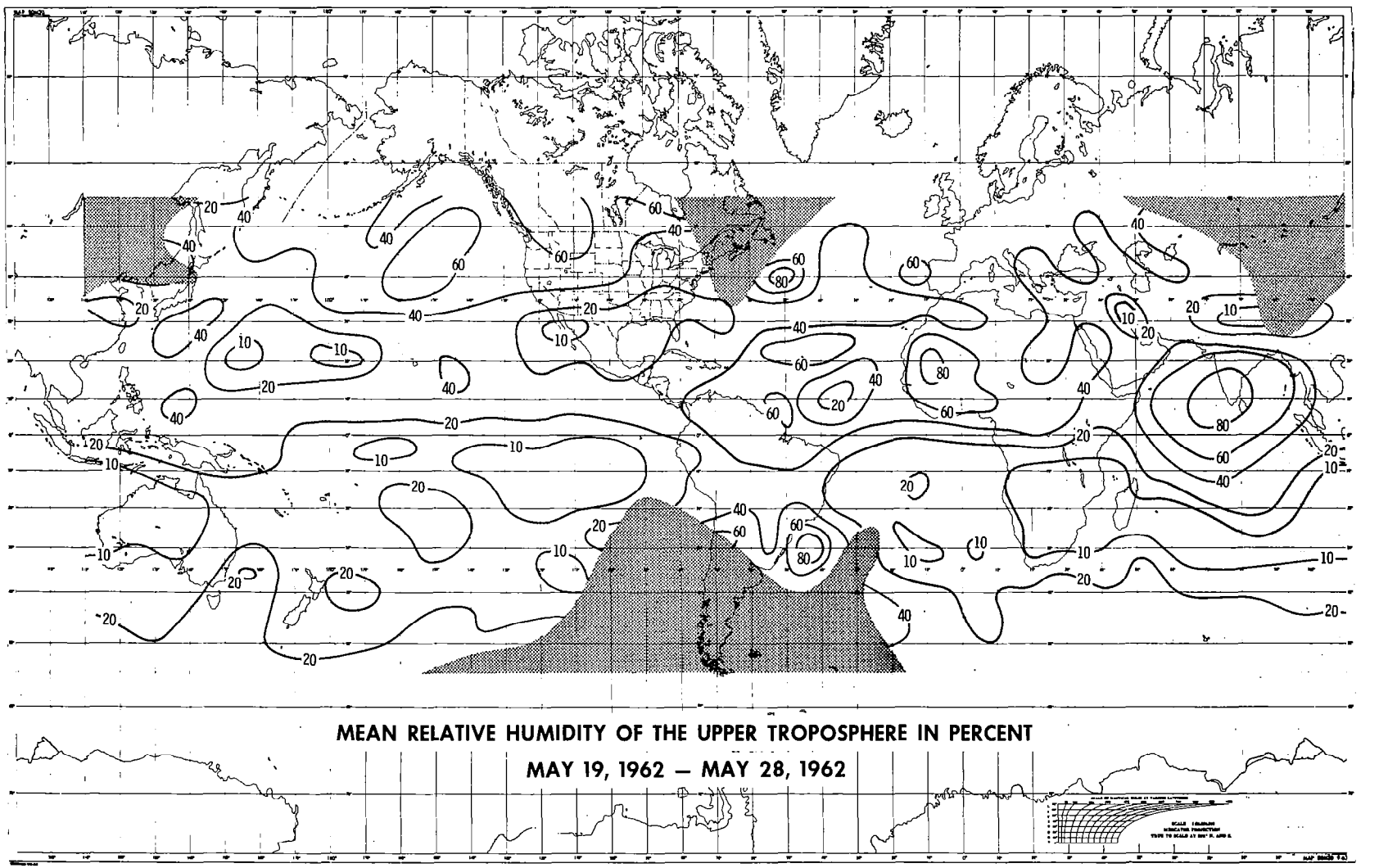
MEAN RELATIVE HUMIDITY OF THE UPPER TROPOSPHERE IN PERCENT
MAY 19, 1962 — MAY 28, 1962

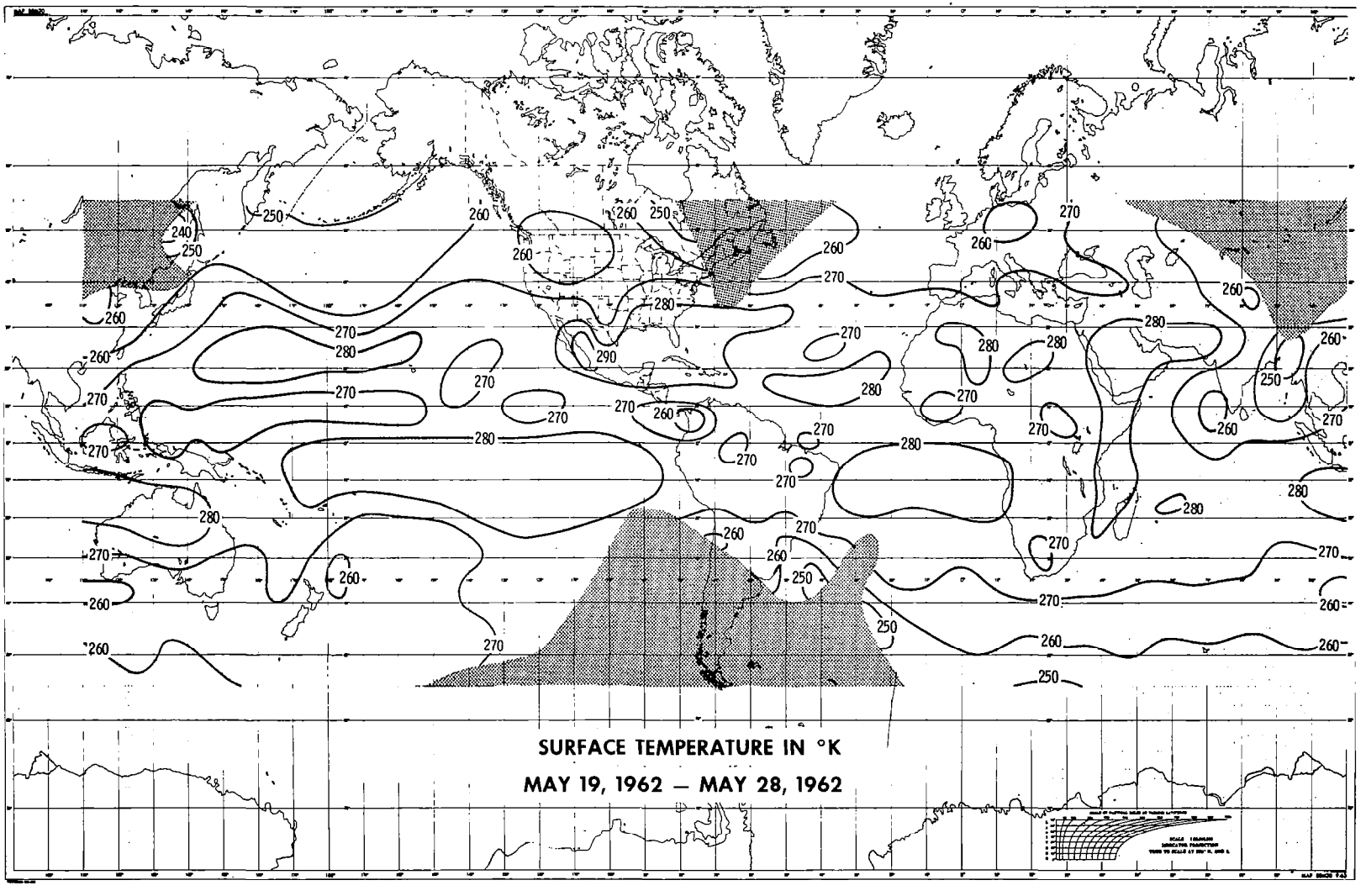
SURFACE TEMPERATURE IN °K
MAY 19, 1962 — MAY 28, 1962

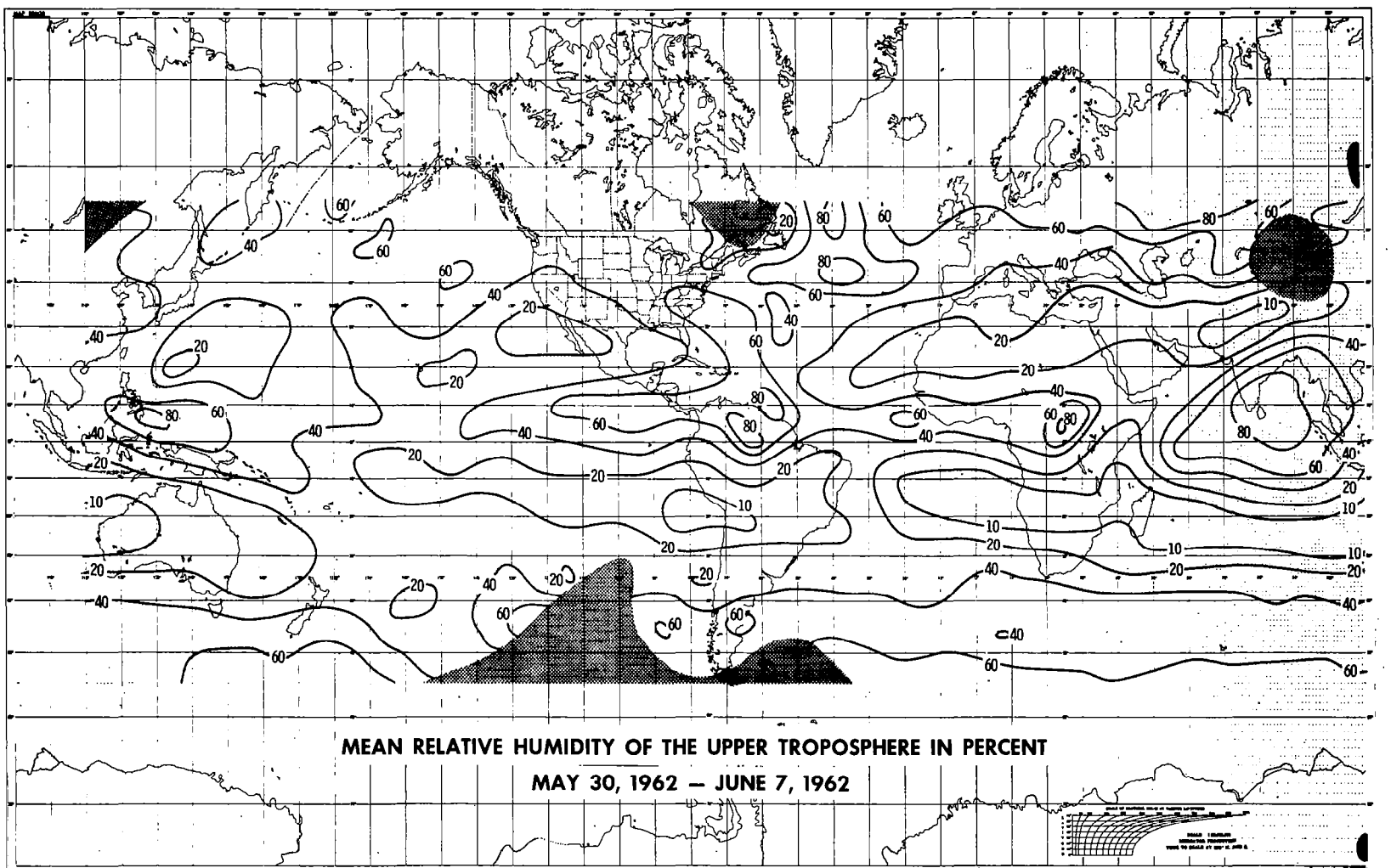
MEAN RELATIVE HUMIDITY OF THE UPPER TROPOSPHERE IN PERCENT
MAY 30, 1962 — JUNE 7, 1962

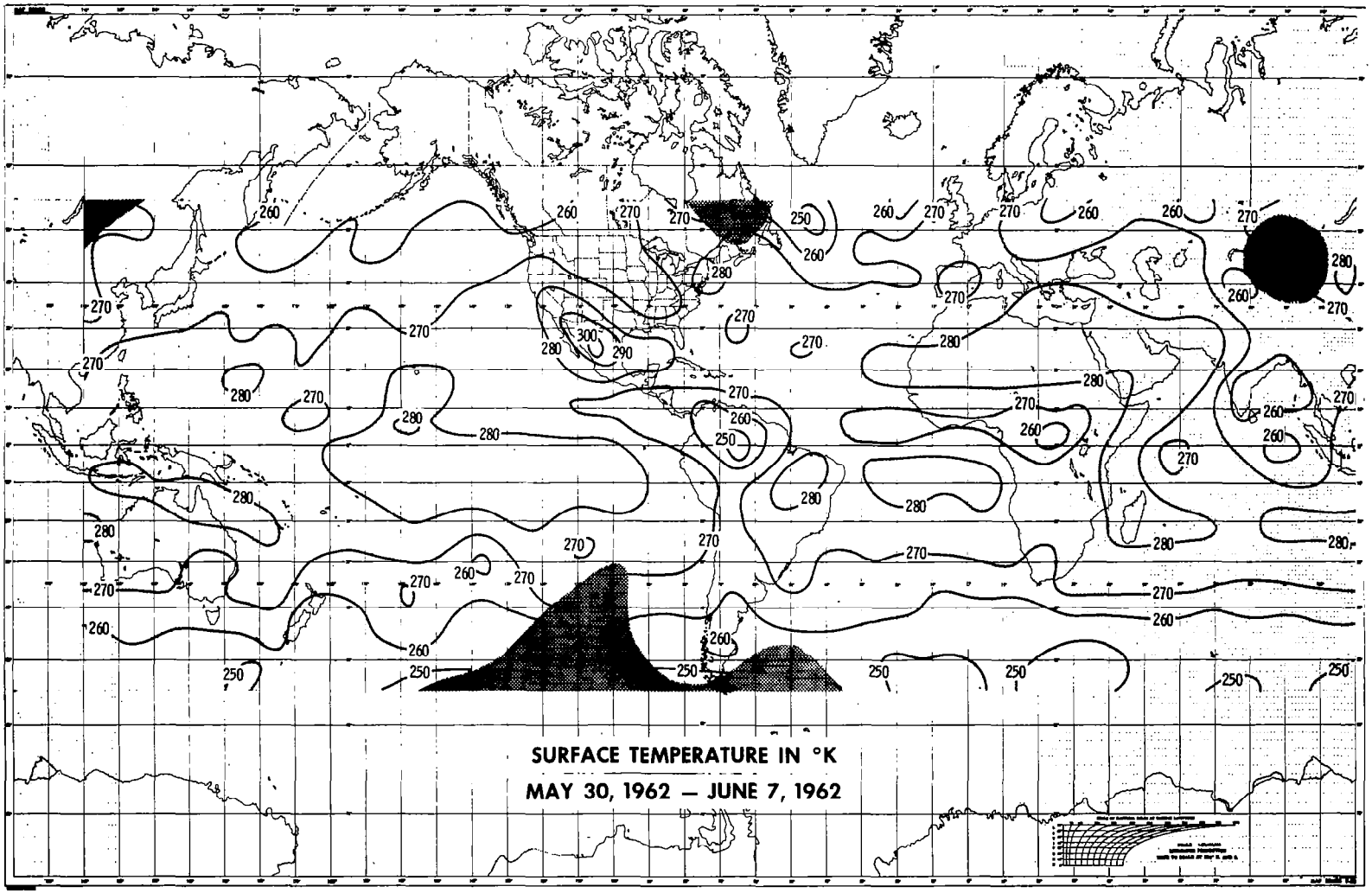
SURFACE TEMPERATURE IN °K
MAY 30, 1962 — JUNE 7, 1962

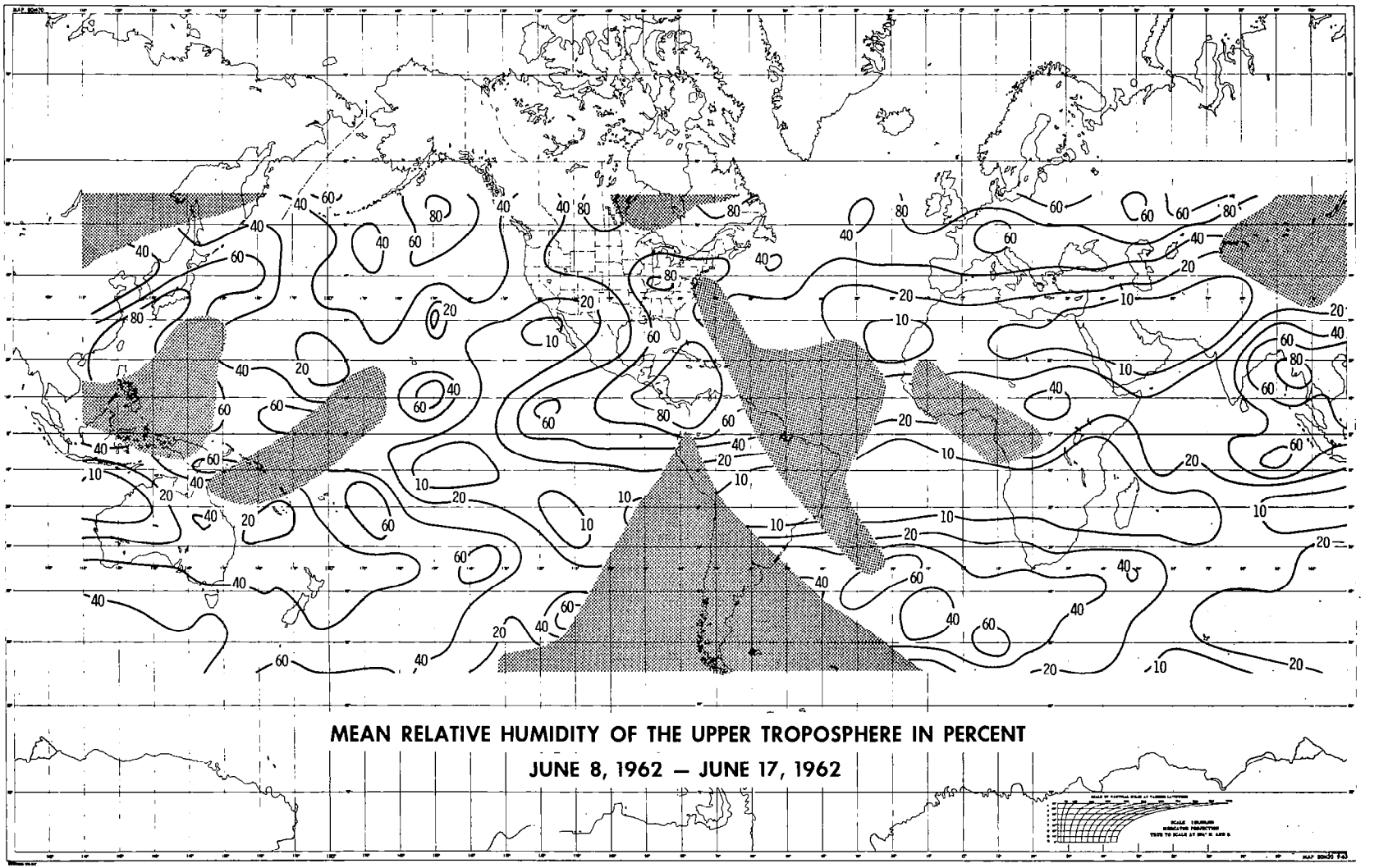

MEAN RELATIVE HUMIDITY OF THE UPPER TROPOSPHERE IN PERCENT

JUNE 8, 1962 — JUNE 17, 1962

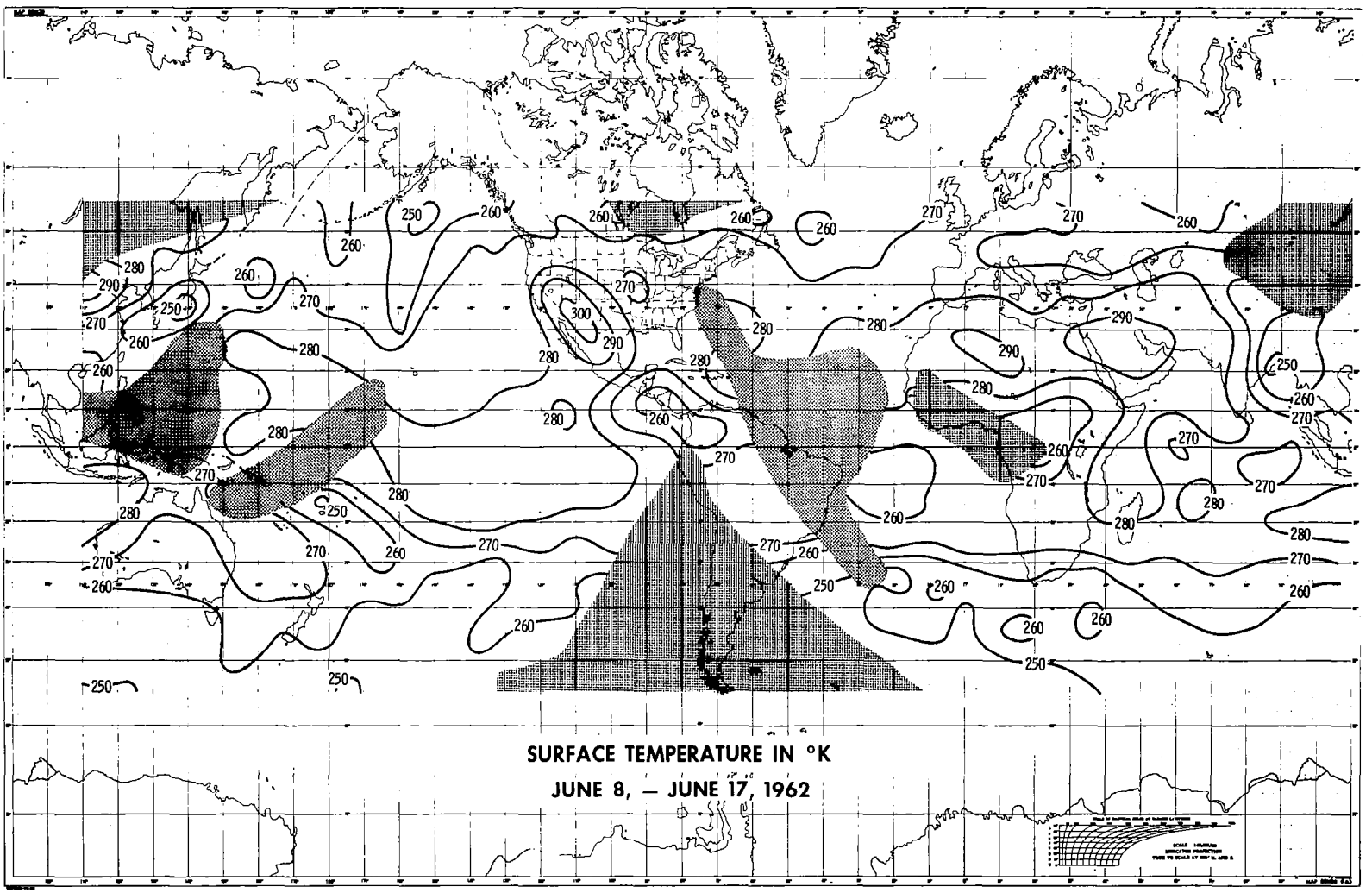
SURFACE TEMPERATURE IN °K
JUNE 8, – JUNE 17, 1962

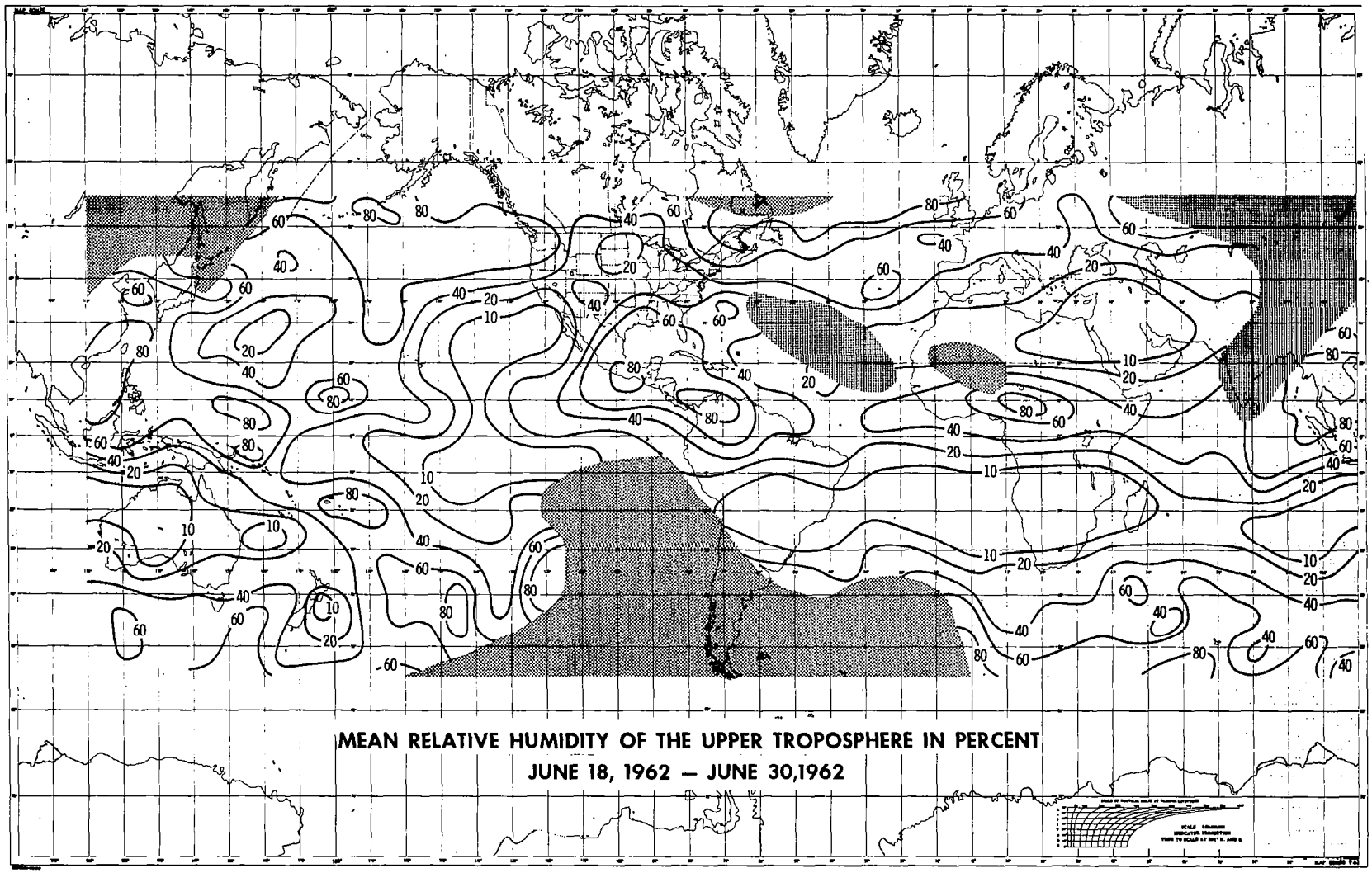

MEAN RELATIVE HUMIDITY OF THE UPPER TROPOSPHERE IN PERCENT
JUNE 18, 1962 — JUNE 30,1962

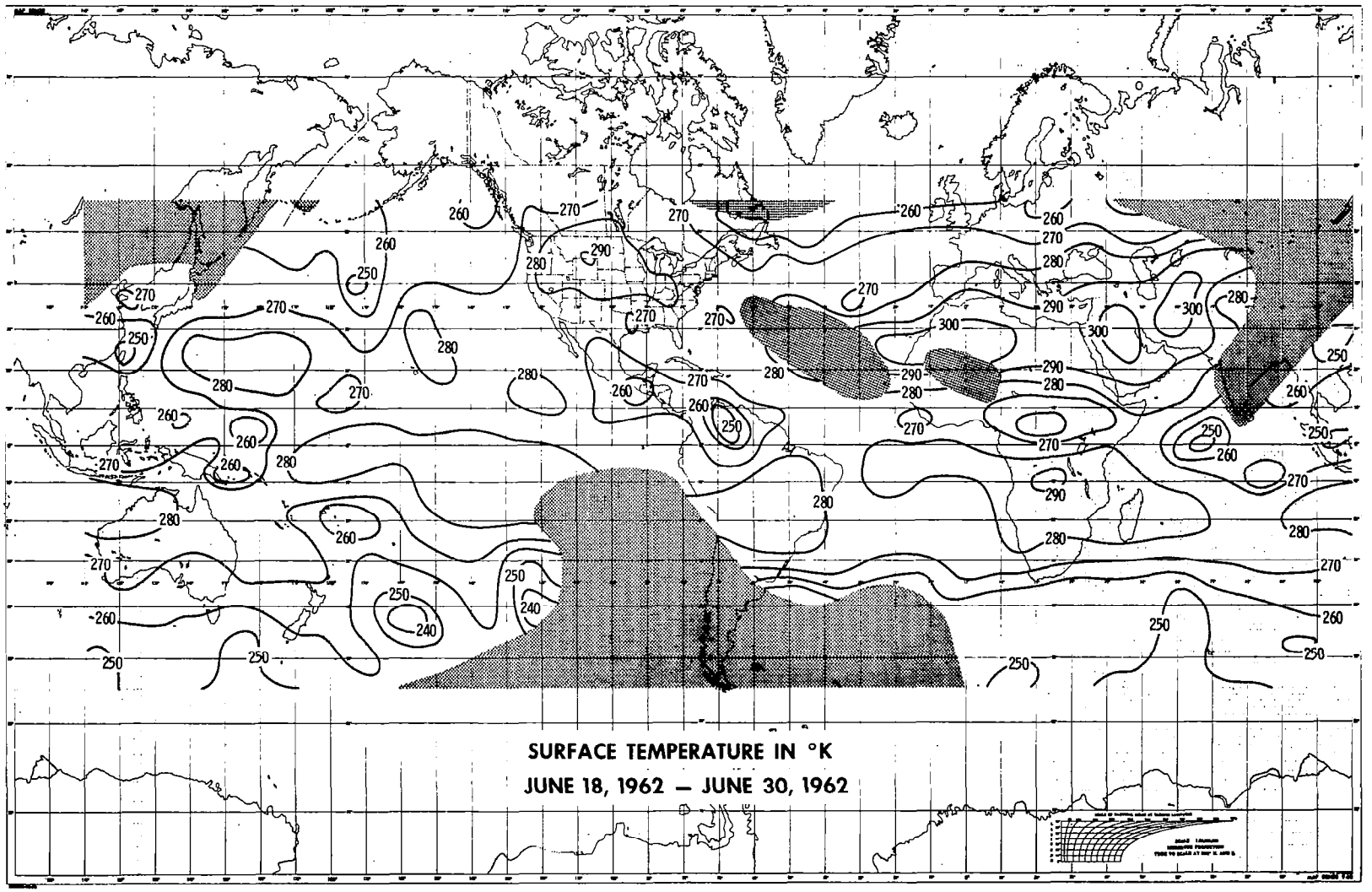
SURFACE TEMPERATURE IN °K
JUNE 18, 1962 — JUNE 30, 1962

1o.o APPENDIX A 2

Maps of the water vapor mass (in g cm^{-2}) above the 5oo mb level for periods of 1o-days covering the period from February 8, 1962 to June 3o, 1962.

(pages 97 - 11o)

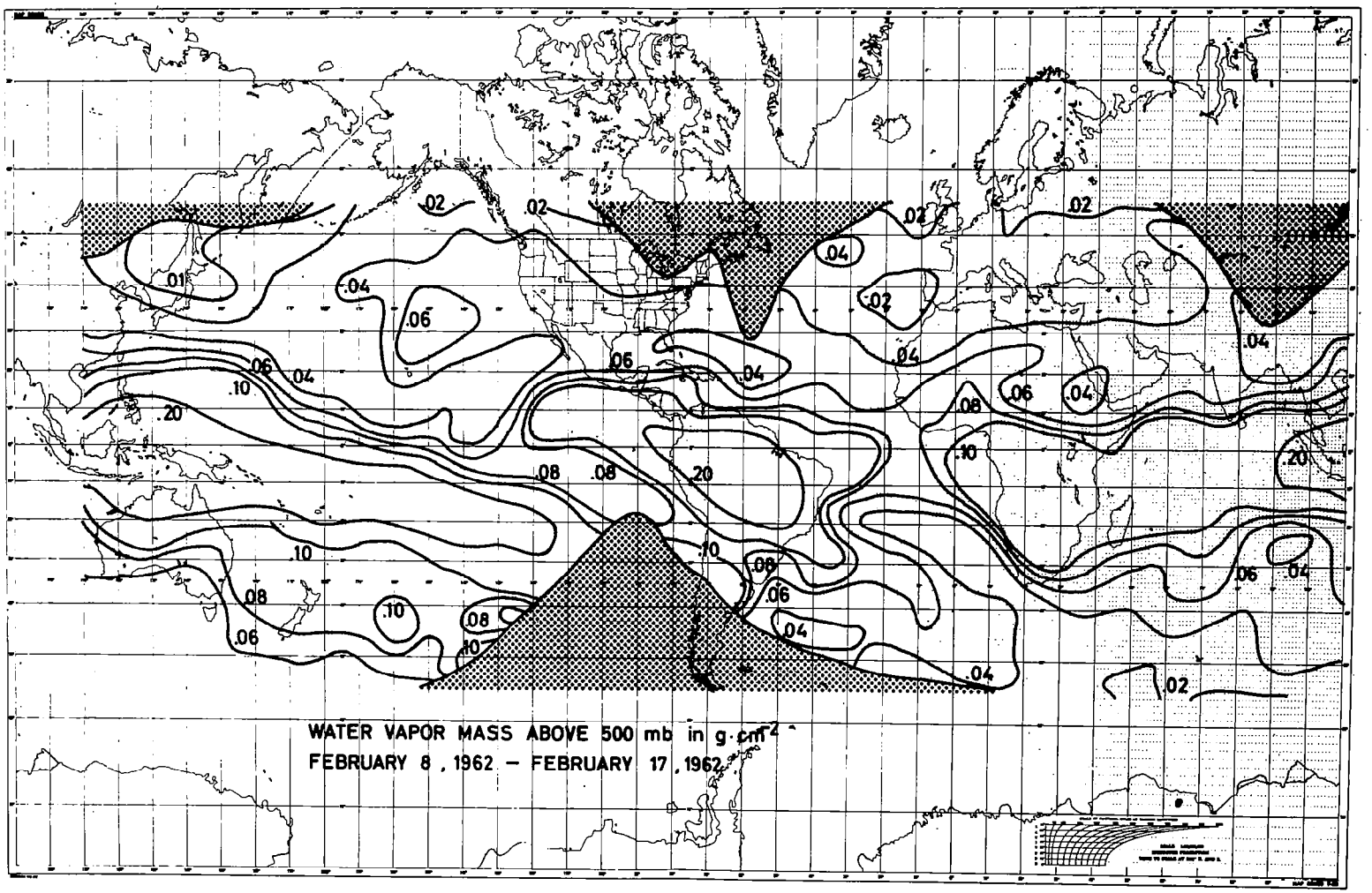
WATER VAPOR MASS ABOVE 500 mb in g·cm⁻²
FEBRUARY 8 , 1962 – FEBRUARY 17 , 1962

WATER VAPOR MASS ABOVE 500 mb in g·cm⁻²
FEBRUARY 18, 1962 — FEBRUARY 27, 1962

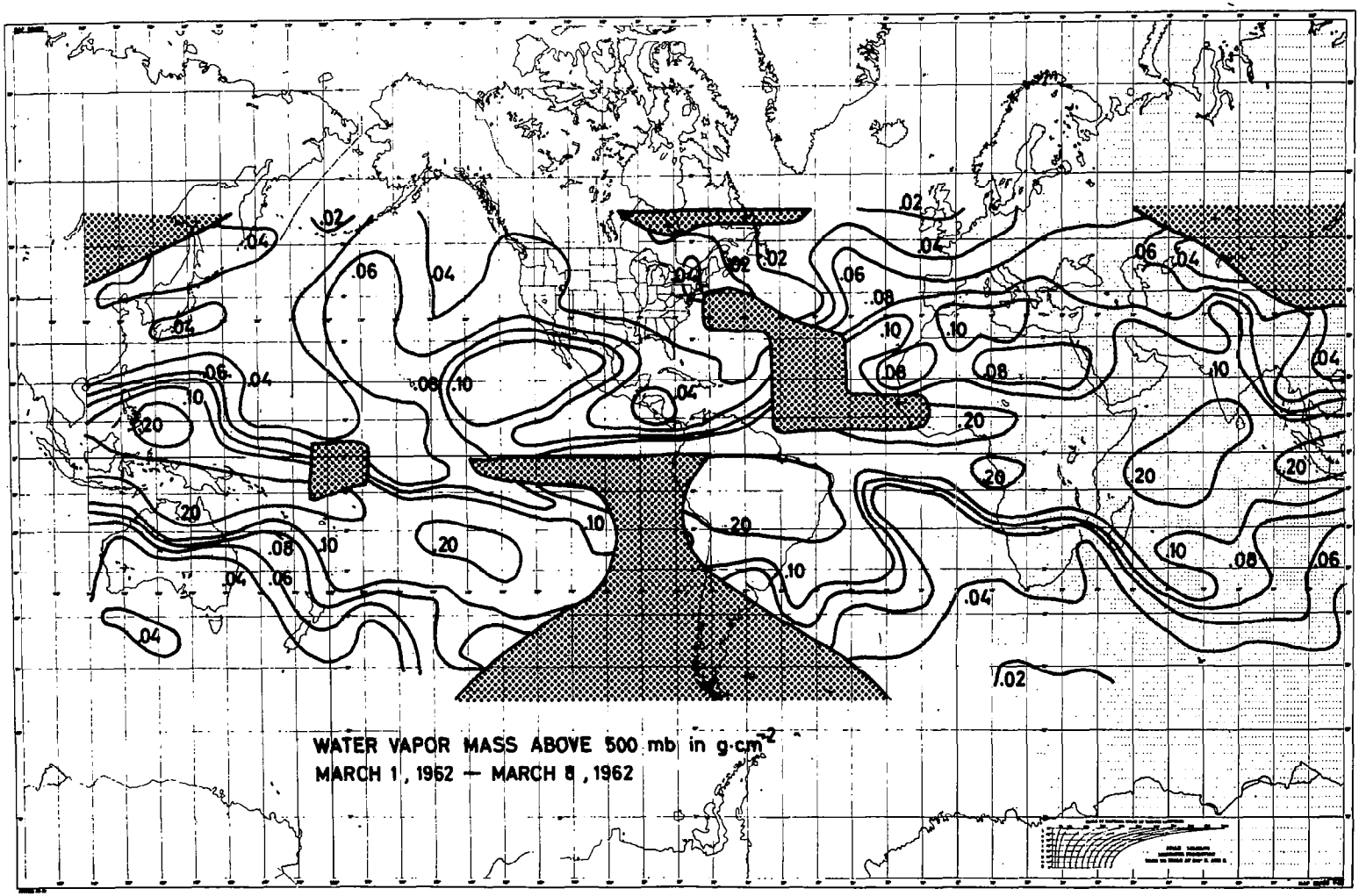
WATER VAPOR MASS ABOVE 500 mb in g·cm⁻²
MARCH 1, 1962 — MARCH 8, 1962

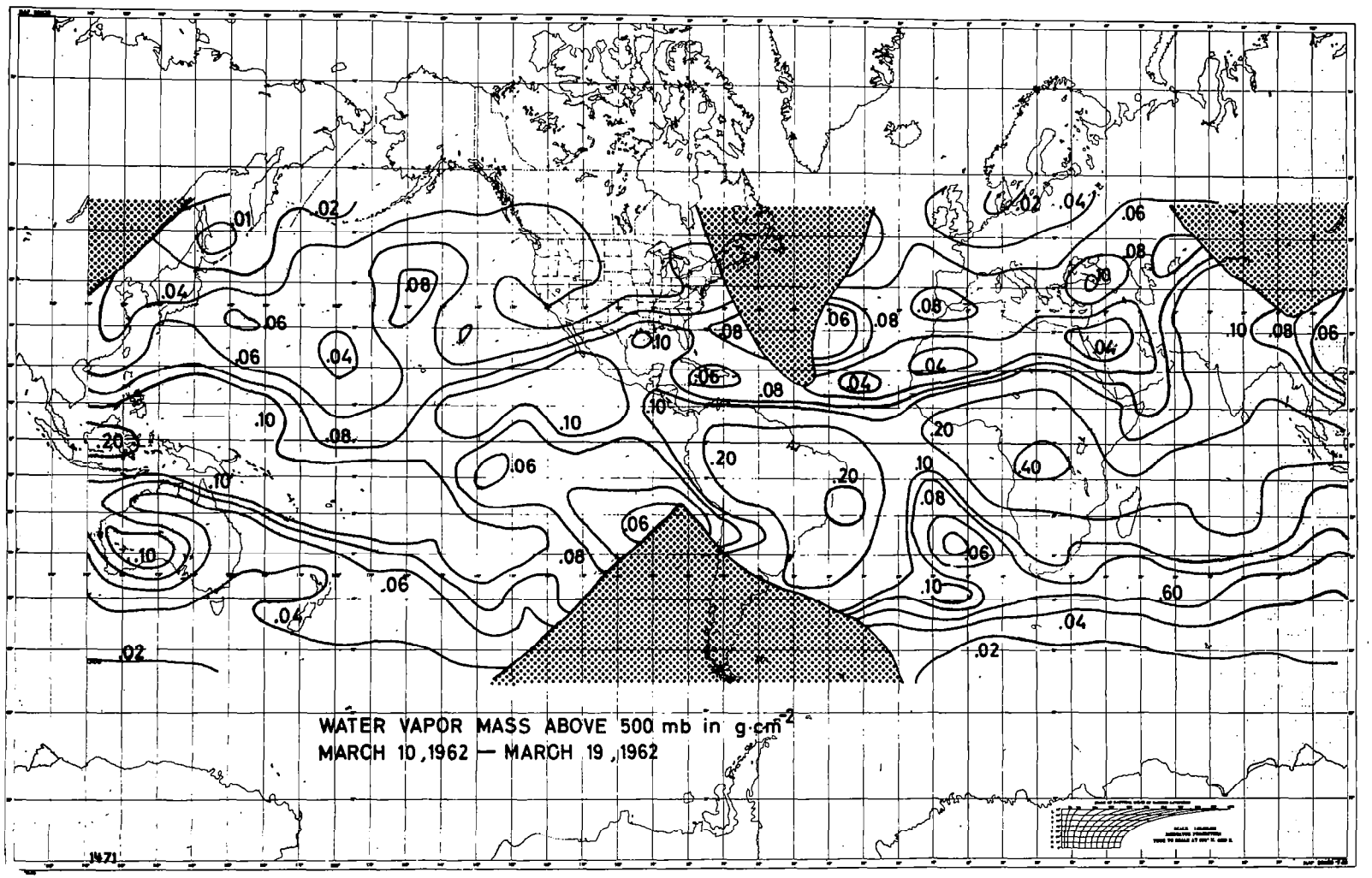
WATER VAPOR MASS ABOVE 500 mb in g·cm⁻²
MARCH 10, 1962 — MARCH 19, 1962

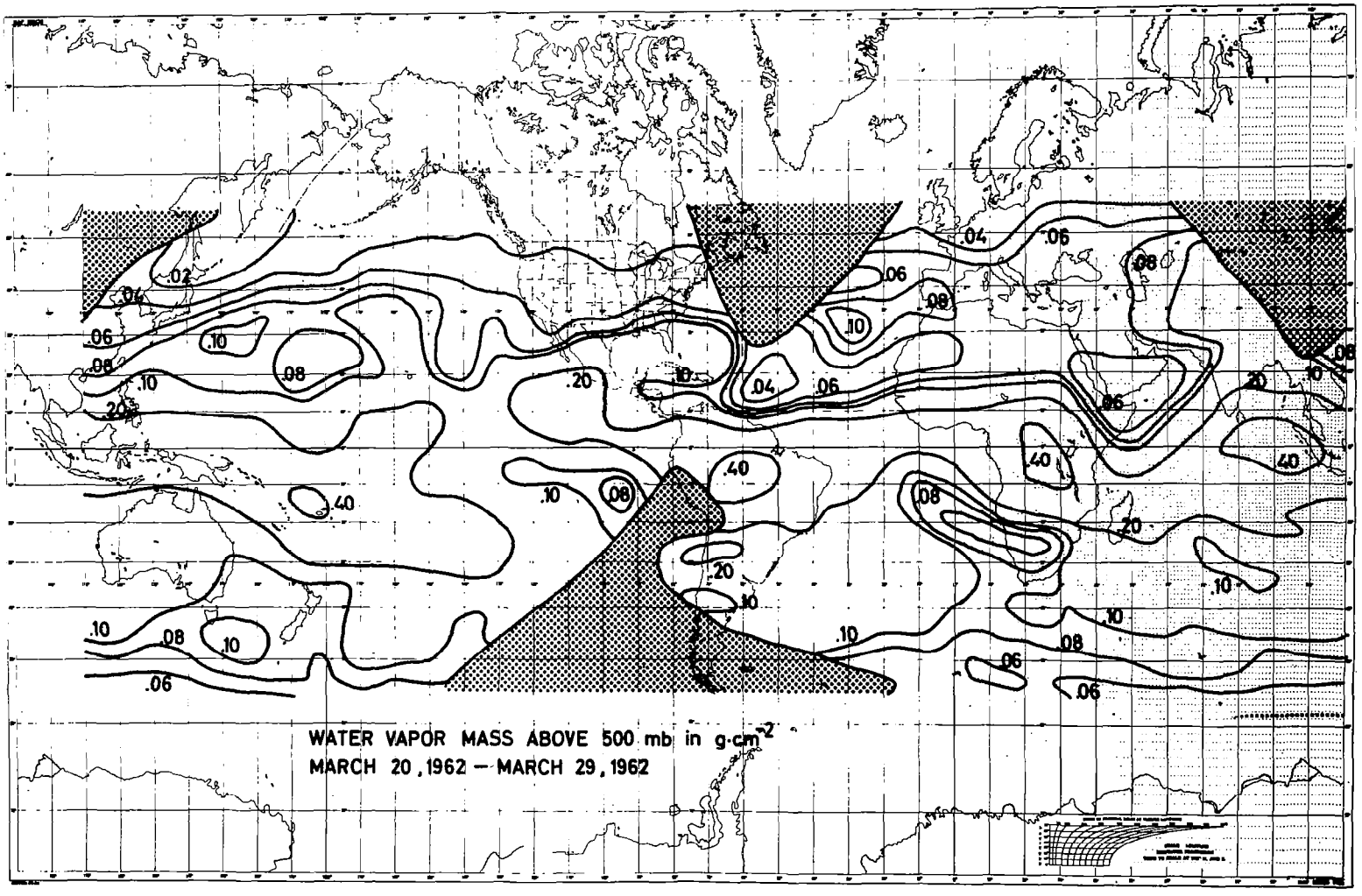
WATER VAPOR MASS ABOVE 500 mb in g·cm⁻²
MARCH 20, 1962 — MARCH 29, 1962

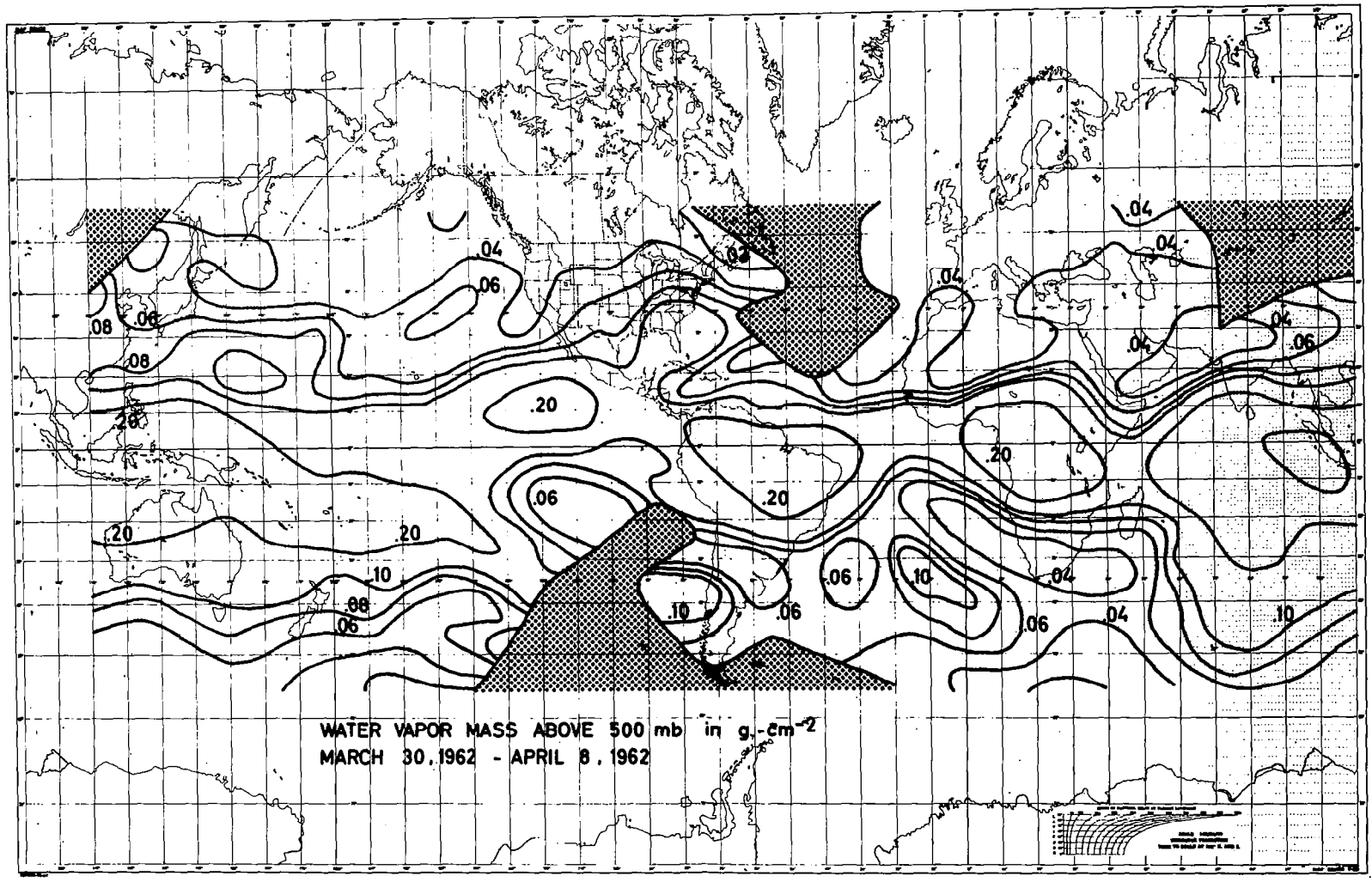
WATER VAPOR MASS ABOVE 500 mb in g.-cm^{-2}
MARCH 30, 1962 - APRIL 8, 1962

WATER VAPOR MASS ABOVE 500 mb in g cm-2
APRIL 9 , 1962 - APRIL 18 , 1962

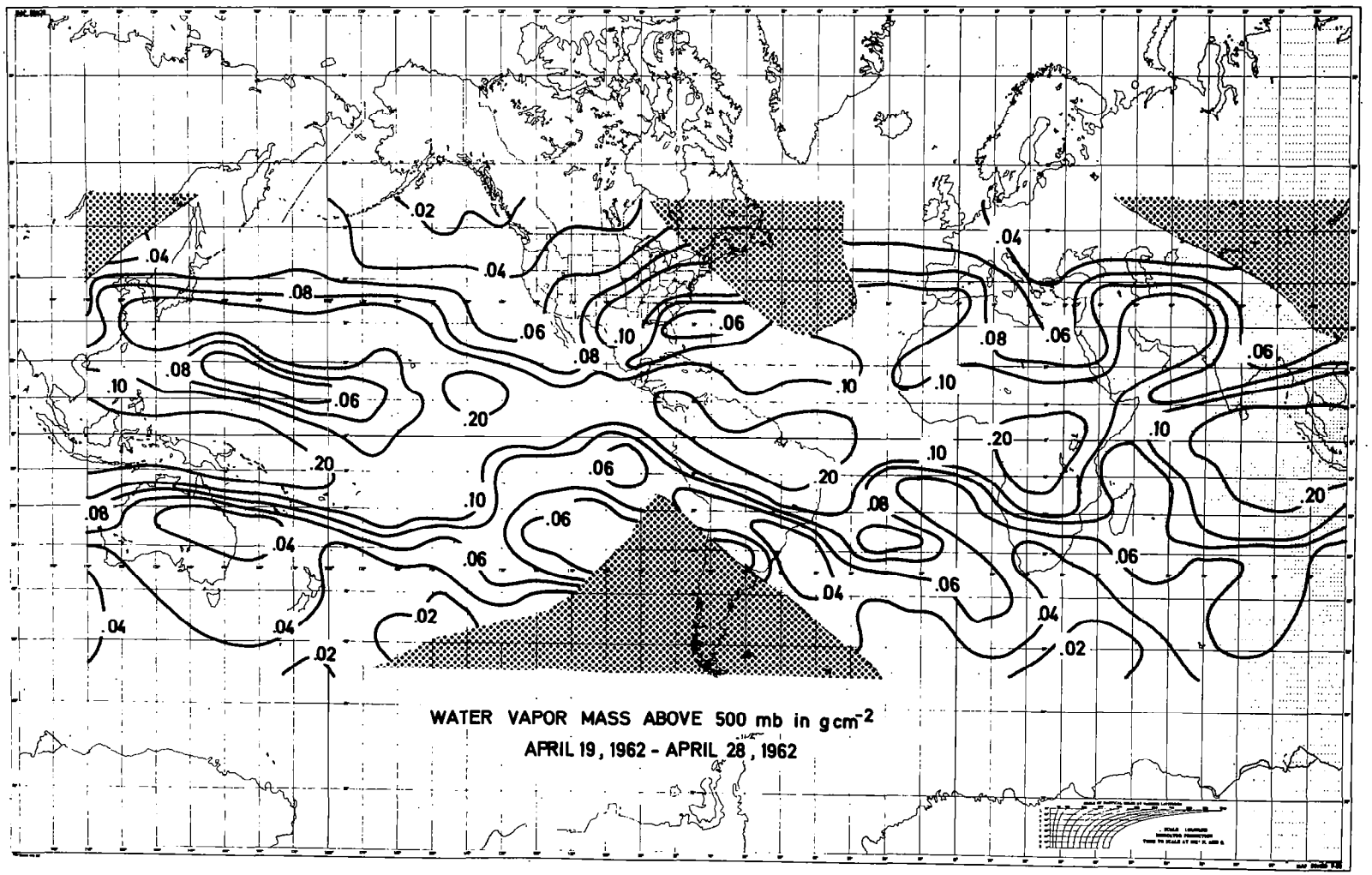
.02
.04
.08
.06
.10
.20
WATER VAPOR MASS ABOVE 500 mb in g cm⁻²
APRIL 19, 1962 - APRIL 28, 1962

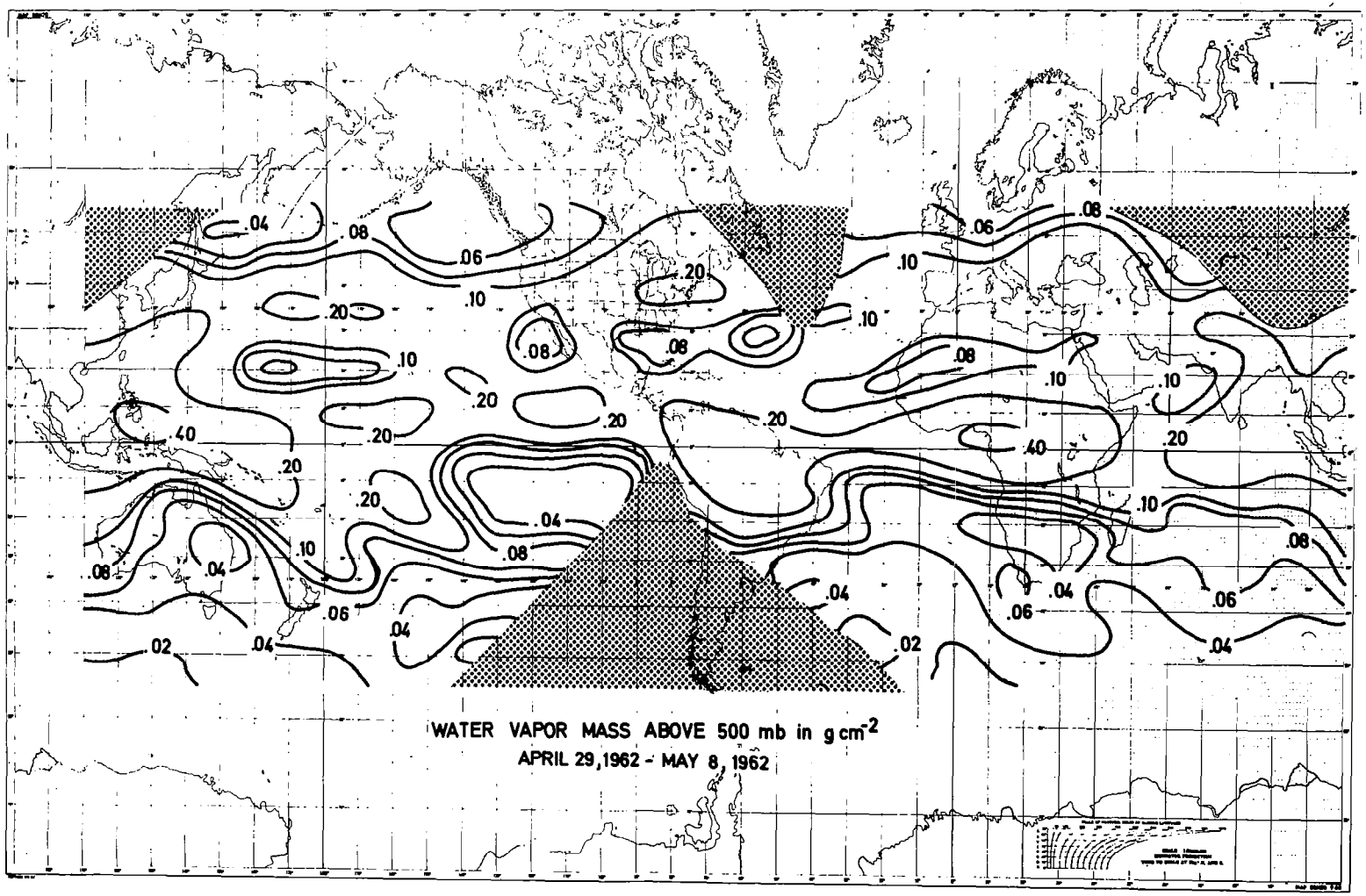
WATER VAPOR MASS ABOVE 500 mb in g cm^{-2}
APRIL 29,1962 - MAY 8, 1962

.08
.06
.10
.20
.10
.10
.08
.10
.08
.20
.10
.08
.40
.10
.20
.20
.20
.10
.20
.04
.08
.06
.10
.06
.04
.04
.02
.04
.02
.02
.02
WATER VAPOR MASS ABOVE 500 mb in g cm-2
MAY 9,1962 - MAY 18, 1962

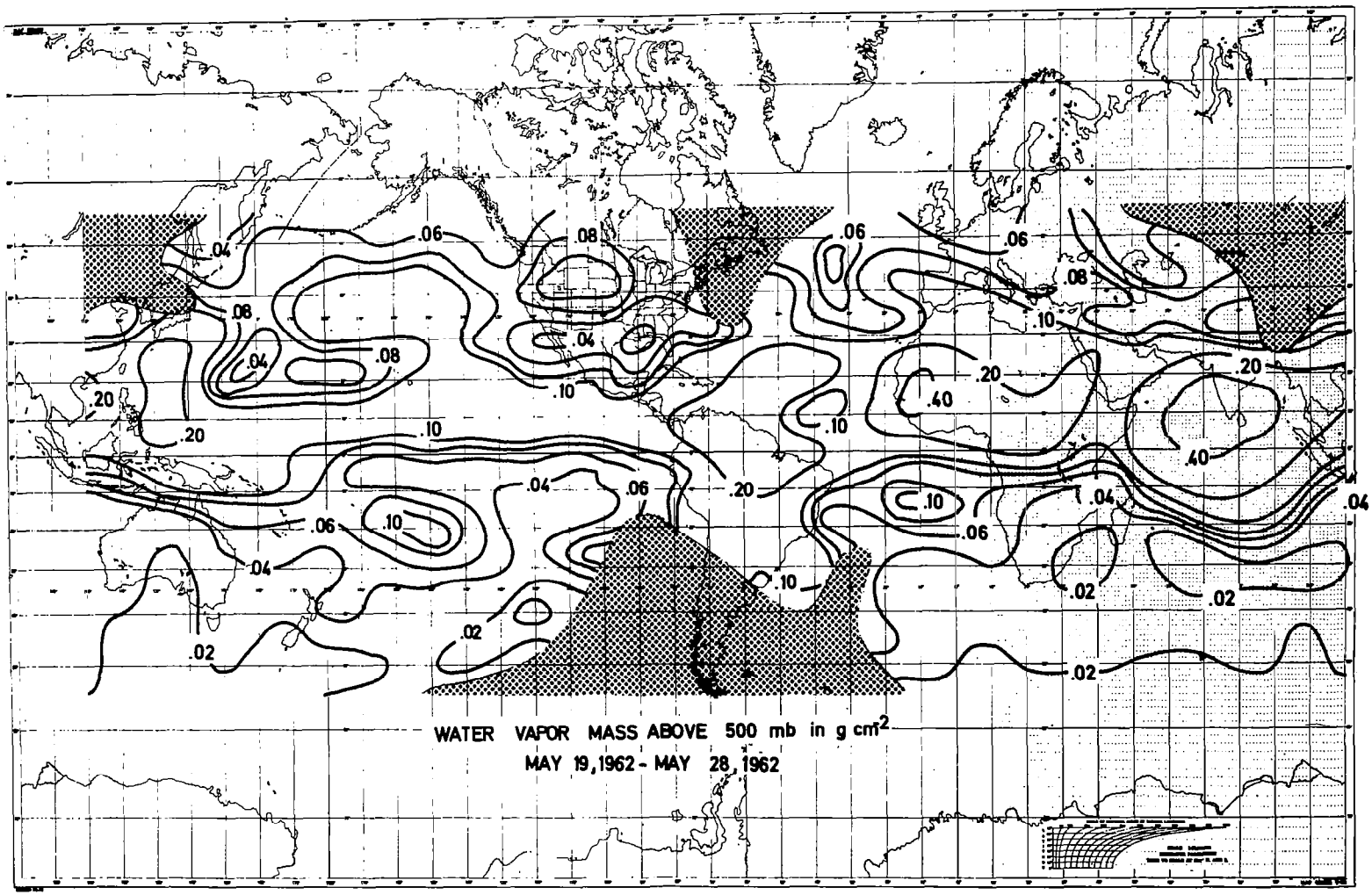
.04
.06
.08
.10
.20
.40
.02
WATER VAPOR MASS ABOVE 500 mb in g cm^2
MAY 19, 1962 - MAY 28, 1962

WATER VAPOR MASS ABOVE 500 mb in g cm^{-2}
MAY 30, 1962 - JUNE 7, 1962

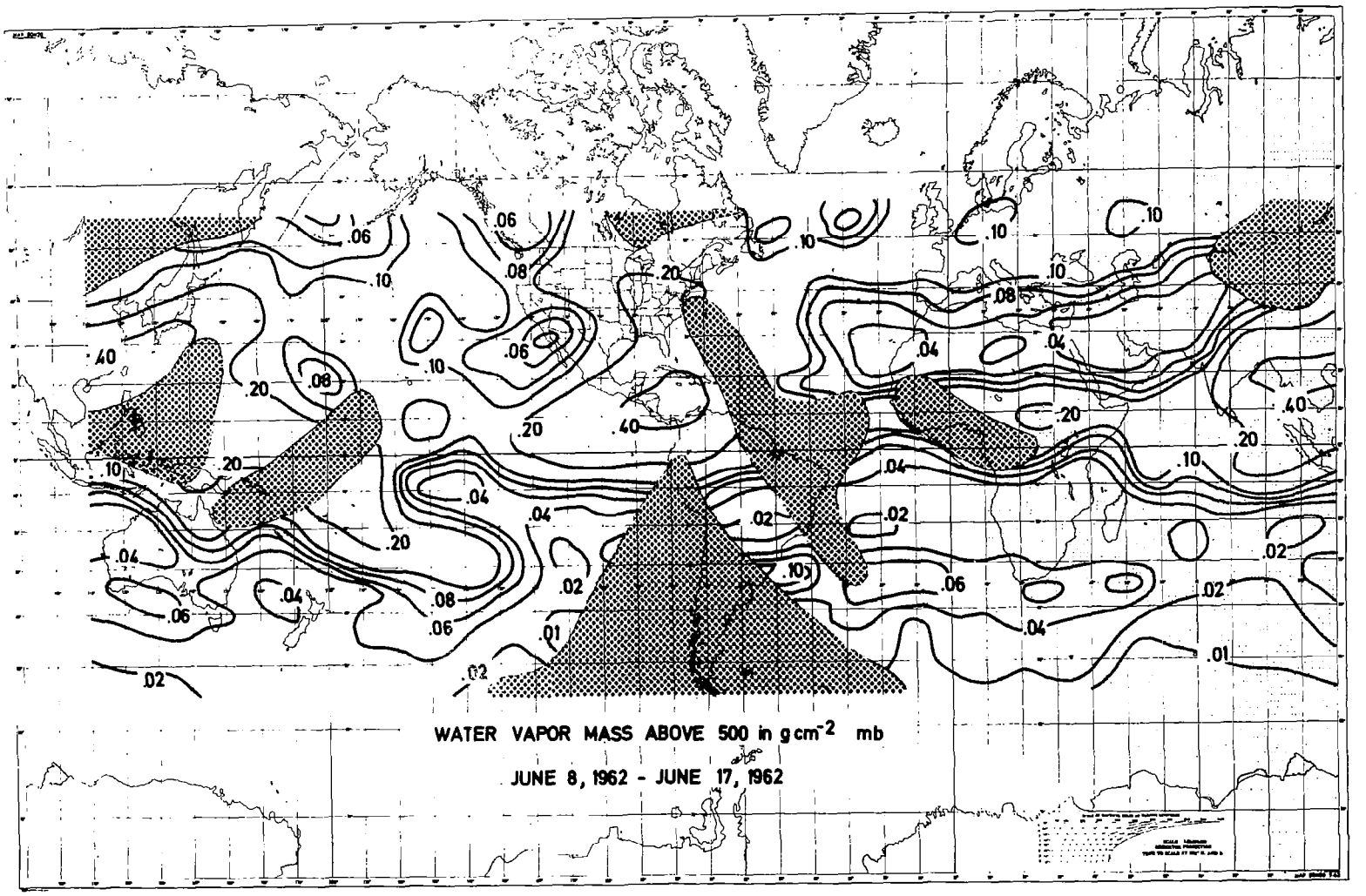
WATER VAPOR MASS ABOVE 500 in g cm⁻² mb
JUNE 8, 1962 - JUNE 17, 1962

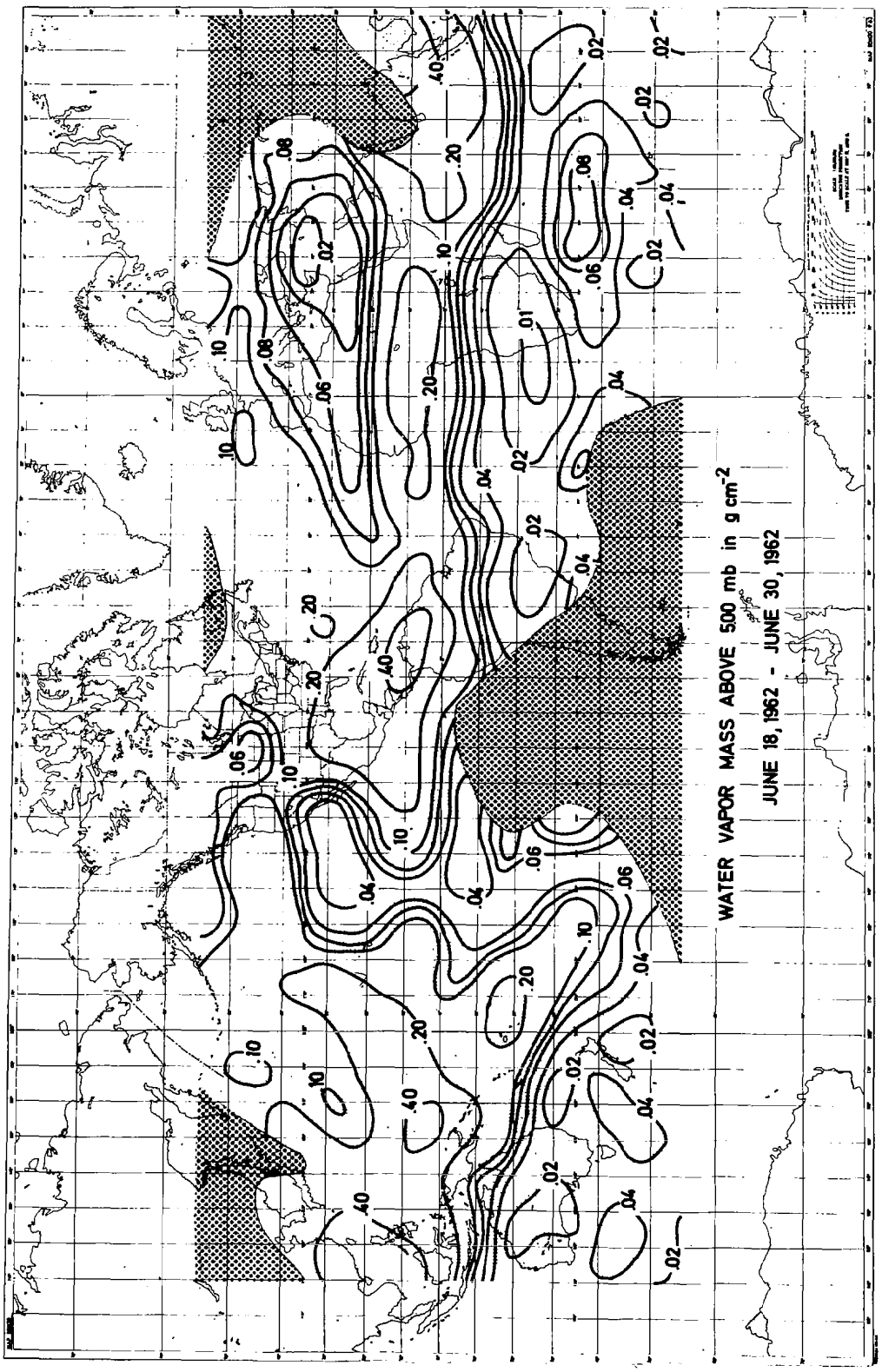

NASA-Langley, 1966 CR-595